SOIL SURFACE SEISMIC HAZARD AND DESIGN BASIS GUIDELINES FOR PERFORMANCE CATEGORY 1 & 2 SRS FACILITIES

COMPUTATION OF USGS SOIL UHS AND COMPARISON TO NEHRP AND PC1 SEISMIC RESPONSE SPECTRA FOR THE SRS

Disclaimer

COMPUTATION OF USGS SOIL UHS AND COMPARISON TO NEHRP AND PC1 SEISMIC RESPONSE SPECTRA FOR THE SRS

by

R.C. Lee

Approved by: Lawrence A. Salomone
Lawrence A. Salomone
SRS Chief Geotechnical Engineer

COMPUTATION OF USGS SOIL UHS AND COMPARISON TO NEHRP AND PC1 SEISMIC RESPONSE SPECTRA FOR THE SRS

EXECUTIVE SUMMARY

Recently, new site-specific seismic design response spectra were developed for Savannah River Site (SRS) performance category (PC) 1,2,3 and 4 structures, systems and components (SSCs) (WSRC, 1997, 1998) in accordance with DOE Standards. The lower performance categories (PC1 and PC2) site-specific design basis were not compatible with the response spectrum generated if building code guidelines were used (National Earthquake Hazard Reduction Program Recommended Provisions for Seismic Regulations for New Buildings, (NEHRP), 1997). These differences in criteria and approach should be documented and understood. Thus, Westinghouse Savannah River Company (WSRC) initiated this study to evaluate the difference between the building code hazard assessment (NEHRP) and the site-specific hazard evaluations used for SRS design.

Using methodologies previously developed (WSRC, 1998) site-specific soil surface hazard was derived from the USGS hard-rock hazard. A site-specific uniform hazard spectrum (UHS) having the same criterion (2/3 of 2500-year return period) as the NEHRP (1997) spectrum was developed from the soil surface hazard and compared to the NEHRP spectrum for the SRS.

The National Map and NEHRP-97 recommended seismic provisions are a significant improvement and accomplishment in building code development. However, for a southeastern U.S. deep-soil site, such as the SRS, serious over-conservatism in the spectral level and bias in the NEHRP-97 spectral shape is apparent from the site-specific evaluation. When National Map consistent hazard curves are developed for SRS hard-rock outcrop and site-specific soil conditions the USGS soil surface hazard is found to be generally greater than Electric Power Research Institute (EPRI) (NEI, 1994) and the Lawrence Livermore National Laboratory (LLNL) (Savy, 1996)) soil PSHAs (WSRC, 1998). Averaging the computed EPRI, LLNL and USGS soil hazard would result in an increase in the SRS design basis.

On the basis of the comparison of the USGS soil UHS and the NEHRP-97 spectrum for the SRS (Figures 8 and 10), it appears application of NEHRP-97 guidance could seriously overestimate (and in some instances underestimate) the design spectrum for other deep soil sites in the southeast U.S.

There are several conclusions based on the results of this evaluation: (1) computation of a site-specific correction to the National Map should be a consideration before using a building code spectrum for a site like the SRS (the cost of a site-specific assessment, using an available bedrock PSHA and disaggregation, may be minor compared to the high cost due to potential design basis excess or underestimation); (2) availability of National Map hard-rock hazard disaggregations would be helpful for routine site-specific hazard assessments; (3) detailed site-specific assessments may not comply with the requirement that a site-specific UHS fall within 20% of the NEHRP spectrum; and (4) NEHRP spectral shape and site classification criteria may not be appropriate for deep soil sites.

INTRODUCTION

Since the release of the National Earthquake Hazard Reduction Program Recommended Provisions for Seismic Regulations for New Buildings (NEHRP, 1997) there has been interest by the Department of Energy (DOE) in comparing these recommended building codes to site-specific analysis conducted for their facilities. In 1997 and 1998 the Defense Nuclear Facilities Safety Board (DNFSB) made specific requests for comparisons of Savannah River Site (SRS) design basis to the NEHRP (1997) spectrum (Kimball, 1998). Review of NEHRP (1997) guidelines for the SRS showed that the level of the NEHRP (1997) spectrum is higher than the site-specific Performance Category 1 (PC1) design basis spectrum (WSRC, 1998). Also, the shape of the NEHRP (1997) spectrum was different from the SRS PC1 spectrum (WSRC, 1998).

The SRS PC1 spectrum (WSRC, 1998) and the NEHRP (1997) (hereafter referred to as NEHRP-97) spectrum for the SRS are illustrated in Figure 1. The PC1 spectrum was derived using mean hazard from the EPRI and LLNL hard-rock probabilistic seismic hazard assessments (PSHAs) that were then continued to the soil surface using site-specific soil amplification functions (WSRC, 1997). The computed soil surface hazards were averaged and fit with site-specific spectral shapes and then enveloped to create a smooth design basis spectrum. The NEHRP-97 spectrum was derived from soft-rock category spectral values taken from the United States Geological Survey (USGS) National Seismic Hazard Map (Frankel et al., 1996) (hereafter referred to as the National Map) and site soil class "D" scaling parameters. Although the NEHRP-97 spectrum was found inappropriate for the SRS, the NEHRP-97 criteria were adopted for SRS PC1 facilities by the DOE and WSRC (WSRC, 1998). Both SRS PC1 and NEHRP-97 spectra (Figure 1) are derived using the same hazard criteria (2/3 of the 2500-year return period).

There were several elements of the National Map and the NEHRP (1997) guidelines responsible for the differences with SRS PC1 design spectrum: (1) the National Map, used for ground motion input to NEHRP-97, contains a highly energetic Charleston source (Mw 7.3, $\Delta\sigma$ = 150 bars, return period = 650 years) as compared to the Charleston sources contained in the hazard models used at the SRS (EPRI and LLNL); (2) ground motion attenuation models used in the National Map contain a conservative feature in the low-frequency portion of the source spectrum (Atkinson and Boore, 1998); (3) the crustal model incorporated in the National Map contains a low-speed gradient (the "soft-rock" outcrop) that is significantly slower than the observed bedrock shear-wave speeds at the SRS (note that the "hard rock" and "soft rock" bedrock distinctions are usually characterized by bedrock shear-wave speeds significantly higher or lower than 5,000 ft/sec respectively); and (4) the NEHRP-97 soil classification model and corresponding design spectrum may not adequately account for a deep soil site such as the SRS (WSRC, 1998). With these differences in mind, and because the DOE design guidance allows use of building code design (for PC1 and PC2 class facilities), it is important for the DOE to have a clear position on the applicability of the National Map and the NEHRP-97 spectrum to the DOE complex. A new SRS-specific soil surface hazard is computed using a (USGS prepared) hard-rock hazard model that is consistent with the National Map together with previously developed site-specific amplification functions. This hard-rock hazard is consistent with the source location, magnitude distribution, and rate of occurrence of earthquake sources used in the National Map. The National Map special source assumptions are very conservative as compared to the EPRI and LLNL PSHAs and this is addressed in the discussion section. The methodology to compute soil surface hazard is described in WSRC (1997, 1998), and requires a hard-rock Probabilistic Seismic Hazard Assessment (PSHA) including hazard disaggregation.

The uniform hazard spectrum (UHS) derived from the computed site-specific hazard (referred to as USGS soil surface hazard) is compared to the NEHRP-97 spectrum (for the SRS). This task is of particular interest for deep-soil eastern U.S. sites because it compares a building code design spectrum to a site-specific spectrum using the same hazard model and identical criteria. The USGS soil surface hazard is also compared to the EPRI and LLNL soil hazard and the SRS PC1 design basis spectrum (WSRC, 1998).

Another issue that is of potential concern for the SRS is the treatment of fault sources in the Charleston "special seismic zone" of the National Map. The impact on finite fault sources that extend outside the defined fault source region require additional study and the USGS was tasked to analyze the impact of these sources (WSRC, 1999). We also briefly review that work below.

DEVELOPMENT OF USGS HARD-ROCK HAZARD

In February 1999, the USGS completed a hard-rock PSHA for the SRS (WSRC, 1999). The scope of work for the USGS consisted of computing seismic hazard (including disaggregation) for a hard-rock outcrop site located centrally at the SRS. The seismic source zones and crustal models are consistent with those models used for the National Map. The ground motion attenuation models used are suitable for hard-rock outcrop sites but differ from those used for the National Map. Hazard disaggregation distance and magnitude bins are consistent with those computed in the EPRI and LLNL hazard studies. Ground motion attenuation models consist of three mutually agreed upon models, Atkinson and Boore (1995) (AB95), Toro et al., (1997) (TORO), and Frankel et al. (1996) modified for hard-rock outcrop conditions (USGS96). The USGS96 and TORO ground motion attenuation models are both single-corner semi-empirical models while the AB95 is a two-corner semi-empirical model.

In a meeting held February 17, 1999, the USGS and the DOE agreed that a composite of hazard models derived from 1- and 2-corner source models would be most appropriate for the southeastern U.S. It was also agreed that a 1/3 weighting for each of TORO, AB95 and USGS96 hazard models would best represent the hazard from a consensus opinion of ground motion experts.

The SRS hazard evaluation was done using the same source geometries and recurrence rates (including Charleston) as was done for the National Map. Hazard evaluations were done for oscillator frequencies of 1, 2, 3.33, 5, 10-Hz and peak ground acceleration (PGA). For each oscillator frequency considered, the USGS96 attenuation model produces the greatest hazard at the SRS. Figures 2a-2f illustrate the 1, 2, 3.33, 5, 10-Hz and PGA hazard computed for each of the models. At 1-Hz, the USGS96 model is about a factor of 3 higher in ground motion ~~or a factor of 9 higher in hazard than~~ the AB95 model as a result of the single corner model used in USGS96. Higher frequency hazard is somewhat more consistent among the models. The factors for ground motion and hazard are respectively: 1.9, 4 at 2 Hz; 1.6, 2.5 at 3 Hz; 1.4, 2.2 at 5 Hz; 1.2, 1.6 at 10Hz; and 0.9, 0.9 for pga. Review of disaggregations indicated that the four models produce consistent hazard contributions by magnitude and distance.

The USGS computed the composite probability of exceedance for hard-rock conditions at the SRS using the 1/3 weighting scheme (Frankel (1999) (this bedrock hazard model will hereafter be referred to as USGS bedrock hazard). The USGS bedrock hazard for 1, 2.5, 5, 10 Hz and PGA are illustrated in Figure 3 (the 2 and 3.33 Hz models were averaged to compare to 2.5 Hz). Comparisons of USGS hard-rock ~~hazard to the EPRI and~~ LLNL bedrock models currently used at the SRS are shown in Figures 4a-4e for 1, 2.5, 5, 10-Hz and PGA respectively. Of the three models, USGS bedrock hazard produces the greatest hazard at nearly all exceedances as compared to either EPRI or LLNL models for 1, 10-Hz, and PGA. However, the differences between LLNL and USGS bedrock hazard are less than the hazard differences between LLNL and EPRI. For 2.5 and 5 Hz, the USGS bedrock hazard is comparable to LLNL. Table 1 contains a comparison of 1,000, 2,500, and 10,000 year return period ground motions based on EPRI and LLNL SRS hard-rock hazard. Also shown in Table 1 are corresponding motions from the USGS96 (single corner model) and USGS weighted average model (includes 2-corner model).

USGS bedrock hazard disaggregations are illustrated in Figures 5a through 5f. For the smaller probabilties, the long-period (1-Hz) hazard is dominated by the Charleston earthquake; the short-period (10-Hz) and PGA is dominated by the Charleston earthquake and a smaller more local event. This differs somewhat from the LLNL and EPRI disaggregations that are not as spiked in magnitude and distance and show broad peaks that tend to show Charleston-type earthquakes controlling long periods and a closer, smaller event controlling the shorter periods.

EVALUATION OF THE USGS CHARLESTON SOURCE ZONE

The USGS Special Source Zones are a potential issue because of the way earthquake source rupture distance is computed for the ground motion attenuation model. The approach used in the development of the National Map is to create a grid of nodes within the confines of the special zone. For each site of interest (e.g., SRS), a line source having the appropriate length, consistent with the special zone magnitude (e.g., 7.3), is centered at each node. The line source orientation is randomized several times and the closest source to site distance of the oriented fault is averaged and then used in the ground motion attenuation model regardless of whether the closest distance is within the confines of the source zone. This algorithm effectively produces hypothetical ruptures outside of the source zone and potentially closer to the SRS.

At the request of WSRC, the USGS performed a sensitivity analysis to understand the effect of the Charleston source zone on hazards at the SRS. The SRS hazard was computed using an alternative representation of the Charleston source zone having the western edge of the zone relocated to the east by 30 km. This modified source zone would ensure that the hypothetical Charleston fault rupture would not extend closer than the original USGS Charleston source zone. Figures 6a through 6f illustrate the SRS hazard using the Frankel et al. (1996) attenuation model and two representations of the Charleston source zone for oscillator frequencies of 0.5, 1, 3.3, 5, 10-Hz and PGA respectively. Hazard differences are less than about 6% at any of the frequencies. Based on this analysis, the original USGS algorithm for computing hazard from finite sources was judged acceptable.

METHODOLOGY TO COMPUTE SITE-SPECIFIC SOIL HAZARD CURVES

The methodology for computation of soil surface hazard using bedrock hazard as input is described in detail in WSRC (1997, 1998). Cornell and Bazzuro (1997) prepared the mathematical formalism described below. Hazard at the surface of a non-linear soil column (soil surface hazard) can be derived using bedrock hazard disaggregation together with a set of frequency, magnitude and ground motion dependent soil amplification functions (SAFs). The discrete form of the soil surface hazard curve is given by:

$$G_Z(z) = \sum_{x_j}\sum_{m_i} \underbrace{G_{Y|M,X}(z/x|m_i,x_j)}_{(1)} * \underbrace{p_{M|X}(m_i|x_j)}_{(2)} * \underbrace{P[X=x_j]}_{(3)}$$

where the sums are over magnitudes (m_i) and bedrock motion amplitude levels (x_j) contained in the hazard disaggregation; $p_{M|X}(m_i|x_j)*P[X=x_j]$ is the probability mass function, and $G_{Y|M,X}$ is the conditional complementary cumulative distribution function (CCDF) on the amplification factor. The three factors in the equation represent:

(1) the conditional CCDF on the amplification of motion caused by the soil, given rock motion of amplitude X=x associated with earthquake of magnitude M=m, (from site amplification functions)
(2) the conditional probability of magnitude M=m, given rock motion X=x, (from hazard disaggregation)
(3) the probability of rock motion X=x (from the probability of exceedence)

The methodology requires disaggregation of bedrock hazard for a suite of bedrock motions. The hazard disaggregation represents the composition of the hazard by earthquake magnitude. For each (bedrock) level of motion, the disaggregated hazard is represented by a table of numbers, where rows represent source distance bins and columns represent source magnitude bins. The sum of all elements of the table is the total probability of exceedance Thus, for a given oscillator frequency and level of bedrock ground motion ($X=x_i$), each element of the hazard disaggregation corresponds to the probability of exceedance of rock ground motion for a specific earthquake magnitude range. For each oscillator frequency, the first differences are taken of the disaggregation elements between adjacent levels of bedrock motion. This results in tables of disaggregations for the probability of occurrence of the mean bedrock control motions. These probability of occurrence disaggregations determine the products of the probability mass function:

$$p_{M|X}(m_i|x_j)*P[X=x_j]$$

where x_j is the geometric average of the jth and j+1 disaggregated hard-rock motions.

$G_{Y|M,X}$, the CCDF on the amplification, is determined using the SAFs developed in WSRC (1997). Magnitude dependence of the SAFs is expressed by the approximate 5^{th}, 50^{th}, and 95^{th} percentile of the EPRI magnitude disaggregation (these three magnitudes are also expressed as ML, MM, and MH respectively). These SAFs for the three magnitudes are interpolated to span the range of the disaggregation magnitude bins (WSRC, 1997).

An exact soil surface hazard computed using this methodology requires disaggregation of bedrock hazard at sufficiently dense amplitudes to span an adequate range of bedrock levels of motion. The disaggregation must also be sufficiently dense in earthquake magnitude bins to account for magnitude dependence of the soil response. This methodology was implemented in FORTRAN Program SOILHAZF. See WSRC (1998) for discussion of SOILHAZF features and flowchart.

Development of equivalent linear soil surface response for the SRS was presented in detail in WSRC (1997). The basic approach to the development of SAFs is to disaggregate the bedrock hazard curves and use the disaggregated magnitudes to develop a suite of magnitude dependent bedrock spectra, or control motions. The site properties including soil column thickness, bedrock type, and the range in material and dynamic properties are then parameterized and randomized. A large number of realizations (30) of the randomized soil and bedrock properties are then derived to develop site response for two bedrock types and six ranges of soil column thickness that span the range of conditions for the SRS. By convolving each magnitude dependent bedrock control motion through the soil profile realizations, statistical distributions on site response are derived for each of the combinations of soil column thickness and bedrock type. Development of bedrock control motions, their site-specific response, frequency, magnitude, and ground motion dependency are discussed in detail in WSRC (1997).

Earthquake distance dependence of the SAF is not considered. It is expected that the effect of distance on the computed SAF is second-order except at the lowest POE's (largest ground motions).

USGS SOIL SURFACE HAZARD

The USGS bedrock hazard magnitude and frequency dependent disaggregated hard-rock seismic hazard results are used to compute the USGS soil surface hazard. The USGS hard-rock hazard results are considered mean values (Frankel, personnel communication) and can be compared directly to the earlier mean LLNL and EPRI hard-rock hazard for the SRS. For each of the five ground motion frequencies (1, 2.5, 5, 10-Hz and PGA), the hazard disaggregation is defined for a suite of bedrock spectral ground motions.

Assumptions and approximations used in the soil surface hazard development:

1. A cubic polynomial interpolation of bedrock hazard was used and appears to be a good approximation for USGS bedrock hazard for all oscillator frequencies based on the goodness of fit.
2. The hazard disaggregation, between bedrock levels of motion, is linearly interpolated on a log-log scale.
3. The three-point magnitude dependence contained in the SAFs is linearly interpolated to account for the magnitude dependence contained in the bedrock disaggregation.
4. The SAFs and corresponding control motions of WSRC (1997) are assumed to cover the necessary ranges of bedrock hazard motions. In addition, the SAFs are assumed to be log-normally distributed and linear interpolation of the log-normal distribution is assumed to be adequate for developing soil surface hazard.
5. Where USGS rock ground motions exceeded the range defined by the SAFs, SAF median and standard deviations were conservatively fixed at the limiting values.
6. A lower bound on the SAF of 0.5 is also applied for all frequencies to limit the non-linearity of the soil column.
7. Truncation of the probability of exceedance at $\pm 2\sigma$ was used to avoid accumulation of extremely low POE's.
8. The 100-Hz soil/rock spectral response was used for the PGA transfer function.

Computed USGS soil surface hazard, using the USGS bedrock hazard model are illustrated in Figures 7a through 7e for oscillator frequencies of 1, 2.5, 5, 10-Hz and PGA. The solid lines represent hazard at the top of the soil column. The dashed line in the figures are the USGS bedrock hazard. Open symbols on the dashed lines indicate extrapolation beyond the computed USGS bedrock hazard values. Each of the figures contain six hazard models that are appropriate for a site depending on whether the site is on crystalline or triassic rock and depending on soil column thickness. The legends are read as follows: the first number (1, 2p5, 5, 10, 100) is oscillator frequency; the first letter (u) is for USGS bedrock hazard disaggregation; the second letter is c or t for crystalline or Triassic bedrock; and the last number is 1, 2, or 3, for soil depth range. Thus, the hazard corresponding to "2p5ut3" corresponds to the 2.5 Hz USGS bedrock hazard for soil depth range 3 (1300-1500 ft) overlying Triassic bedrock. As expected, the level and features of these hazard curves are very similar to those of LLNL (WSRC, 1998). For oscillator frequencies of 1 and 2.5 Hz, non-linear effects of the soil column are evident for annual probabilities of exceedence of about 10^{-4} or less. For higher oscillator frequencies (5-, 10-Hz, and PGA), non-linear soil response is apparent for annual probabilities of $5x10^{-4}$.

There are general features in common among the soil surface hazard curves. At higher annual probabilities, the soil surface hazard approximately parallels the rock hazard curve (i.e., nearly the same slope) until ground motions are sufficiently large that non-linear soil effects begin. For larger ground motions, frequency dependent nonlinear soil response increasingly reduces the probability of exceedance as compared to the bedrock hazard (soil surface hazard increasing slope). Significant nonlinear behavior of the soil, manifest in the soil surface hazard curves for the five frequencies, does not become clearly evident until annual probabilities of exceedance are less than about 10^{-4}. At much lower POEs ($\cong 10^{-6}$), the soil surface hazard curves again begin to parallel the bedrock hazard curve. This behavior occurs at lower annual probabilities because of the constraint placed on reduction of motion due to non-linear soil response. This is partially an artifact of the limited range of SAFs; however, the calculation of site response for the upper range of control motion is approaching the limits of the reliability of the equivalent linear method and the reliable range of measured strain-dependent damping for some soil layers used in the analysis (WSRC, 1996). For computation of very low probability soil surface hazard ($<10^{-6}$), limiting the upper range of control motions (or equivalently limiting the peak soil strains) adds more conservatism to those segments of the soil surface hazard curve than would otherwise be based on extrapolations of laboratory testing data. In addition, the added conservatism obtained by limiting the degree of soil degradation may compensate for the additional uncertainty in the equivalent linear approximation at these strain levels (WSRC, 1998).

Most of the assumptions and limitations of the computation of soil surface hazard, described in WSRC (1998), apply in this application as well. As discussed in WSRC (1998), there are two important assumptions. First, the soil hazard results depend critically on the reliability of the site amplification models. It is assumed that the equivalent linear model of wave propagation through the soil and the laboratory determined, strain-dependent soil modulus and hysteretic damping, are valid for bedrock control motions of up to 0.75g. It is also assumed that the site response distribution is fixed for motions exceeding that amount. Also, the importance of earthquake distance dependence in the soil SAFs has not been explored. For lower probabilities, the most likely event distance becomes small and angle of incidence effects could alter the soil/rock transfer function.

COMPARISON OF USGS SOIL UHS TO NEHRP-97 SPECTRUM

The NEHRP-97 spectrum applies the National Map for the reference soft-rock site category (2,500 < Vs < 5,000 ft/sec) (Frankel et al., 1996). Following the NEHRP-97 guidelines, USGS soft-rock spectral values (for the central SRS location) were adjusted for site class "D" which is characterized by shallow soils having shear wave speeds of 600< Vs <1,200 ft/sec and standard penetration test resistance values (N-values) of 15-50 in the upper 100 ft (the SRS median shear-wave speed is about 1,150 ft/sec and N-values typically range from about 10-70) (WSRC, 1997). In addition, as recommended in NEHRP-97, the design response spectrum was taken as 2/3 of the maximum considered ground motions (2500 year return period). The resulting NEHRP-97 spectrum for the SRS is illustrated in Figure 8.

The envelope of the USGS soil surface hazard curve is used to develop the USGS soil UHS at each frequency (Figure 8). The same NEHRP-97 design criteria (2/3 of 2500-year return period) were used to compute the USGS soil UHS. The difference in the two spectra is remarkable considering the difference is a result of generic vs. site-specific evaluation.

DISCUSSION

Bedrock Hazard

The National Map hazard, once corrected to account for SRS bedrock outcrop, is consistent with the mean LLNL bedrock hazard model for the SRS at oscillator frequencies of 2.5 and 5-Hz. The USGS bedrock hazard is significantly higher than both LLNL and EPRI at 1 and 10 Hz. This is not a surprising result as the National Map hazard model employs a large magnitude earthquake (Mw 7.3) having a short return period (650 yr.) that occurs in an area source zone as close as 80 km to the site. This source model is based on an end-member model developed from paleoseismic data recovered along the Georgia, North and South Carolina coasts (Obermeir et al. 1990; Amick et al. 1990). The National Map characteristic earthquake uses a best estimate of the 1886 earthquake, however, the return period is based on the highest recurrence computed from the average of the last four episodes of observed liquefaction. According to Amick et al., the minimum earthquake magnitude that could be associated with a given episode of liquefaction is about Mw 6 or lower. In the absence of any observable Quaternary tectonic deformation in the southeastern U.S., repeated large displacements expected from a Mw 7 earthquake (estimated to be 4-8 m), seem excessive for a best estimate or mean model. The LLNL and EPRI hazard models contain a range of earthquake recurrence rates, and to a degree the National Map model is contained as a subset. However, it is expected that the National Map characteristic earthquake model is considerably more conservative than the mean EPRI and LLNL probabilistic hazard models. We believe that the USGS characteristic earthquake model is considerably more conservative than the mean hazard model that would be derived from contemporary expert opinion on the Charleston source. Specifically, questions that should be addressed for the National Map, or incorporated as alternate models are:

- Should a mean or best estimate earthquake source model have only a Poisson model of a characteristic earthquake for the Charleston zone?
- Should the best estimate Charleston seismic zone have a western extent that runs over 100 km inland?

- Should the return period based on the paleoseismic data use only the last four episodes resulting in the shortest possible average period?
- Should the characteristic earthquake magnitude be based on the best estimate of the 1886 Charleston earthquake magnitude (Mw 7.3) when the paleoseismic data may be explained by the occurrence of Mw 6 earthquakes (Dave Amick, personal communication) and there is no indication of high deformation rates in the SEUS?
- How is a maximum magnitude of Mw 7.5 justified for seismic zones other than Charleston in the SEUS?

USGS Soil Surface Hazard and UHS

The methodology to compute soil surface hazard from USGS hard-rock hazard is identical to that used to develop site-specific hazard from the LLNL and EPRI hard-rock PSHAs (WSRC, 1998). The computed USGS soil hazard indicates significant non-linearity at annual exceedences of 10^{-4} or greater. At annual exceedences of 10^{-5} or less, the reliability of the hazard is significantly reduced because of the limitations on the equivalent linear model used to derive the site amplification functions.

Figure 9a illustrates the individual USGS, LLNL, and EPRI soil surface UHS using the criterion of 2/3 of 2500-year return period. The USGS soil UHS exceed both LLNL and EPRI UHS at 1 and 10-Hz. The average EPRI+LLNL UHS is compared to the average EPRI+LLNL+USGS UHS in Figure 9b. The USGS UHS exceed the EPRI and LLNL average by significant margins: 28% at 10-Hz, 12% at 5-Hz, 18% at 2.5 Hz and 60% at 1-Hz. At 1-Hz, the average EPRI+LLNL+USGS spectral value exceeds the average EPRI+LLNL spectral value by about 35%.

Comparison of NEHRP and USGS soil UHS for the SRS

There are significant differences between the NEHRP-97 spectrum prescribed for SRS soil conditions, and the USGS soil UHS derived using the same criteria (return period) (Figure 8). In the range of 1-10 Hz, the NEHRP-97 spectrum is about 70% greater than the USGS soil UHS. The National Map 1-Hz bedrock spectral acceleration is higher by about a factor of two as compared to the average of EPRI/LLNL. Atkinson and Boore (1998) have shown that the 1-Hz single corner attenuation model is biased-high as compared to two corner attenuation models.

The National Map expresses the probability of exceedence of ground motions for a "soft-rock" reference site condition to be consistent with the western U.S. hazard evaluation. That site condition is the boundary between NEHRP-97 classes B and C. This B-C Boundary is defined to have an average shear-wave speed of 2,500 ft/sec (760 m/sec) in the upper 30 m of the profile. At the SRS, directly measured shear-wave speeds in shallow bedrock range from about 8,000 to 11,000 ft/sec (2.4-3.3 km/sec), a "hard-rock" site condition.

In the development of the National Map used in NEHRP-97, two attenuation models were used. One was an internal USGS BLWN model that employed a "soft-rock" velocity profile. The other attenuation model was a published hard-rock attenuation model (Toro et al., 1993) with a correction applied for soft-rock site conditions. The soft-rock/hard-rock factors applied were 1.52, 1.76, 1.72, and 1.34 for PGA, 5-, 3.3, and 1-Hz response spectral values respectively (Frankel, et al., 1996). These factors were derived from the comparisons of the results of the internal model with and without the "soft-rock" velocity gradient. Note that the USGS96 model discussed above is the same internal model with a hard-rock profile that also contains a velocity gradient with additional site amplification factors. Kimball (1998) has indicated that the soft-rock to hard-rock amplification factors applied by the National Map are inconsistent with those assumed by NEHRP. This inconsistency would also increase the NEHRP design as compared to the site-specific assessment.

~~From Figure 8, it appears that the~~ site-specific corrections account for the difference between the NEHRP-97 spectrum and the USGS soil UHS. Note that the the NEHRP-97 spectrum appears conservative at the five spectral values, at long periods the NEHRP-97 spectrum could be unconservative if the response of a deep soil column were not properly taken into account.

To better illustrate the long-period problem with the NEHRP-97 spectral shape, we fit a site-specific spectral shape from a deterministic earthquake to the long-period portion of the USGS UHS (Figure 10). The most likely earthquake controlling the long-period portion of the USGS spectrum is represented by the Mw 7.5 bin at 150 km, based on the USGS 1-Hz magnitude disaggregation (Figures 5a and 5b). A Charleston 50th percentile spectrum (WSRC, 1997) derived assuming an Mw 7.3 at 150 km is scaled to the 1-2.5 Hz spectral average of the USGS UHS (scale factor of 1.24). As shown in Figure 10, the fundamental mode of the scaled site-specific spectrum falls well outside the NEHRP-97 spectrum. Clearly, the NEHRP-97 spectral shape for a deep soil site such as the SRS does not have adequate breadth. For the SRS, the large differences in the NEHRP-97 spectrum and the USGS soil UHS are a result of an inappropriate NEHRP-97 site response correction.

Comparison of USGS Soil UHS and PC1 Design Spectrum for the SRS

A detailed comparison of the design spectrum inferred from the USGS soil UHS as compared to the *PC1 design* spectrum is beyond the scope of this report. In order to make a detailed comparison, appropriate site-specific spectral shapes would be fit to the 1-2 and 5-10 Hz UHS and smooth enveloping curves would be drawn. A design basis spectrum based on the combined USGS, EPRI and LLNL soil UHS, with an appropriate enveloping shape, would be greater than the design spectrum using the combined EPRI and LLNL soil UHS.

NEHRP-97 Guidelines

The computation of USGS soil hazard from a hard-rock hazard disaggregation is illustrative of the methodology to develop a site-specific PSHA from a more general purpose hazard evaluation like the National Map. The site-specific PSHA is consistent with the earthquake source zones and recurrence rates assumed in developing the National Map. This evaluation, starting from a hard-rock disaggregation, is in principle, a suitable approach to make a site-specific assessment for any rock or soil site. If the National Map and the NEHRP-97 guidelines provide a hard-rock PSHA (with magnitude and distance disaggregation), a site-specific design spectrum could be easily developed following the necessary site characterization. Hard-rock hazard disaggregations add only a limited amount of additional tabular data that an agency can easily maintain, or if an online system is employed, the hazard disaggregation can be computed at the users request.

For the SRS, large differences between the NEHRP-97 spectrum and the USGS soil UHS are too great to be dismissed as a site-specific variation from the NEHRP-97 site classification criteria. NEHRP-97 criteria allow a 20% reduction in the design spectrum to account for possible reduction to accommodate a site-specific hazard assessment. One interpretation of the adjustment factor is that site-specific variability should be more or less within 20% of the NEHRP-97 spectrum. This investigation shows that site-specific effects can be much larger than the allowed ± 20%.

SUMMARY OF FINDINGS

Regarding the application of NEHRP-97 to the SRS the following statements are warranted:

- The National Map hazard is excessively conservative for a site such as the SRS;
- For frequencies greater than 1-Hz, the NEHRP-97 spectrum is overly conservative for the SRS and
- For deep-soil sites such as the SRS, the shape of the NEHRP-97 spectrum is unconservative at long periods.

Regarding development of SRS site-specific hazard from National Map input, the following statements are warranted:

- The hard-rock PSHA is consistent with the earthquake source definition and recurrence rates contained in the National Map but results in different hazard because of differences in the assumed bedrock conditions;
- The USGS hard-rock hazard is close to LLNL at 2.5 and 5-Hz, but is greater than LLNL and EPRI for 1, 10-Hz and PGA;
- The USGS hard-rock hazard is generally more conservative than either EPRI or LLNL hazard because of the highly energetic source assumed for the Charleston zone.
- The computed USGS soil surface hazard is less than the NEHRP spectrum recommended for shallow SRS soils;
- The computed USGS soil surface hazard is greater than the SRS design basis at 1 Hz and
- The methodology of WSRC (1998) is useful to derive site-specific soil surface hazard from hard-rock hazard disaggregation.

CONCLUSIONS

The National Map and NEHRP-97 recommended seismic provisions are a significant improvement and accomplishment in building code development, however, for a southeastern U.S. deep soil site, such as the SRS, the National Map ground motion attenuation adjustments and site response are not appropriate. Serious bias in the National Map ground motion hazard exists because of the inappropriate bedrock and NEHRP-97 spectral shape. When National Map consistent hazard curves are developed for SRS hard-rock outcrop and site-specific soil conditions the USGS soil surface hazard is generally greater than EPRI and LLNL soil hazard. The National Map hazard for the SRS is greater than EPRI and LLNL hazard because of the highly energetic source used for the Charleston special zone. Averaging the computed EPRI, LLNL and USGS soil hazard would increase the SRS design basis.

There are several conclusions based on the results of this evaluation: (1) computation of a site-specific correction to the National Map should be considered before acceptance of a building code spectrum (the cost of a site-specific assessment, using an available hard-rock PSHA and disaggregation, may be minor compared to the high cost due to potential design basis excess or underestimation); (2) availability of National Map hard-rock hazard disaggregations would be helpful for routine for site-specific hazard assessments; (3) detailed site-specific assessments may exceed the requirement that a site-specific UHS fall within 20% of the NEHRP spectrum; and (4) NEHRP spectral shape and site classification criteria may not be appropriate for deep soil sites.

FUTURE WORK

Additional work will be required to better clarify and understand the difference between EPRI, LLNL, and USGS hazard assessments including site response. There are three areas for comparison: (1) the USGS/NEHRP inferred site amplification from hard-rock to the Class D soil-site should be evaluated to compare directly to the SRS site amplification functions; (2) a comparison of 1- and 2-corner attenuation models used in all three hazard studies should be completed using the same Charleston source configuration. This will permit a direct comparison of the attenuation models and assist in the comparison of the source models; (3) PSHA sources, particularly Charleston should be compared for the SRS. This would entail selection of a small earthquake magnitude range and comparing probabilistic ground motion at SRS hard-rock for several frequencies. Based on inferences from the attenuation model study in 2, a rough comparison can be made of the Charleston source from the three studies.

The distance dependence of soil amplification functions and its impact on soil hazard should be evaluated. In general, it is possible that sites close to source zones could require site amplification functions incorporating non-vertical angles of incidence. An evaluation of the significance of this effect on site response could be easily evaluated.

ACKNOWLEDGEMENTS

Document reviews by Jeff Kimball, Brent Gutierrez, Carl Costantino and Allin Cornell significantly improved the text.

REFERENCES

Amick, D., R. Gelinas, R. Cannon, D. Moore, E. Billington, and H. Kemppinen, 1990. Paleoliquefaction features along the Atlantic Seaboard. NUREG/CR-5613 RA. Prepared for U.S. Nuclear Regulatory Commission by Ebasco Services Inc., 146 pp.

Atkinson, G.M., and D.M. Boore, 1995. New ground motion relations for eastern North America, Bull. Seis. Soc. Am., Vol. 85, 17-30.

Atkinson, G.M., and D.M. Boore, 1998. Evaluation of Models for Earthquake Source Spectra in Eastern North America, Bull. Seis. Soc. Am., Vol. 88, 917-934.

Bernreuter, D.L., 1997. Letter report from Don Bernreuter to Jeff Kimball. Lawrence Livermore National Laboratory, Fission Energy and Systems Safety Program, May 15, 1997, NTFS97-123.

Cornell, C.A., and P. Bazzurro, 1997. Efficient probabilistic hazard analysis for non-linear soil sites with uncertain properties.

Frankel, A. 1999. Letter report of calculation results to R.C. Lee, March 9, 1999.

Frankel, A., C. Mueller, T. Barnhard, D. Perkins, E.V. Leyendecker, N. Dickman, S. Hanson, and M. Hopper, 1996. National Seismic Hazard Maps, June 1996, U.S. Geol. Surv. Open-File Rept. 96-532.

Kimball, J., 1998. Supplemental Response to Issues 3, 4, and 9. Seismic Action Items for Defense Nuclear Facilities Safety Board, WSRC letter from L.A. Salomone to A.H. Hadjian, PECD-SGS-98-0124, July 6, 1998.

NEHRP, 1997. National Earthquake Hazards Reduction Program (NEHRP) Recommended Provisions. For Seismic Regulations For New Buildings And Other Structures, Building Seismic Safety Council, Part 1 Provisions (FEMA 302).

NEI, 1994. Nuclear Energy Institute, Washington, D.C., Seismic Siting Decision Process, May 24, 1994.

Obermeir, S.F., R.B. Jacobson, J.P. Smout, R.E. Weems, G.S. Gohn, J.E. Monroe, and D.S. Powars, 1990. Earthquake induced liquefaction features in the coastal setting of South Carolina and in the fluvial setting of the New Madrid Zone, U.S. Geological Survey Prof. Paper 1504.

Savy, J.B., 1996. Fission Energy and Systems Safety Program, April 24, 1996, SANT96-147JBS, letter from J.B. Savy, Deputy Associate Program Leader Natural Phenomena Hazards to Jeff Kimball, DOE.

Toro, G., N. Abrahamson, and J. Schneider, 1993. Engineering model of strong ground motions from earthquakes in the central and eastern United States, in Guidelines for determining design basis ground motions, EPRI TR-102293, J.F. Schneider, ed., Electric Power Research Institute.

Toro, G., N. Abrahamson, and J. Schneider, 1997. Model of strong ground motion in eastern and central North America: best estimates and uncertainties, Seism. Res. Lett. Vol. 68, 41-57.

WSRC, 1996. Investigations of Nonlinear Dynamic Soil Properties at the Savannah River Site, by R.C. Lee,WSRC-TR-96-0062, Rev. 0.

WSRC, 1997. SRS Seismic Response Analysis and Design Basis Guidelines, by R.C. Lee, M.E. Maryak, and M.D. McHood,WSRC-TR-97-0085, Rev. 0.

WSRC, 1998. Soil Surface Seismic Hazard and Design Basis Guidelines for Performance Category 1 & 2 SRS Facilities, by R.C. Lee,WSRC-TR-98-00263, Rev. 0.

WSRC, 1999. Letter from Maryak to Hyman of 2/2/99, Funding for USGS Hazard Study, PECD-SGS-99-0021.

TABLE 1

Comparison of SRS hard-rock hazard models at return periods of 1000, 2500 and 10000 years. "USGS96" is a single corner attenuation model and "USGS wt. Ave." is a weighted average of 1- and 2-corner attenuation models.

Ret. Period (yrs)	1-Hz Sa (g's)			
	USGS96	USGS wt. Ave.	LLNL	EPRI
1000	0.080	0.057	0.033	0.013
2500	0.13	0.10	0.062	0.024
10000	0.27	0.20	0.12	0.061

Ret. Period (yrs)	5-Hz Sa (g's)			
	USGS96	USGS wt. Ave.	LLNL	EPRI
1000	0.18	0.14	0.14	0.061
2500	0.30	0.23	0.22	0.11
10000	0.58	0.48	0.48	0.21

Ret. Period (yrs)	PGA (g's)			
	USGS96	USGS wt. Ave.	LLNL	EPRI
1000	0.092	0.081	0.071	0.048
2500	0.17	0.15	0.12	0.078
10000	0.31	0.30	0.22	0.15

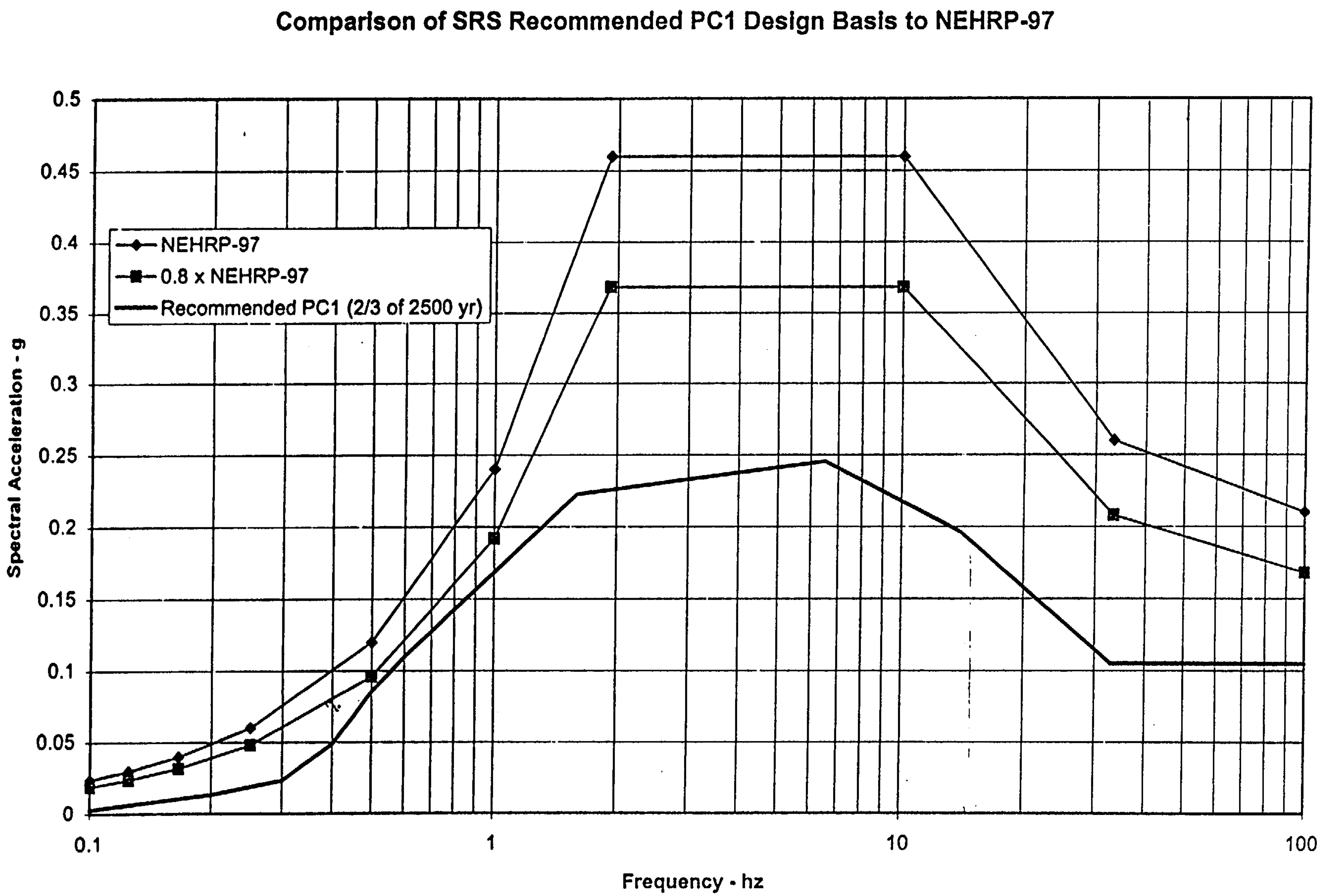

Figure 1 – Comparison of SRS PC1 spectrum to NEHRP-97 spectrum and 80% of NEHRP-97 spectrum for SRS (WSRC, 1998). The PC1 spectrum was derived using EPRI and LLNL hard rock hazard that was continued to the soil surface, averaged, and enveloped with a site-specific spectral shape. The NEHRP-97 spectrum was derived from soft-rock category spectral values taken from the National Map and site soil class "D" scaling parameters. Both spectra are derived using the same hazard criteria (2/3 of the 2500 year return period).

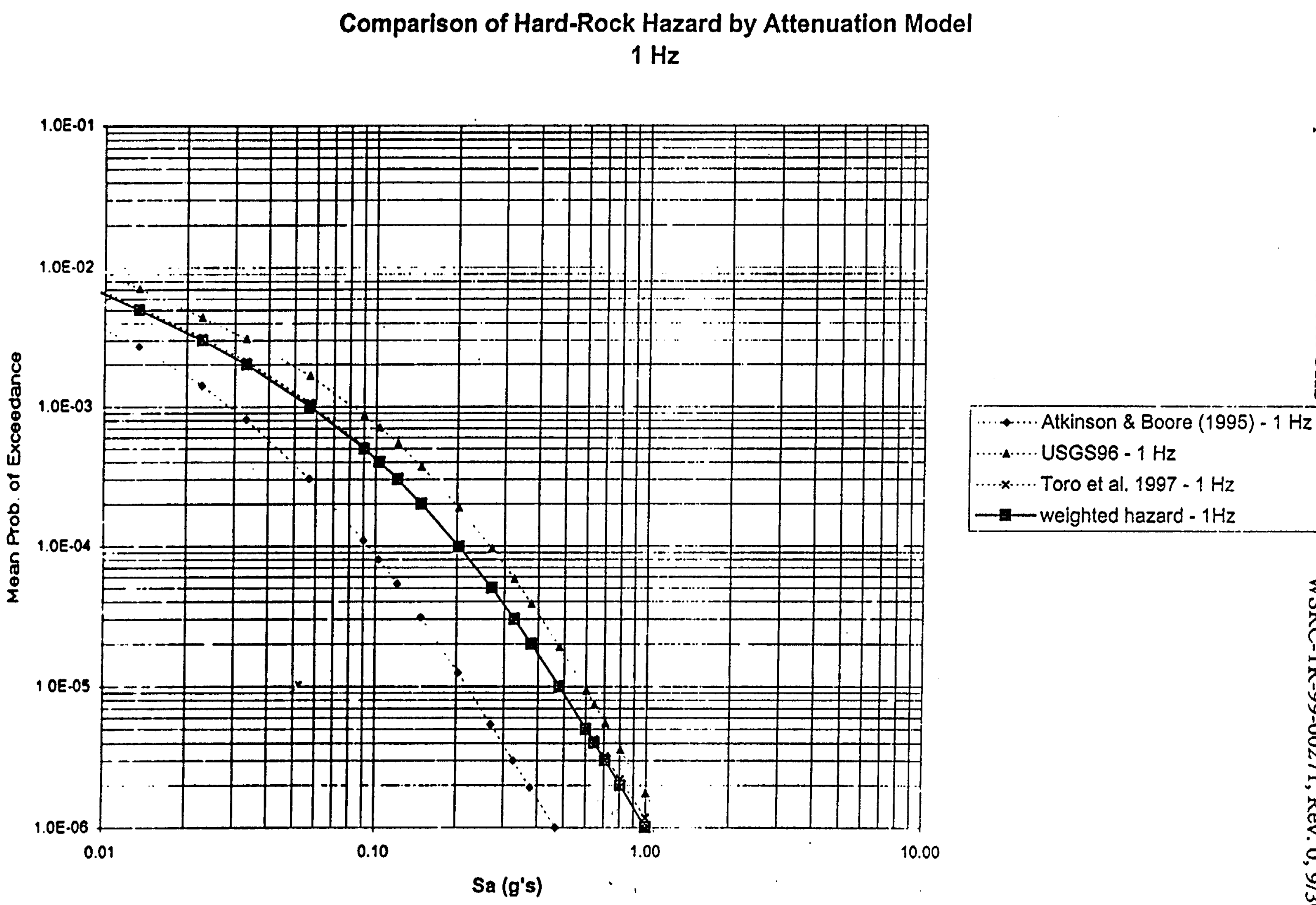

Figure 2a – USGS bedrock 1-Hz hazard computed using National Map source model assumptions and hard-rock site conditions for central SRS. Hard-rock attenuation models used are Atkinson and Boore (1995), USGS96 and Toro et al., 1997. Also shown (solid line) is the weighted hazard model.

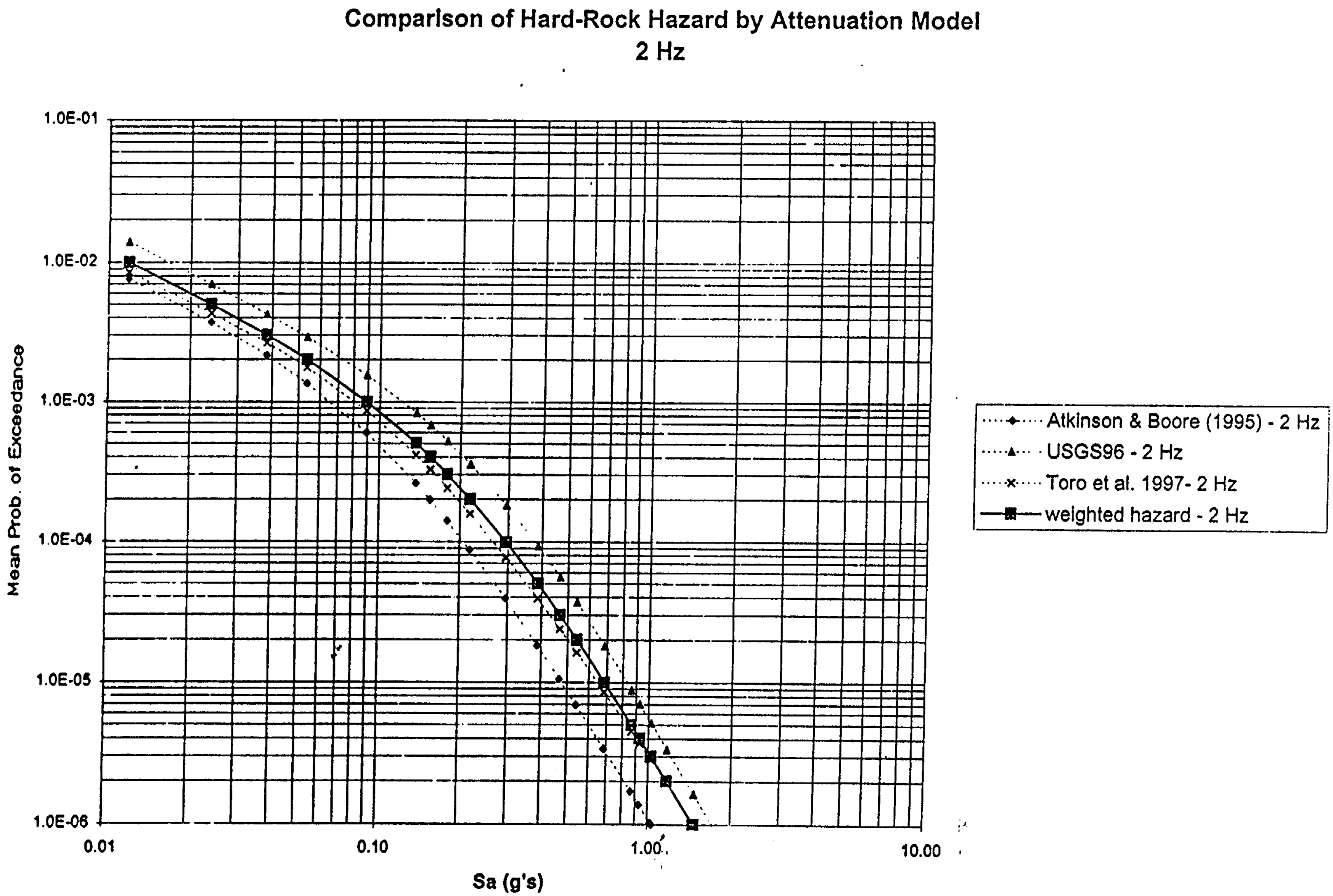

Figure 2b – USGS bedrock 2-Hz hazard computed using National Map source model assumptions and hard-rock site conditions for central SRS. Hard-rock attenuation models used are Atkinson and Boore (1995), USGS96 and Toro et al., 1997. Also shown (solid line) is the weighted hazard model.

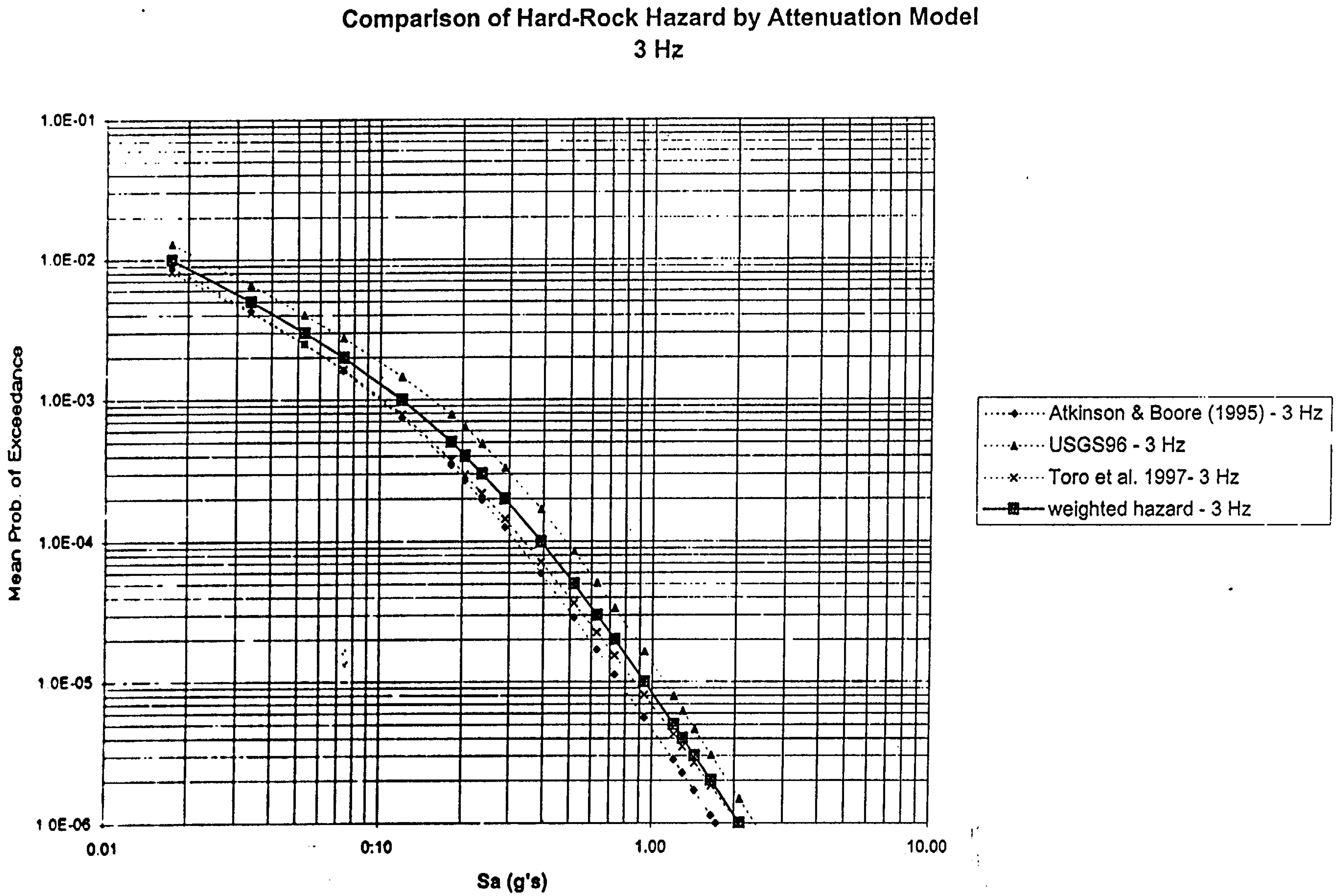

Figure 2c – USGS bedrock 3-Hz hazard computed using National Map source model assumptions and hard-rock site conditions for central SRS. Hard-rock attenuation models used are Atkinson and Boore (1995), USGS96 and Toro et al., 1997. Also shown (solid line) is the weighted hazard model.

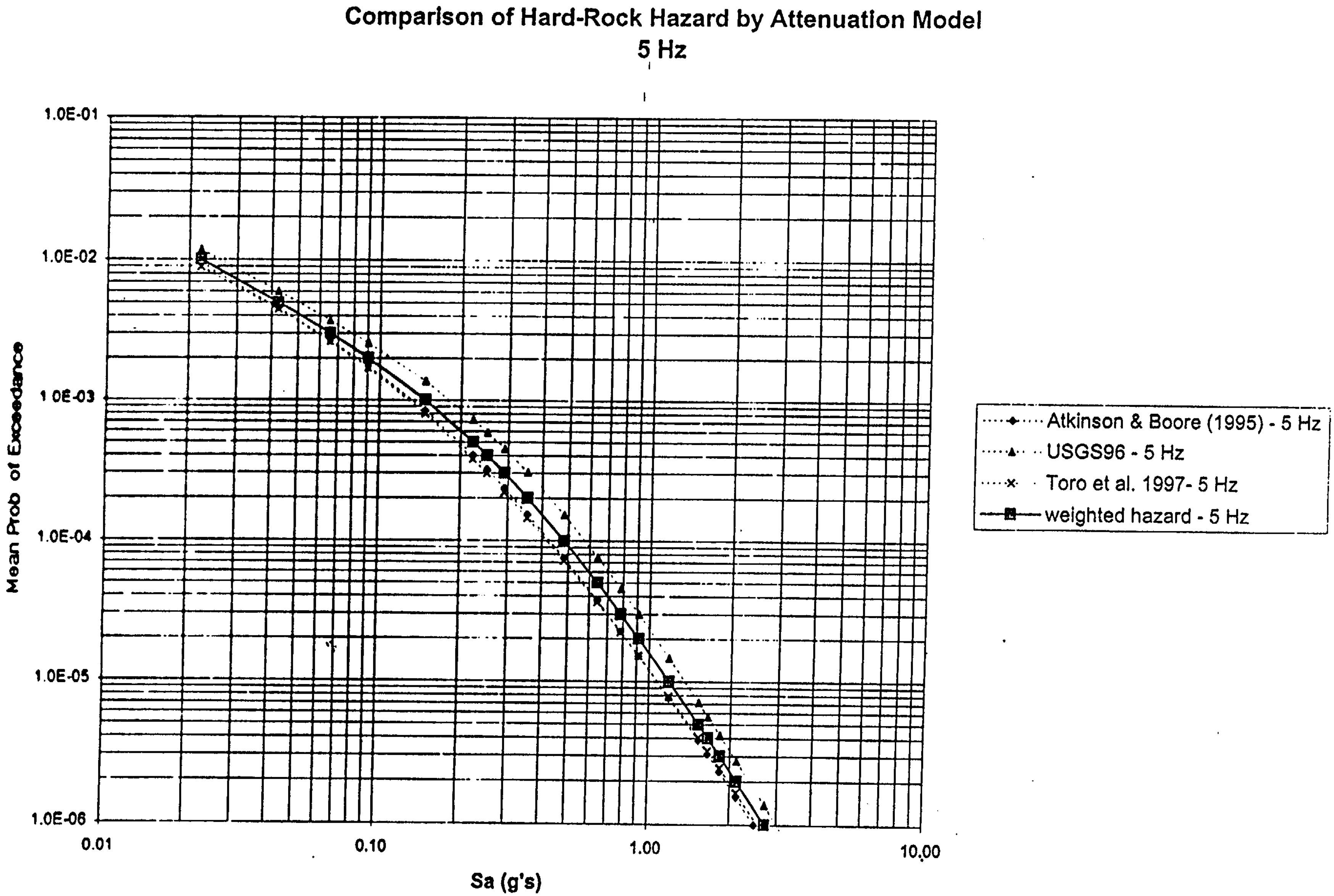

Figure 2d – USGS bedrock 5-Hz hazard computed using National Map source model assumptions and hard-rock site conditions for central SRS. Hard-rock attenuation models used are Atkinson and Boore (1995), USGS96 and Toro et al., 1997. Also shown (solid line) is the weighted hazard model.

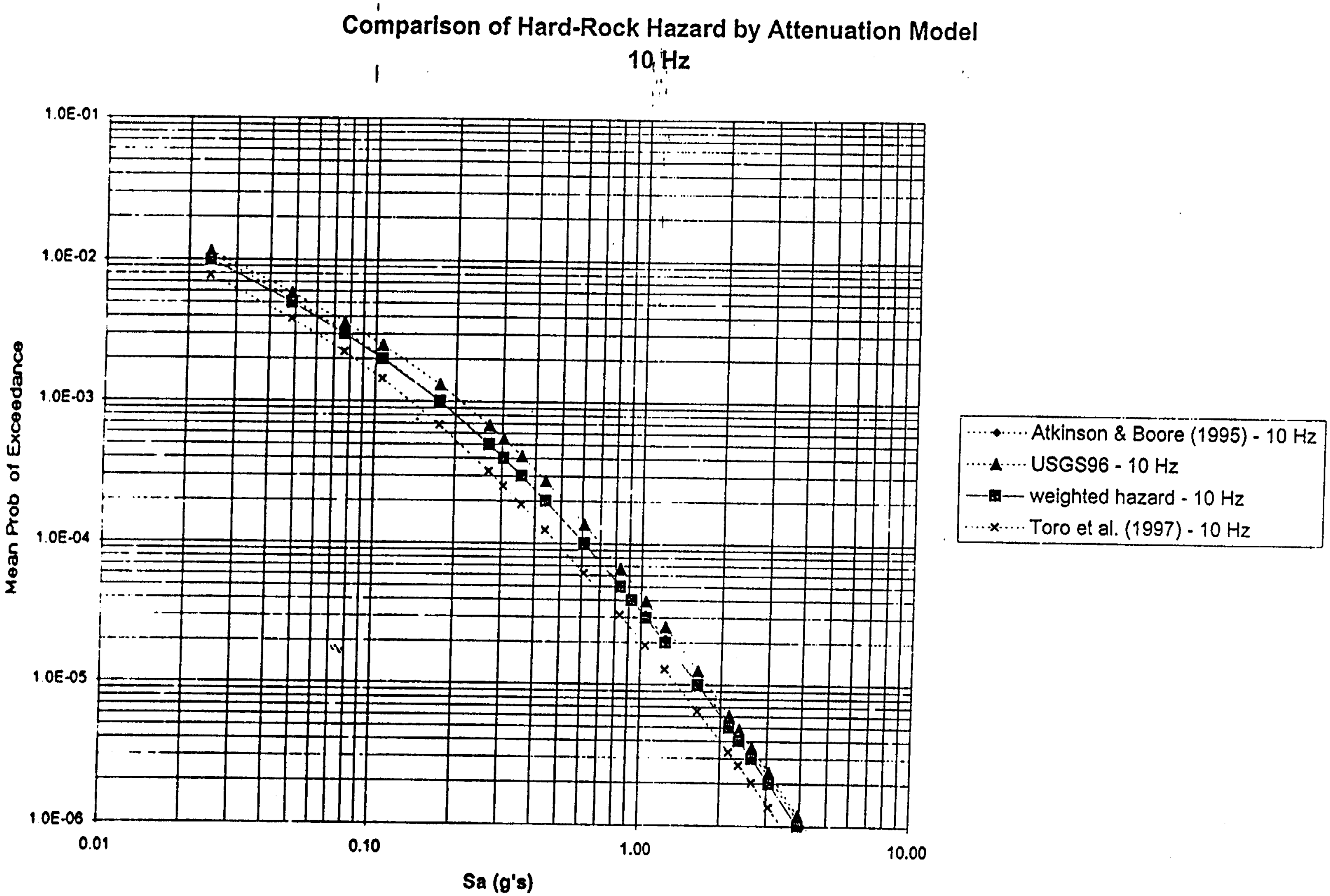

Figure 2e – USGS bedrock 10-Hz hazard computed using National Map source model assumptions and hard-rock site conditions for central SRS. Hard-rock attenuation models used are Atkinson and Boore (1995), USGS96 and Toro et al., 1997. Also shown (solid line) is the weighted hazard model.

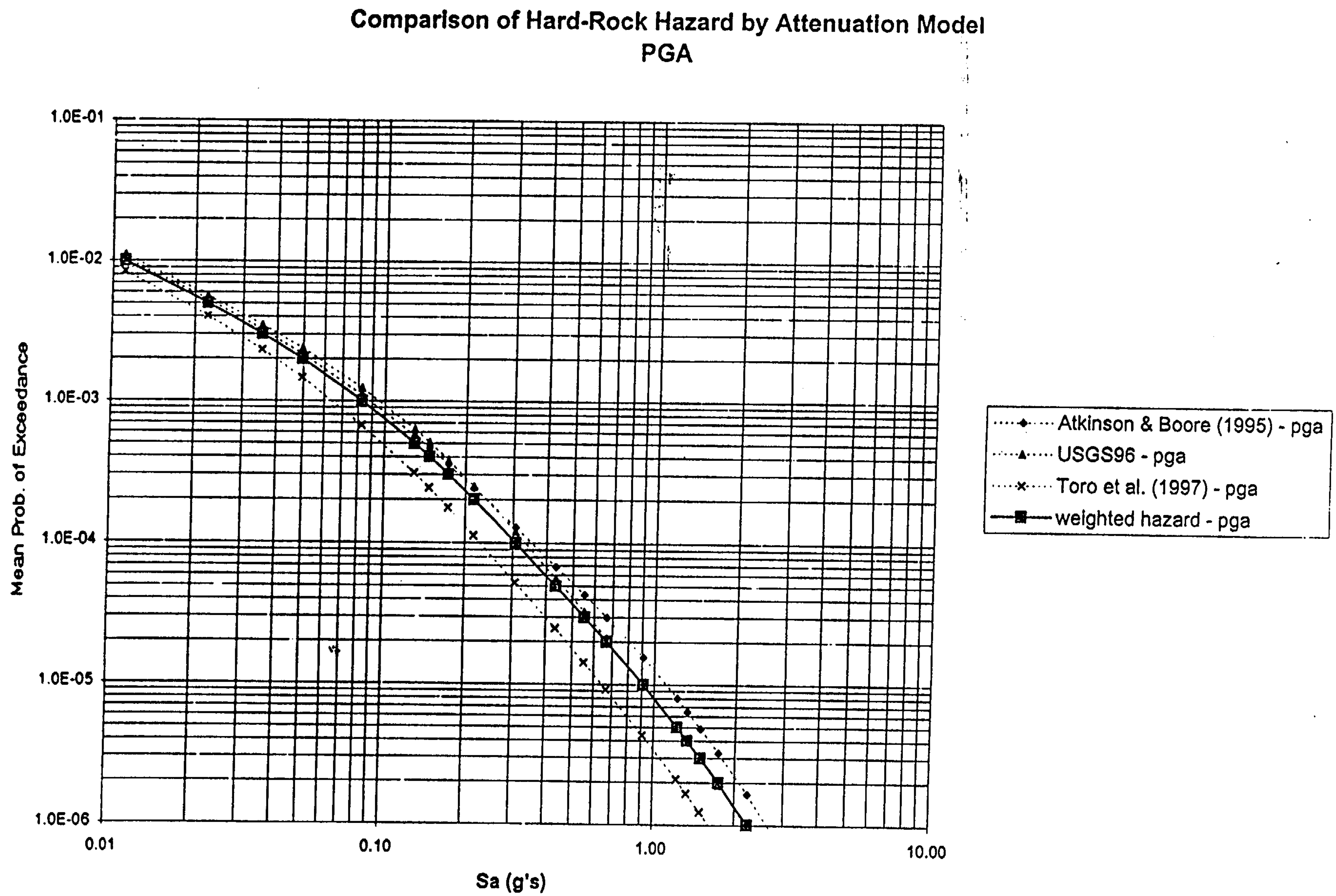

Figure 2f – USGS bedrock PGA hazard computed using National Map source model assumptions and hard-rock site conditions for central SRS. Hard-rock attenuation models used are Atkinson and Boore (1995), USGS96 and Toro et al., 1997. Also shown (solid line) is the weighted hazard model.

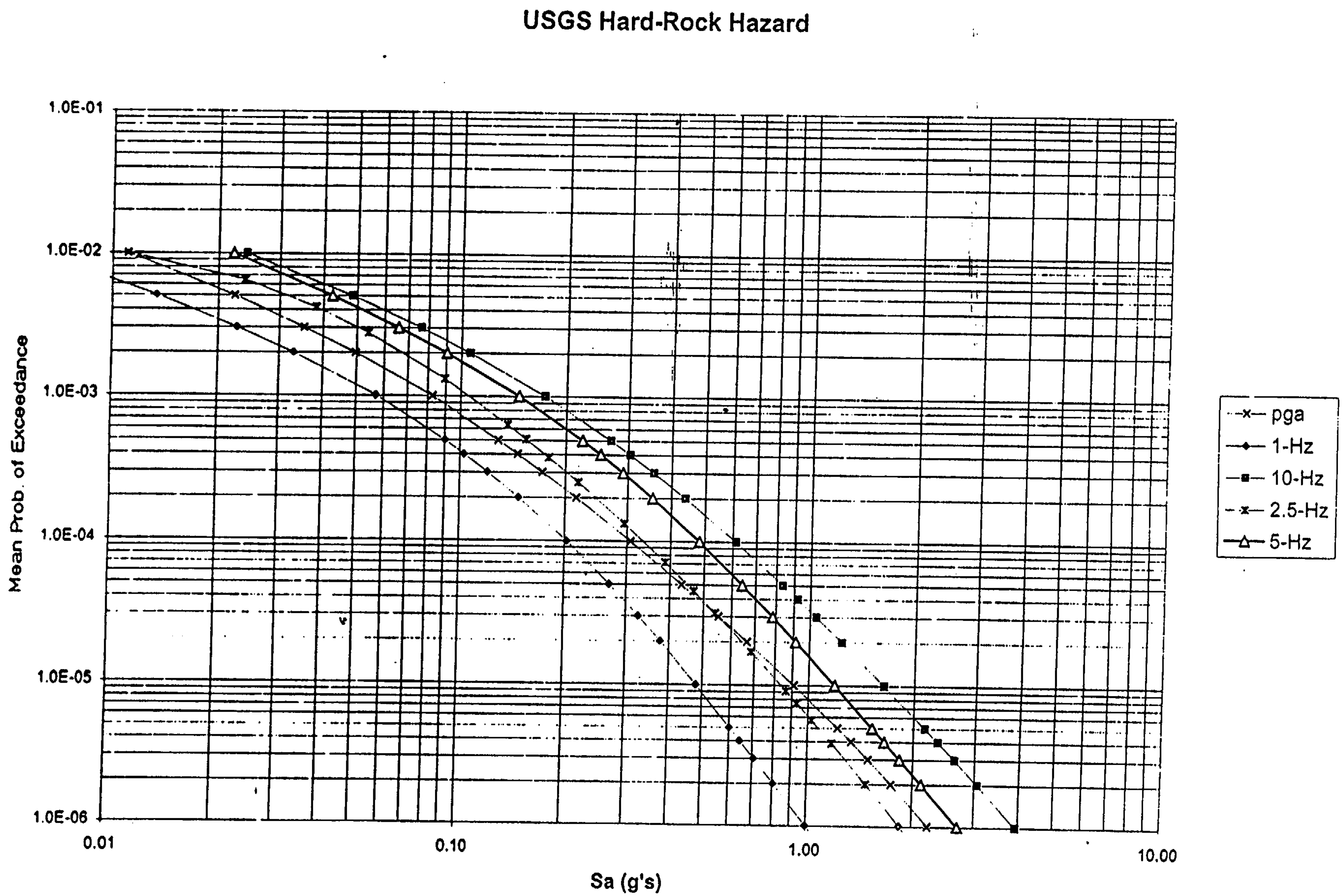

Figure 3 – Composite USGS bedrock hazard computed using National Map source model assumptions and hard-rock site conditions for central SRS.

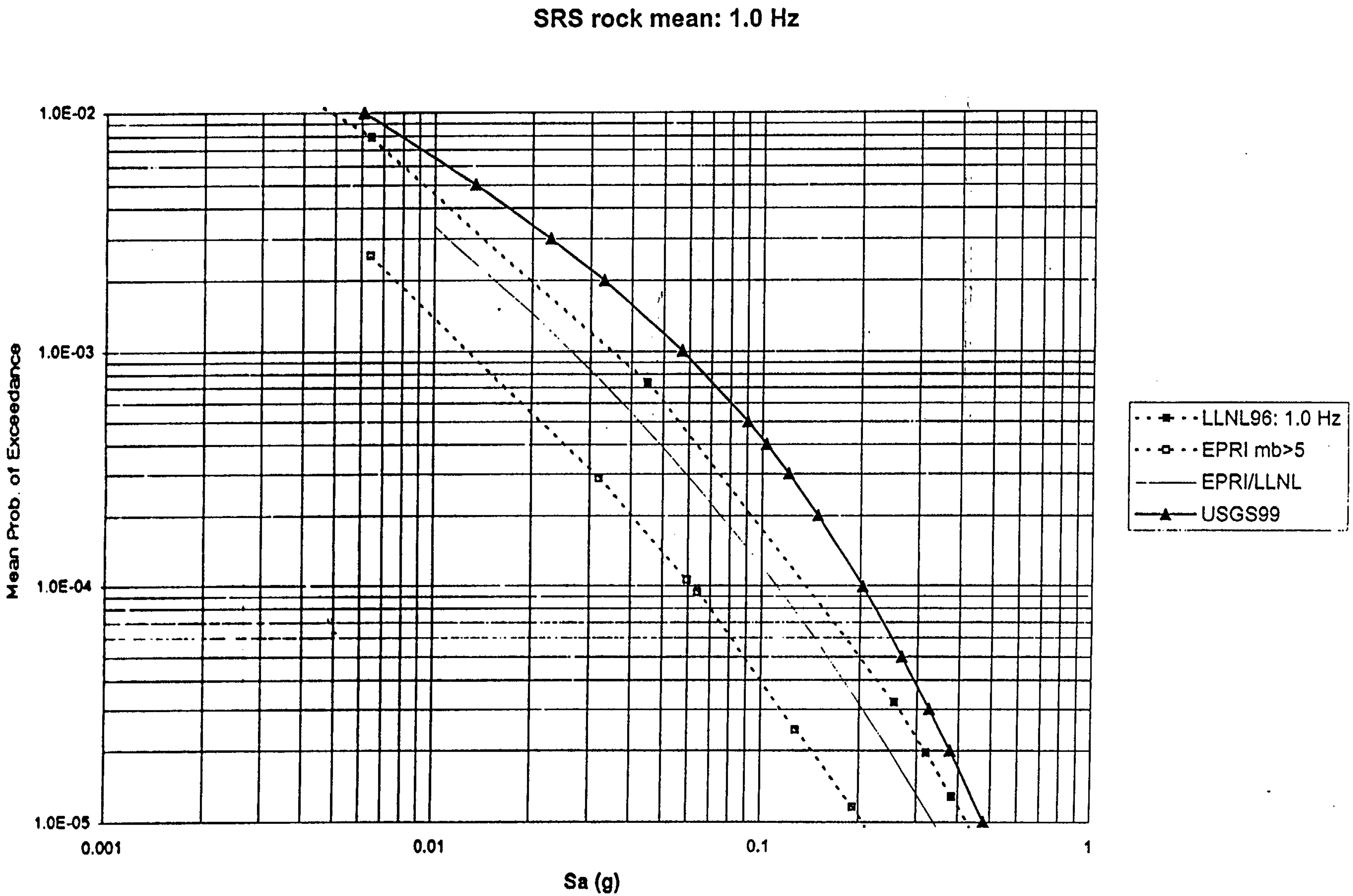

Figure 4a – Comparison of USGS bedrock 1-Hz hazard to EPRI and LLNL bedrock hazard for a central SRS site and hard-rock site conditions.

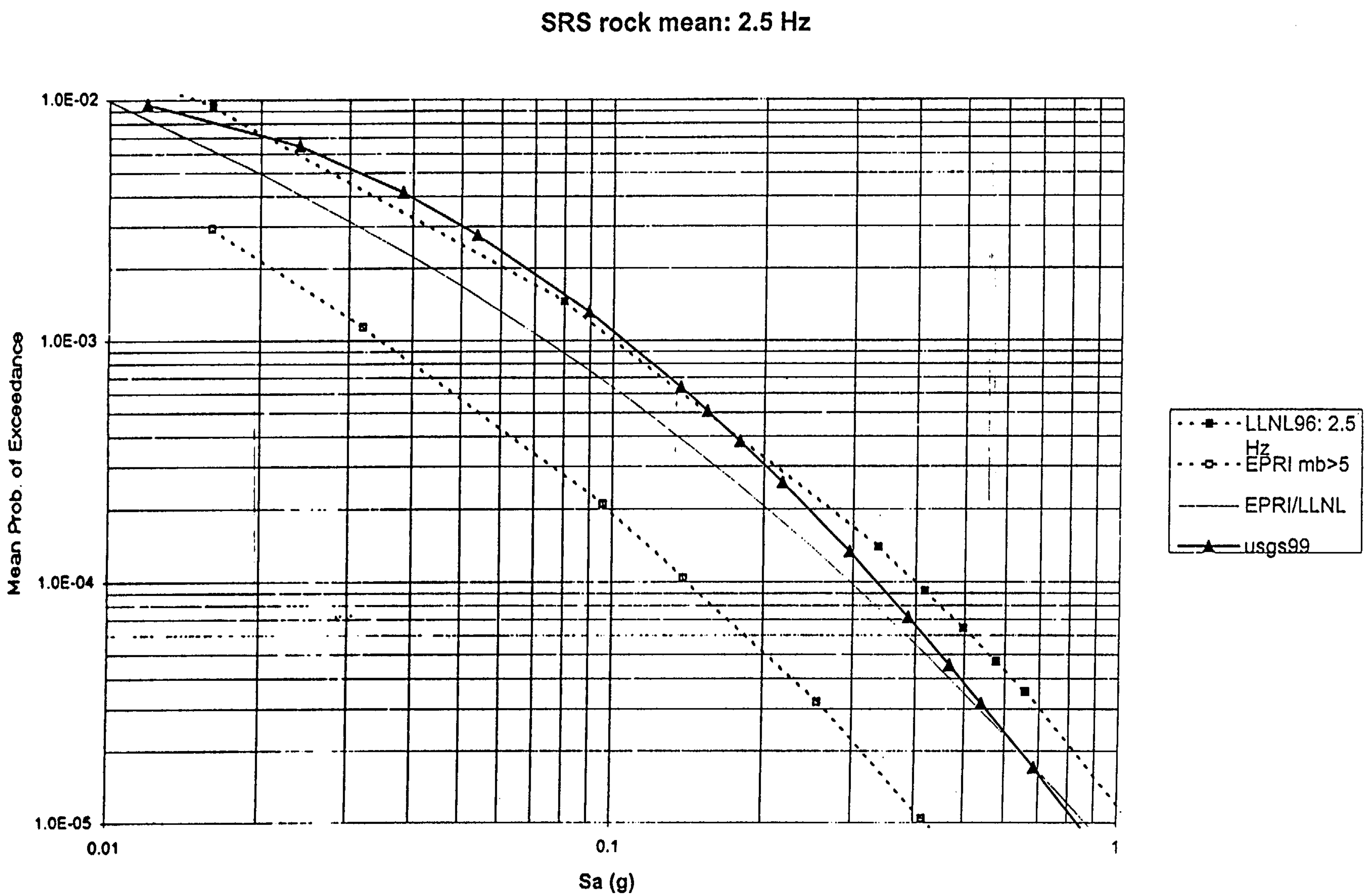

Figure 4b – Comparison of USGS bedrock 2.5-Hz hazard to EPRI and LLNL bedrock hazard for a central SRS site and hard-rock site conditions.

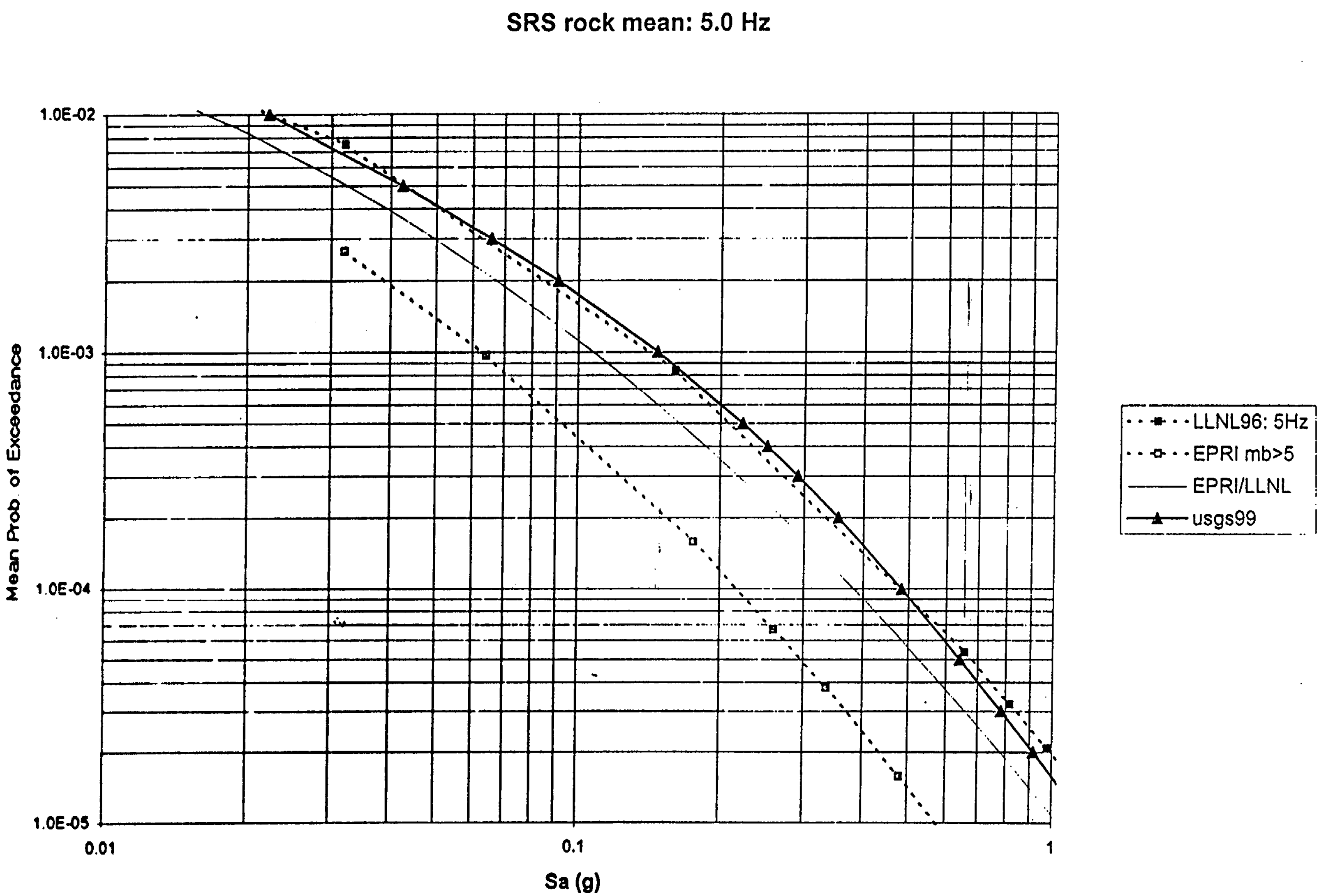

Figure 4c – Comparison of USGS bedrock 5-Hz hazard to EPRI and LLNL bedrock hazard for a central SRS site and hard-rock site conditions.

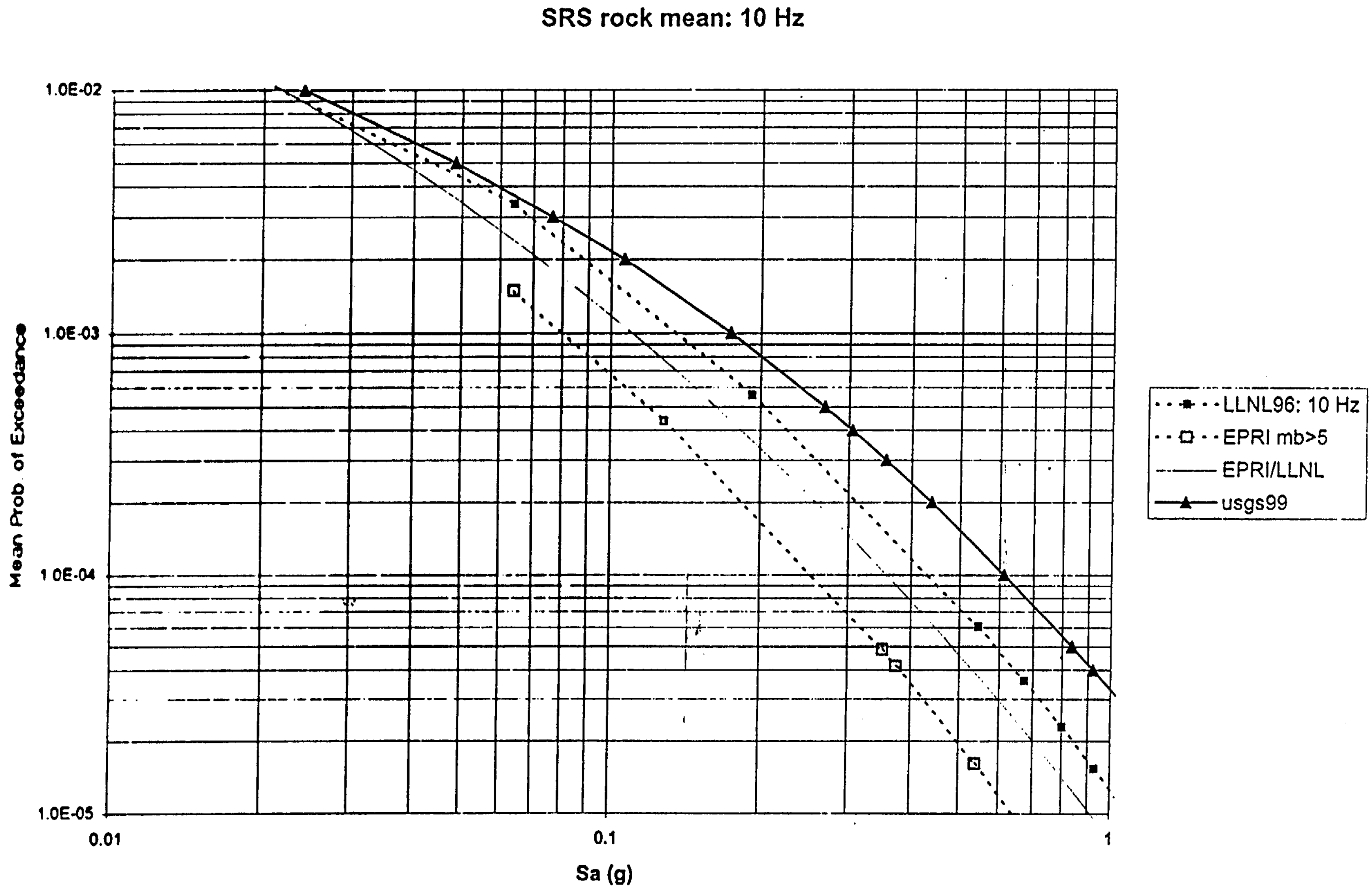

Figure 4d – Comparison of USGS bedrock 10-Hz hazard to EPRI and LLNL bedrock hazard for a central SRS site and hard-rock site conditions.

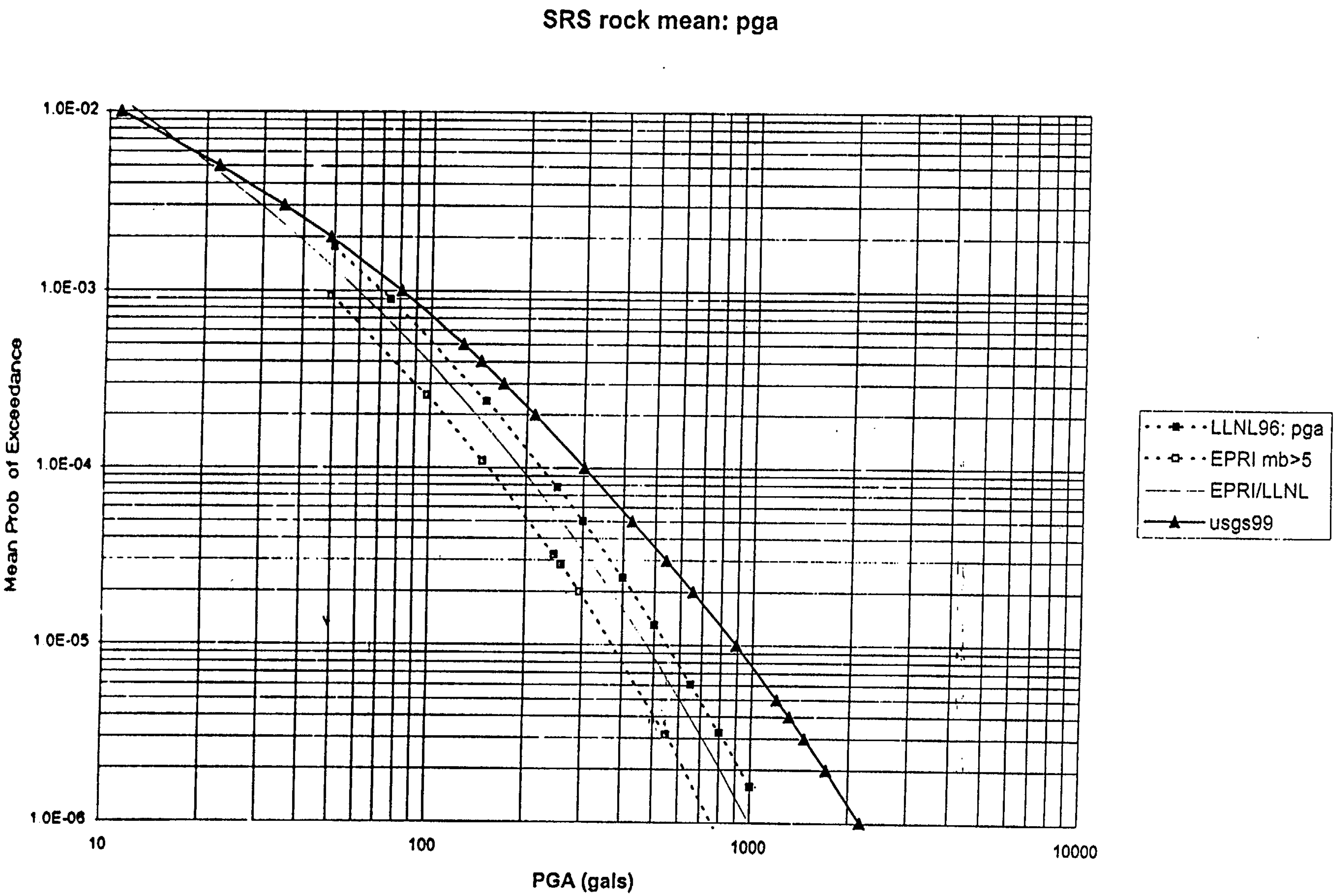

Figure 4e – Comparison of USGS bedrock PGA hazard to EPRI and LLNL bedrock hazard for a central SRS site and hard-rock site conditions.

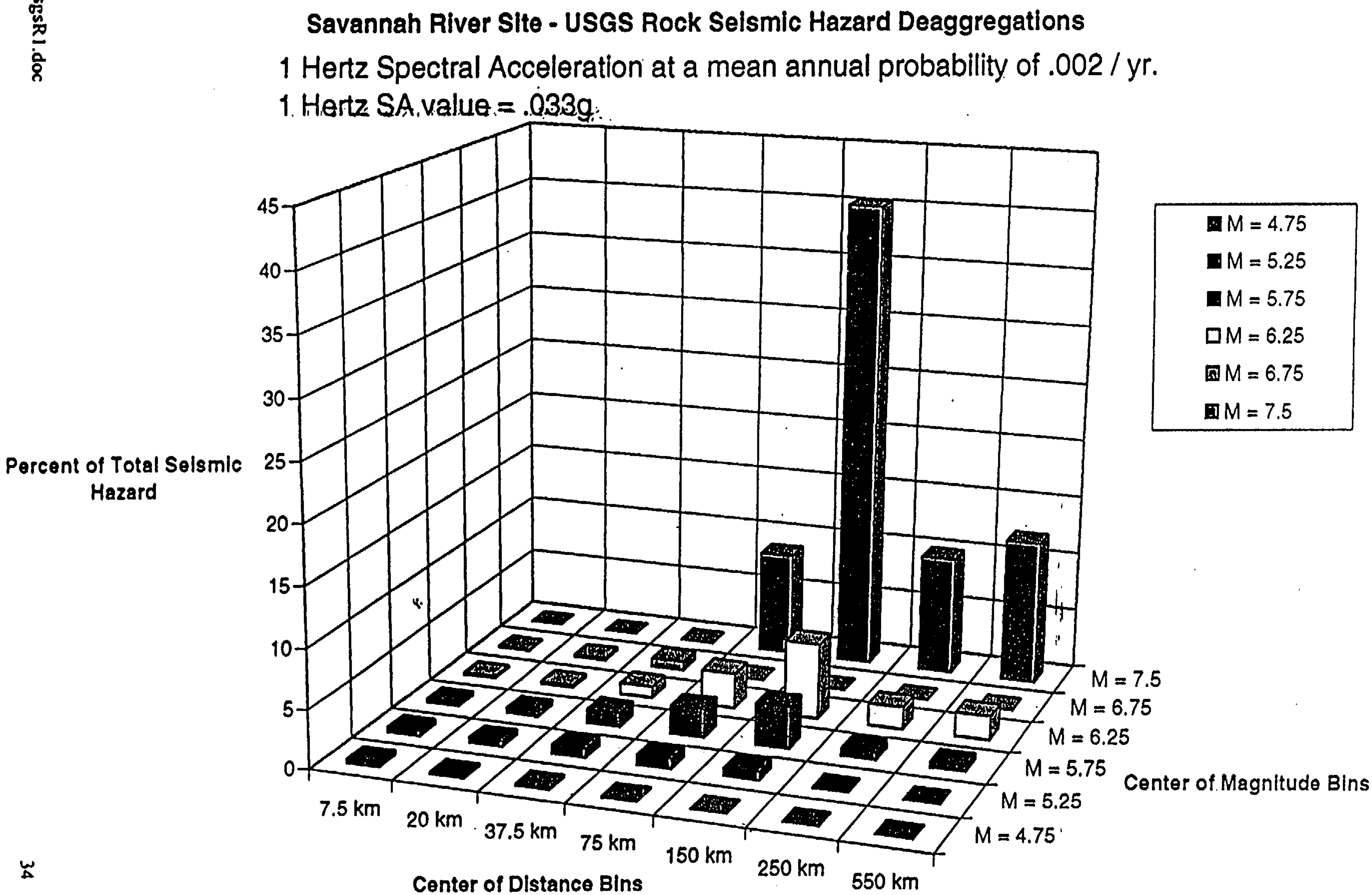

Figure 5a – USGS bedrock 1-Hz hazard disaggregation for SRS with mean annual probability of exceedence of $2x10^{-3}$.

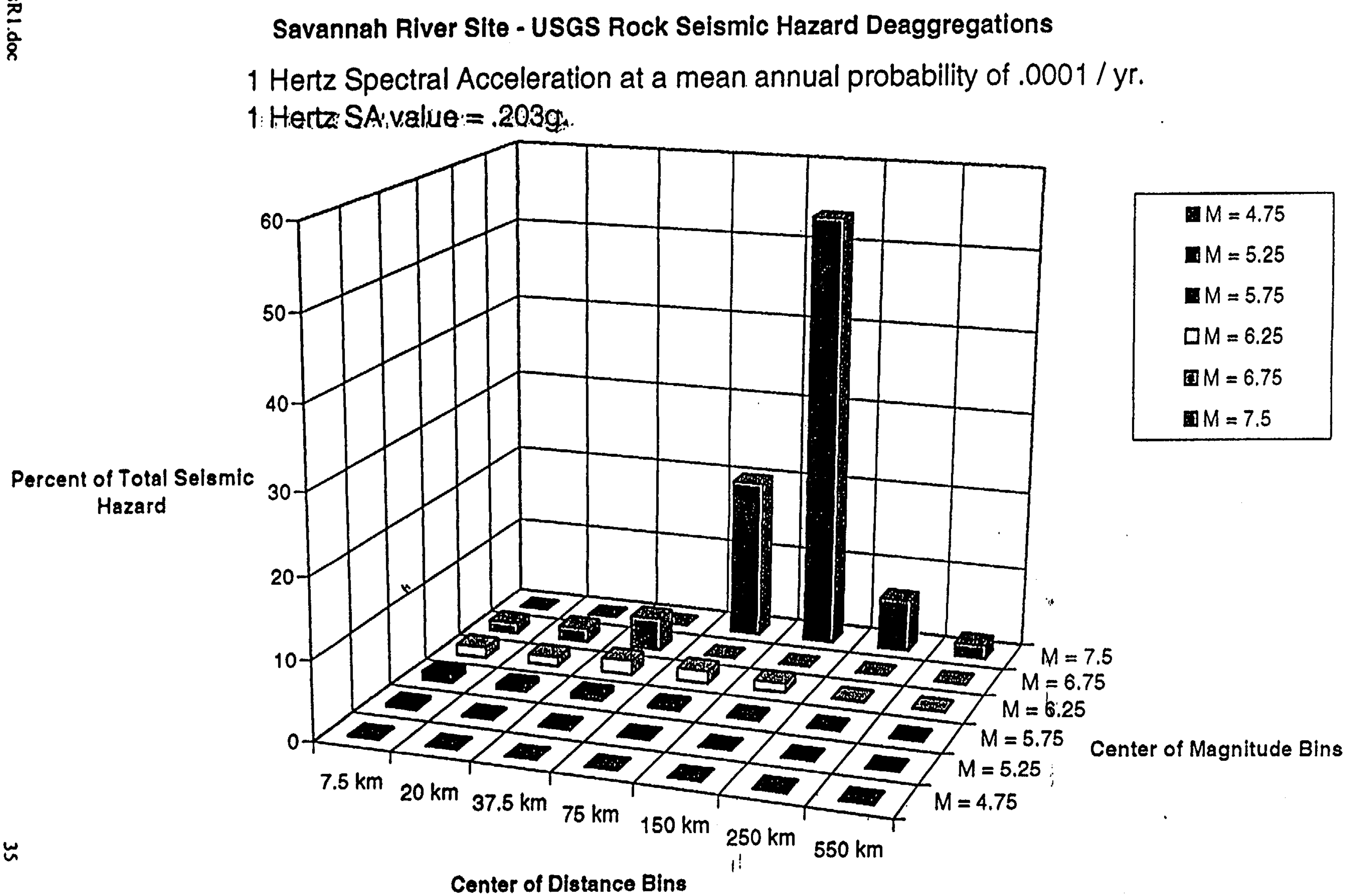

Figure 5b – USGS bedrock 1-Hz hazard disaggregation for SRS with mean annual probability of exceedence of $1x10^{-4}$.

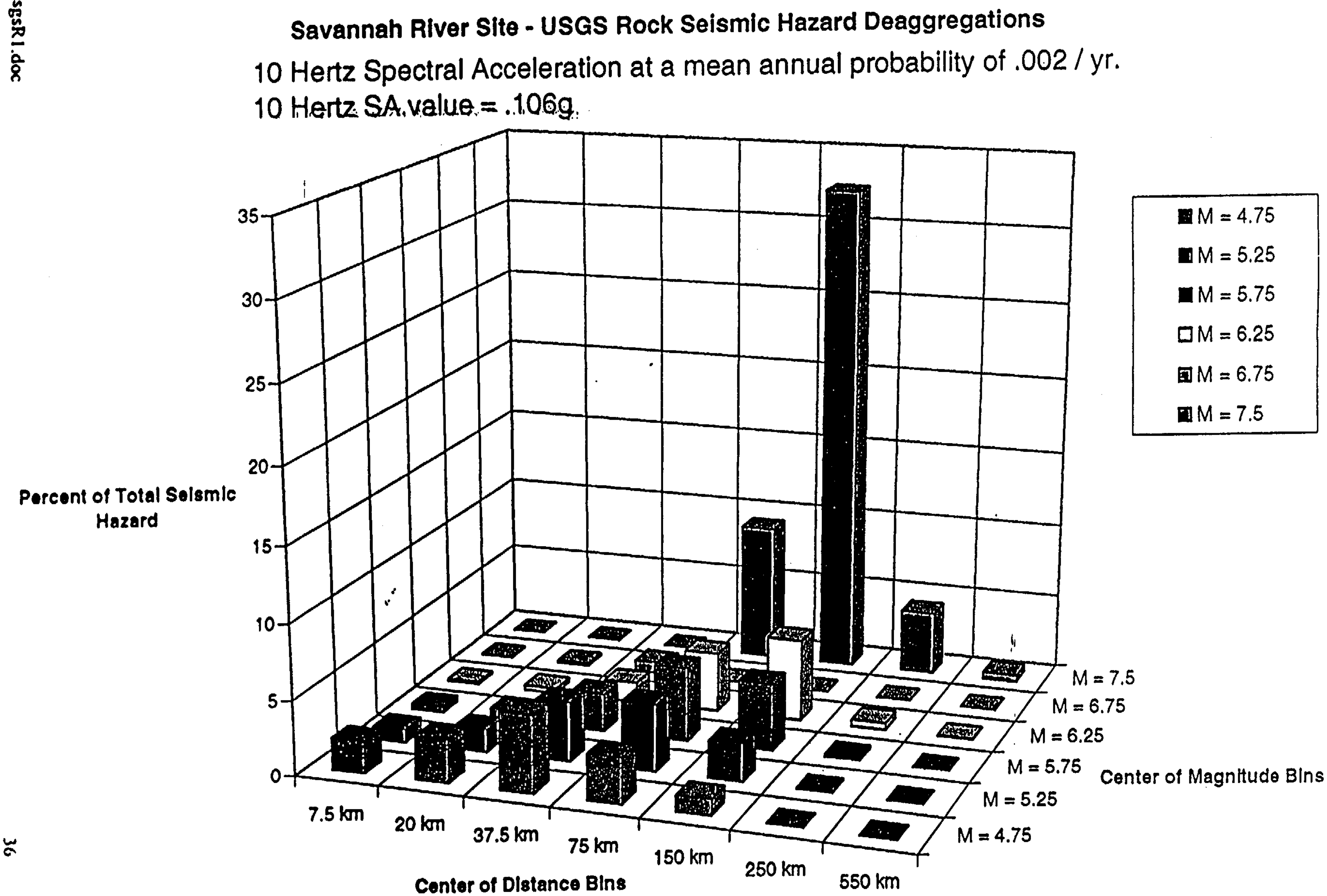

Figure 5c – USGS bedrock 10-Hz hazard disaggregation for SRS with mean annual probability of exceedence of $2x10^{-3}$.

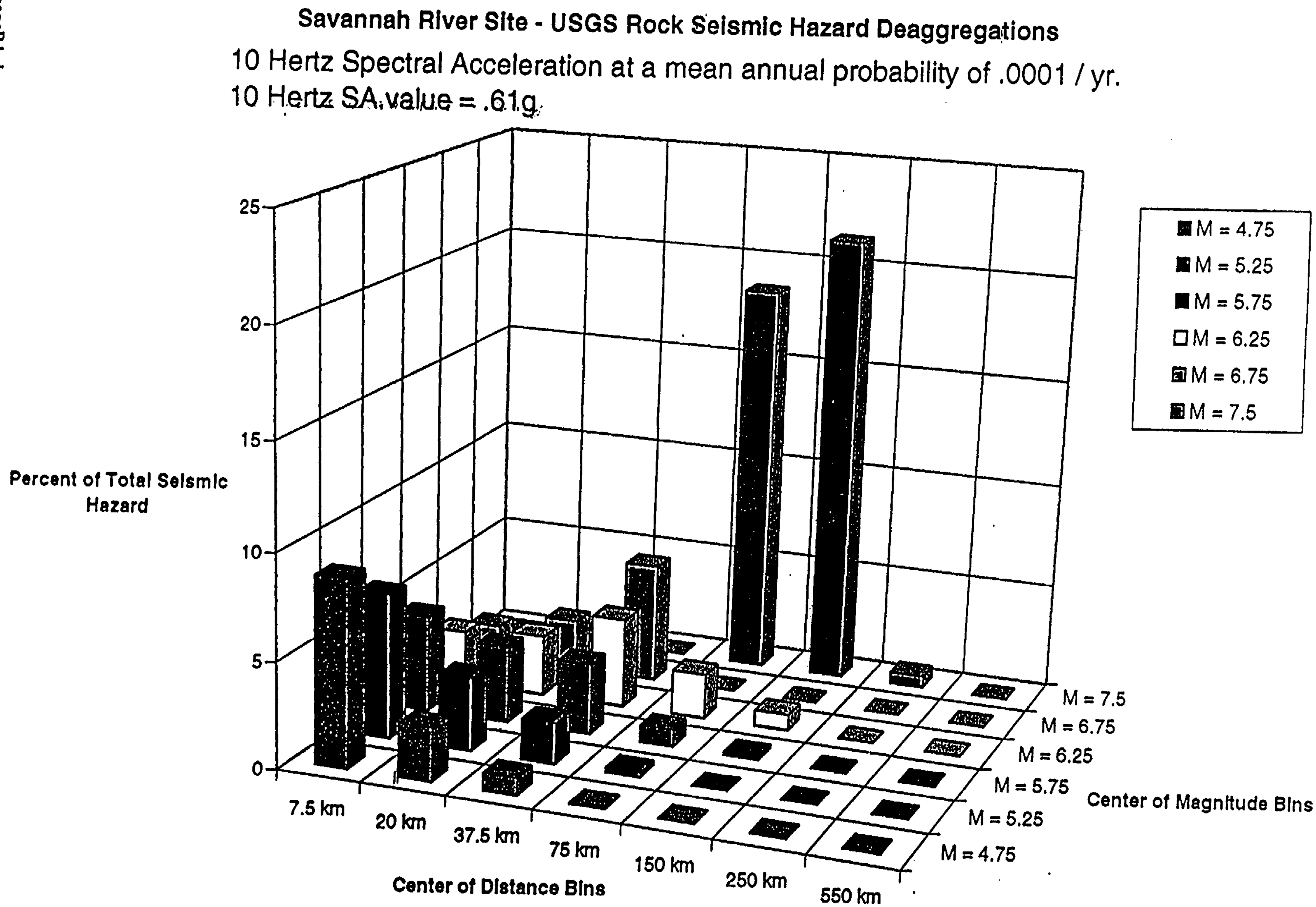

Figure 5d – USGS bedrock 10-Hz hazard disaggregation for SRS with mean annual probability of exceedence of 1×10^{-4}.

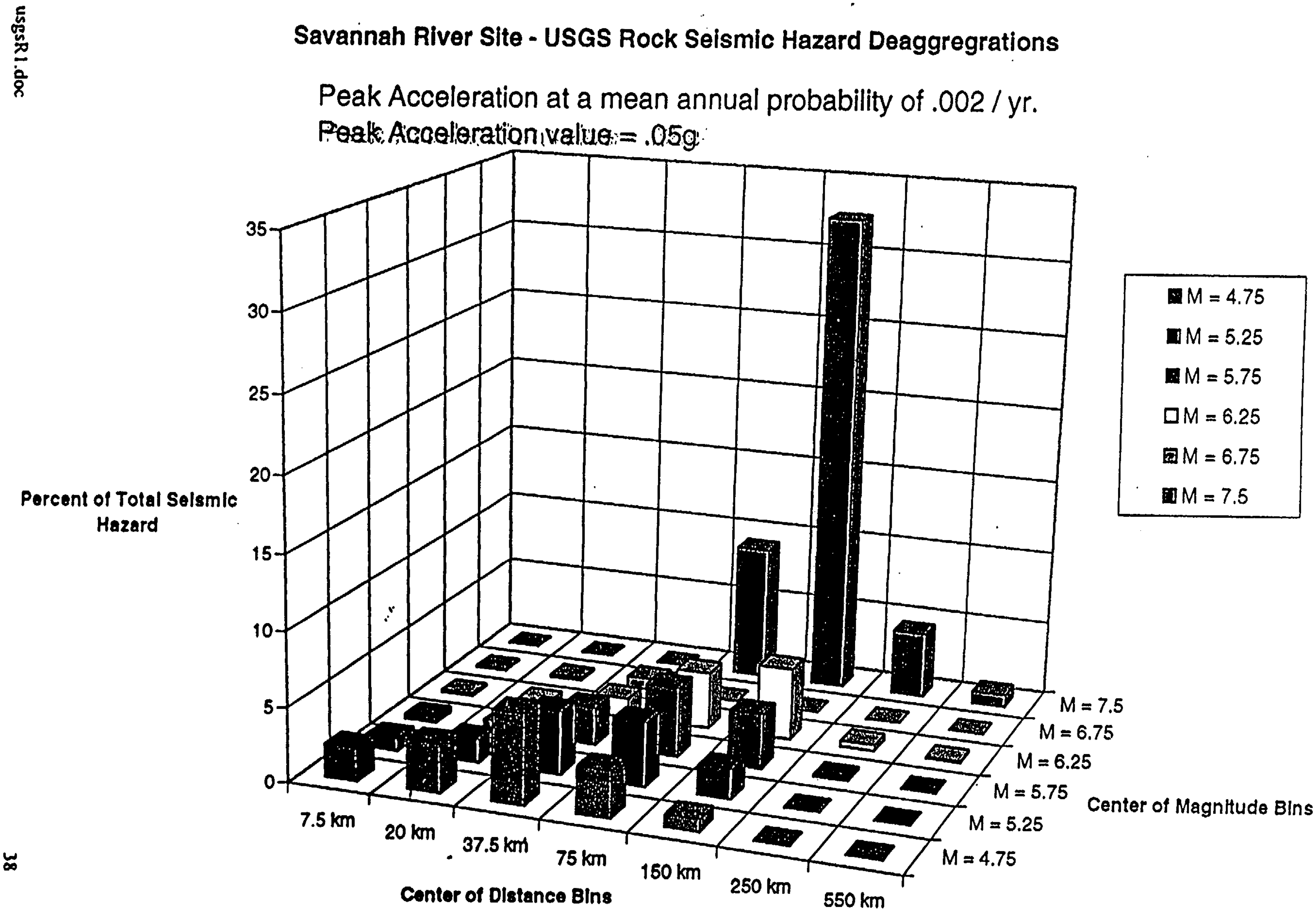

Figure 5e – USGS bedrock PGA hazard disaggregation for SRS with mean annual probability of exceedence of $2x10^{-3}$.

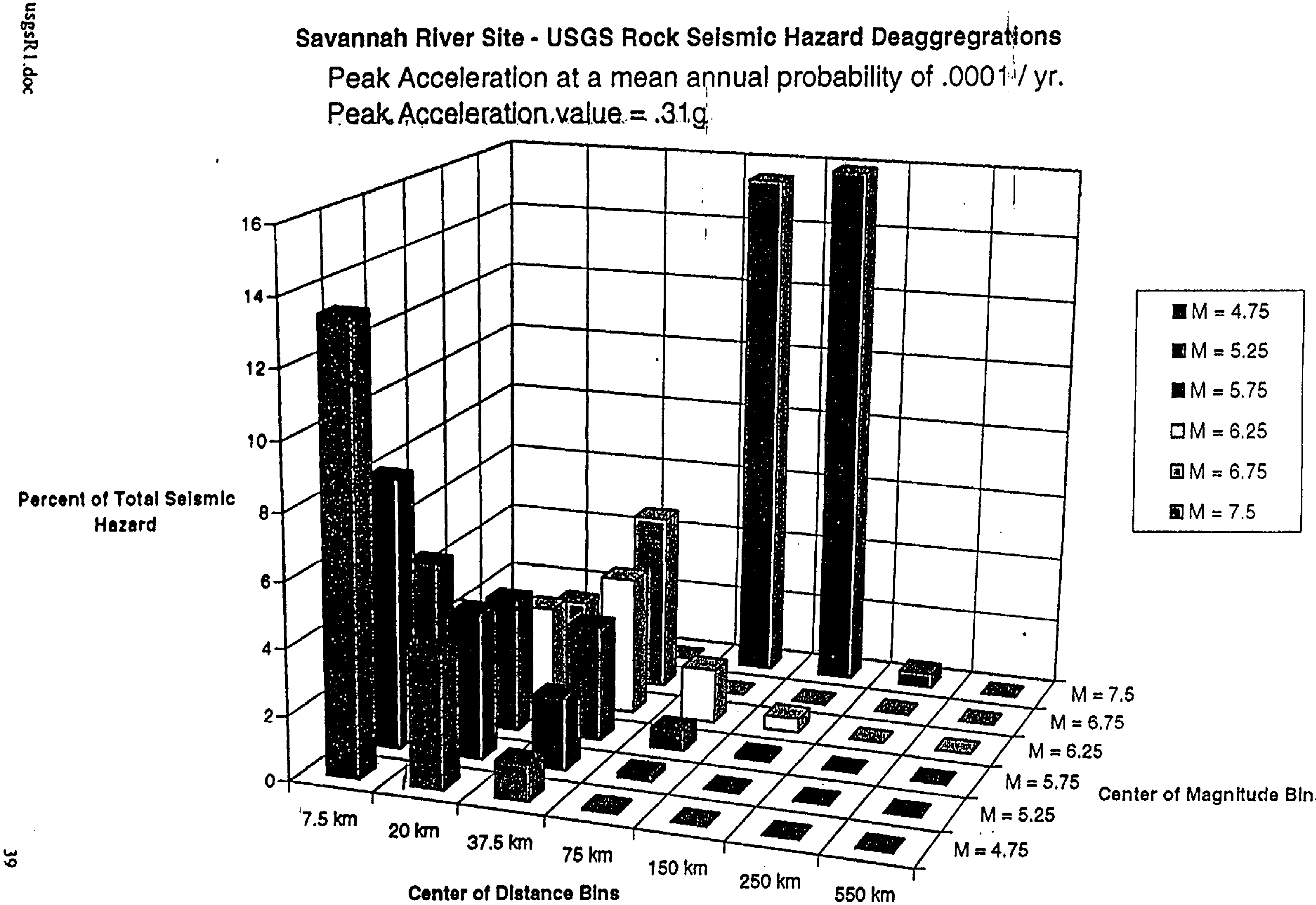

Figure 5f – USGS bedrock PGA hazard disaggregation for SRS with mean annual probability of exceedence of 1×10^{-4}.

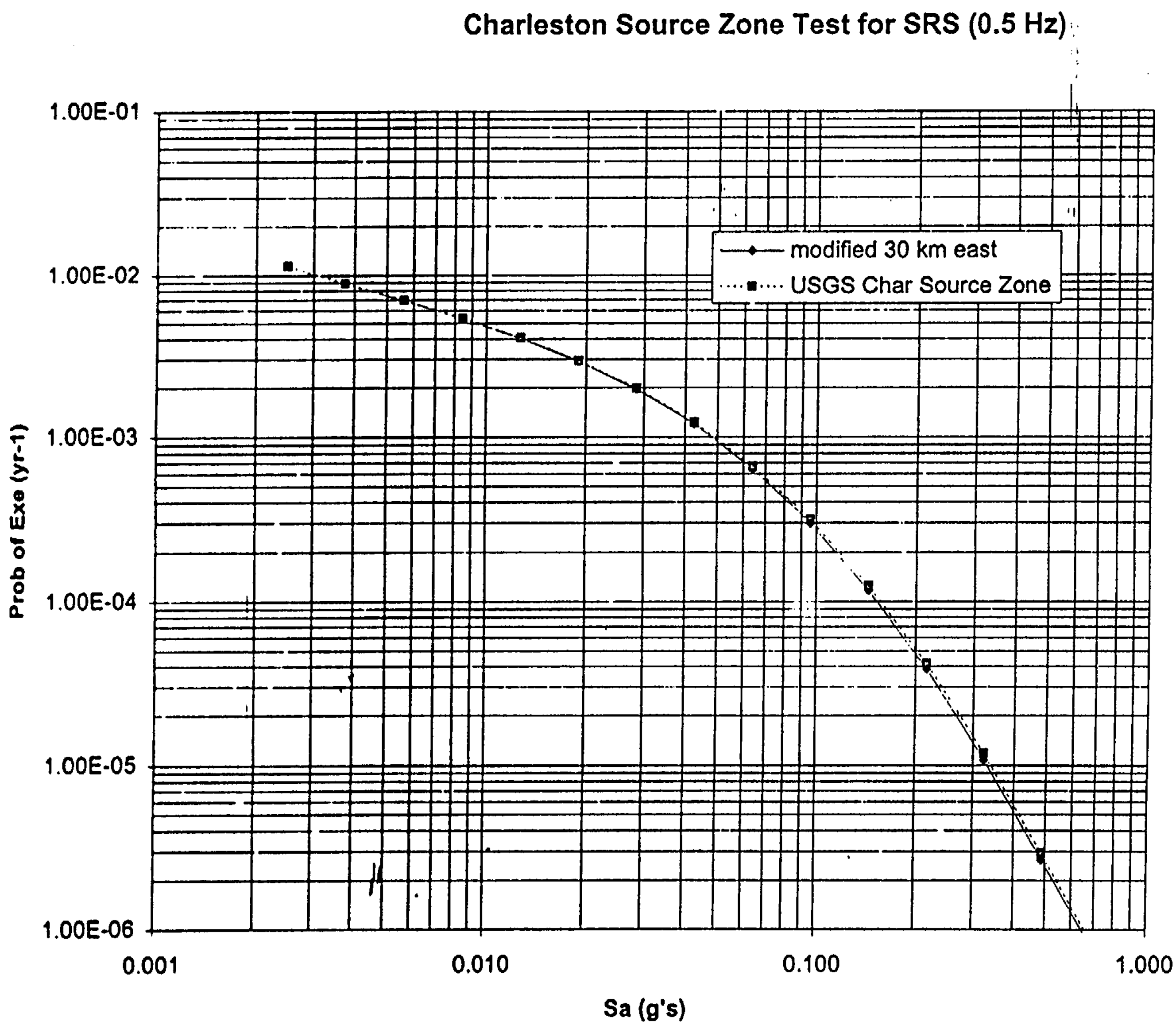

Figure 6a – Comparison of SRS bedrock 0.5-Hz hazard using USGS96 attenuation model and alternate Charleston source zones.

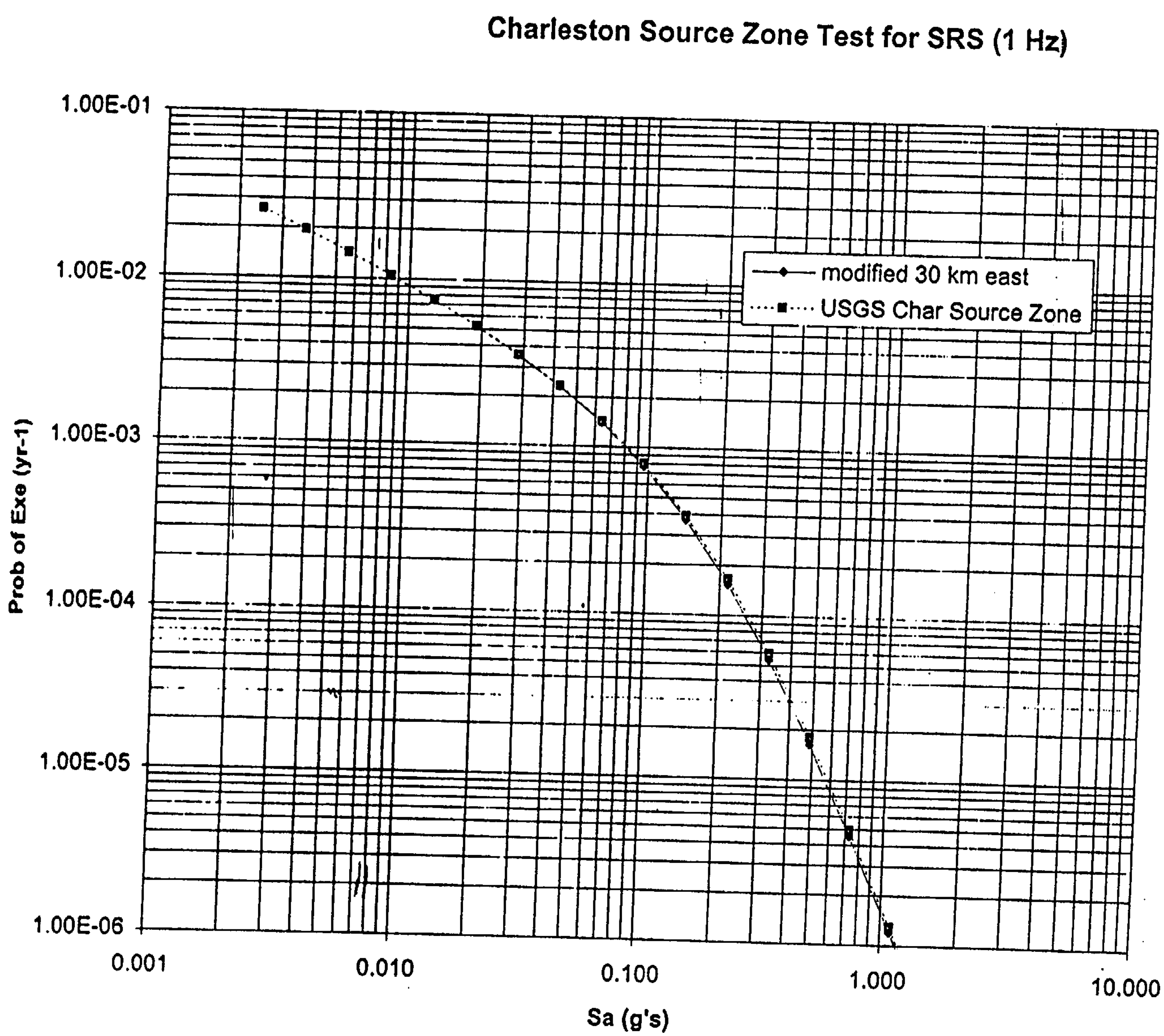

Figure 6b – Comparison of SRS bedrock 1-Hz hazard using USGS96 attenuation model and alternate Charleston source zones.

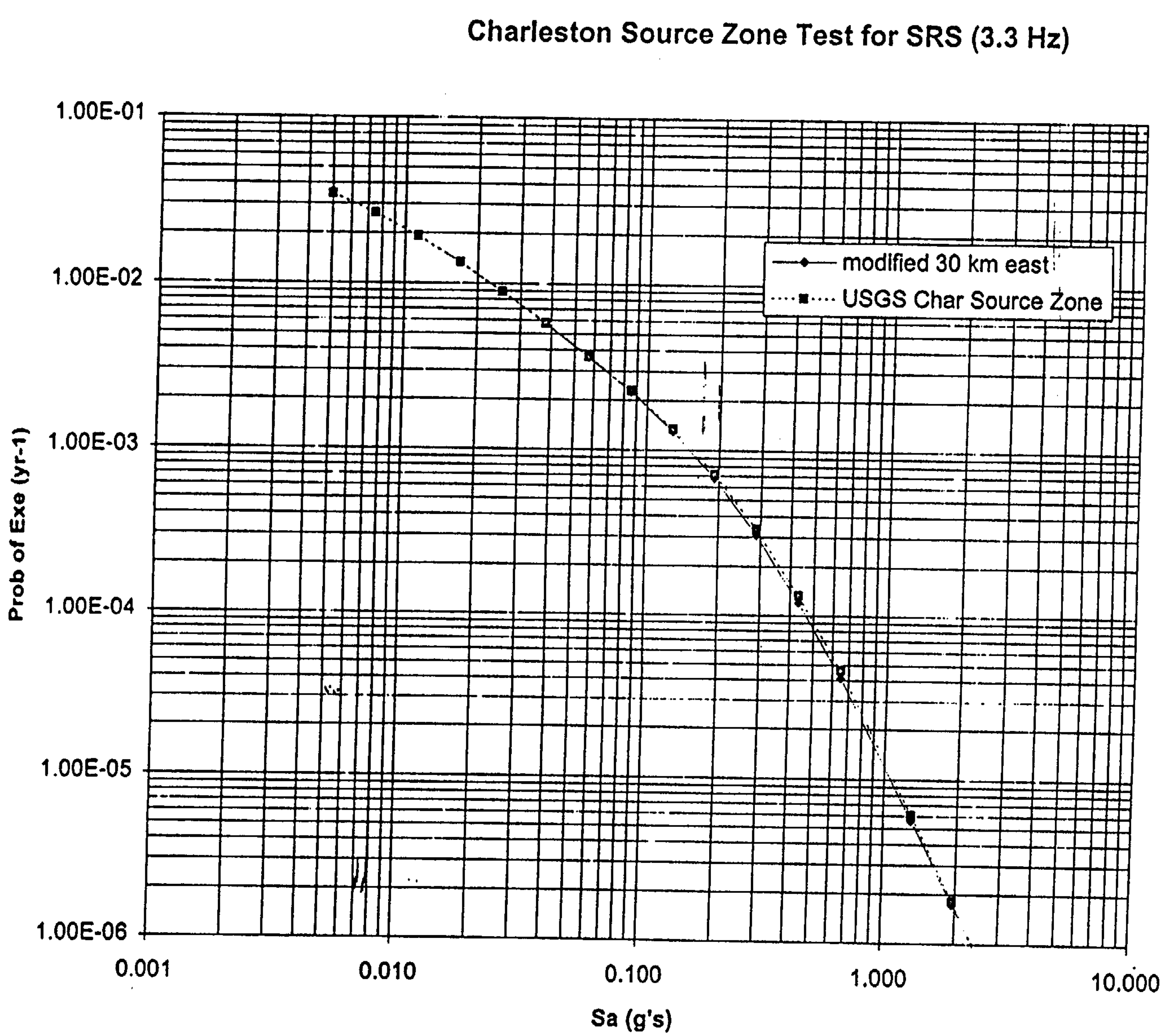

Figure 6c – Comparison of SRS bedrock 3.3 Hz hazard using USGS96 attenuation model and alternate Charleston source zones.

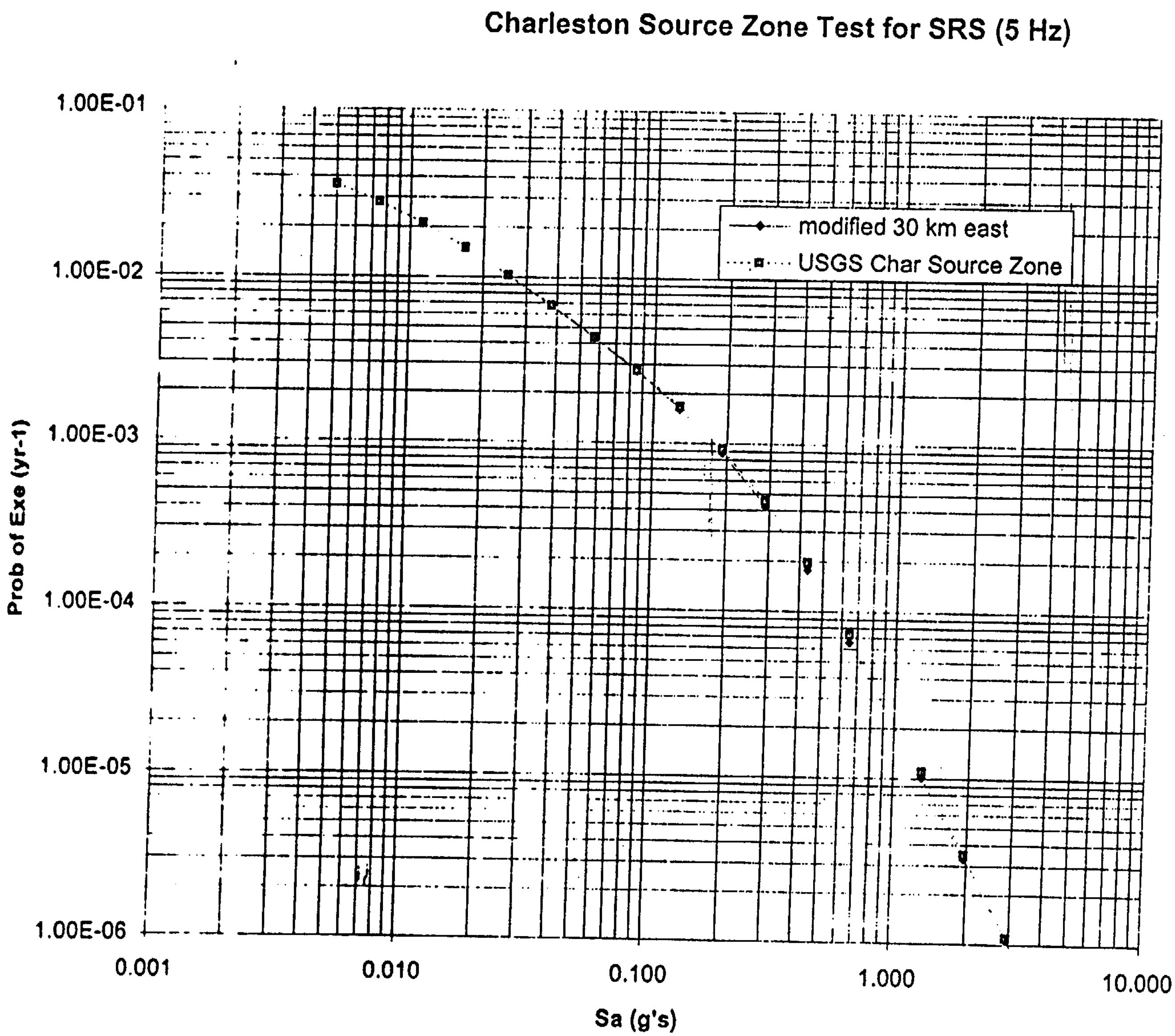

Figure 6d – Comparison of SRS bedrock 5 Hz hazard using USGS96 attenuation model and alternate Charleston source zones.

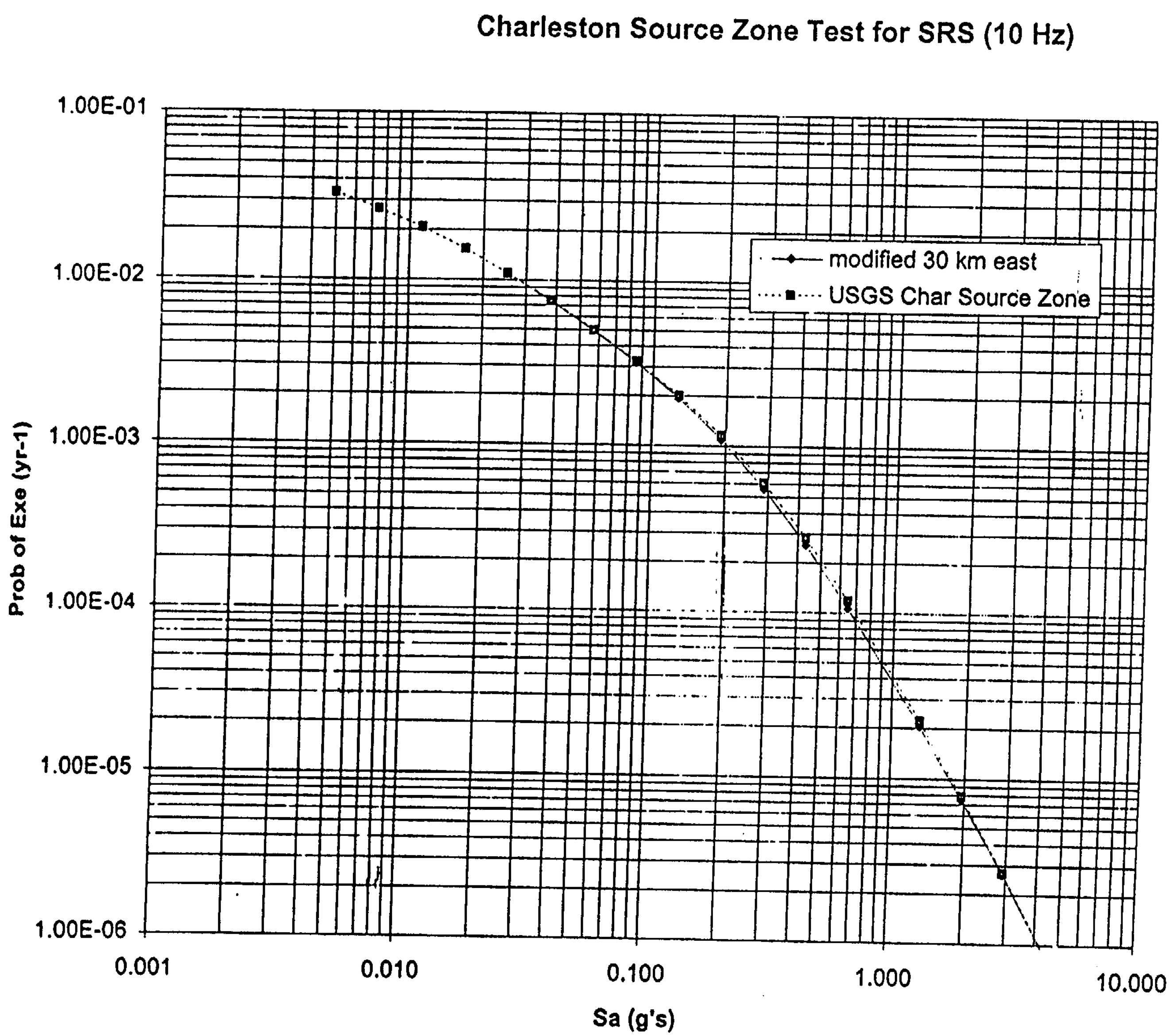

Figure 6e – Comparison of SRS bedrock 10 Hz hazard using USGS96 attenuation model and alternate Charleston source zones.

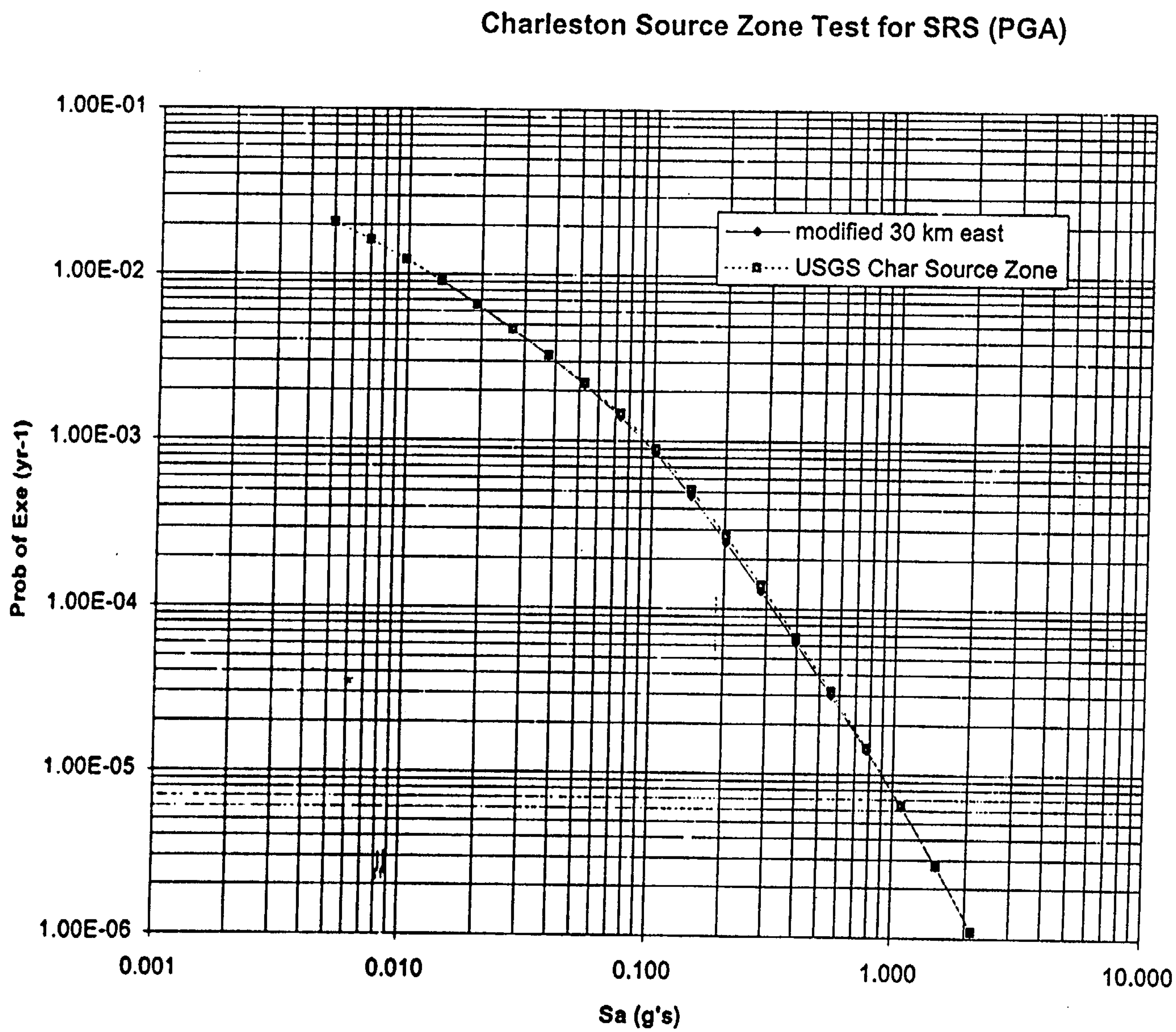

Figure 6f – Comparison of SRS bedrock PGA hazard using USGS96 attenuation model and alternate Charleston source zones.

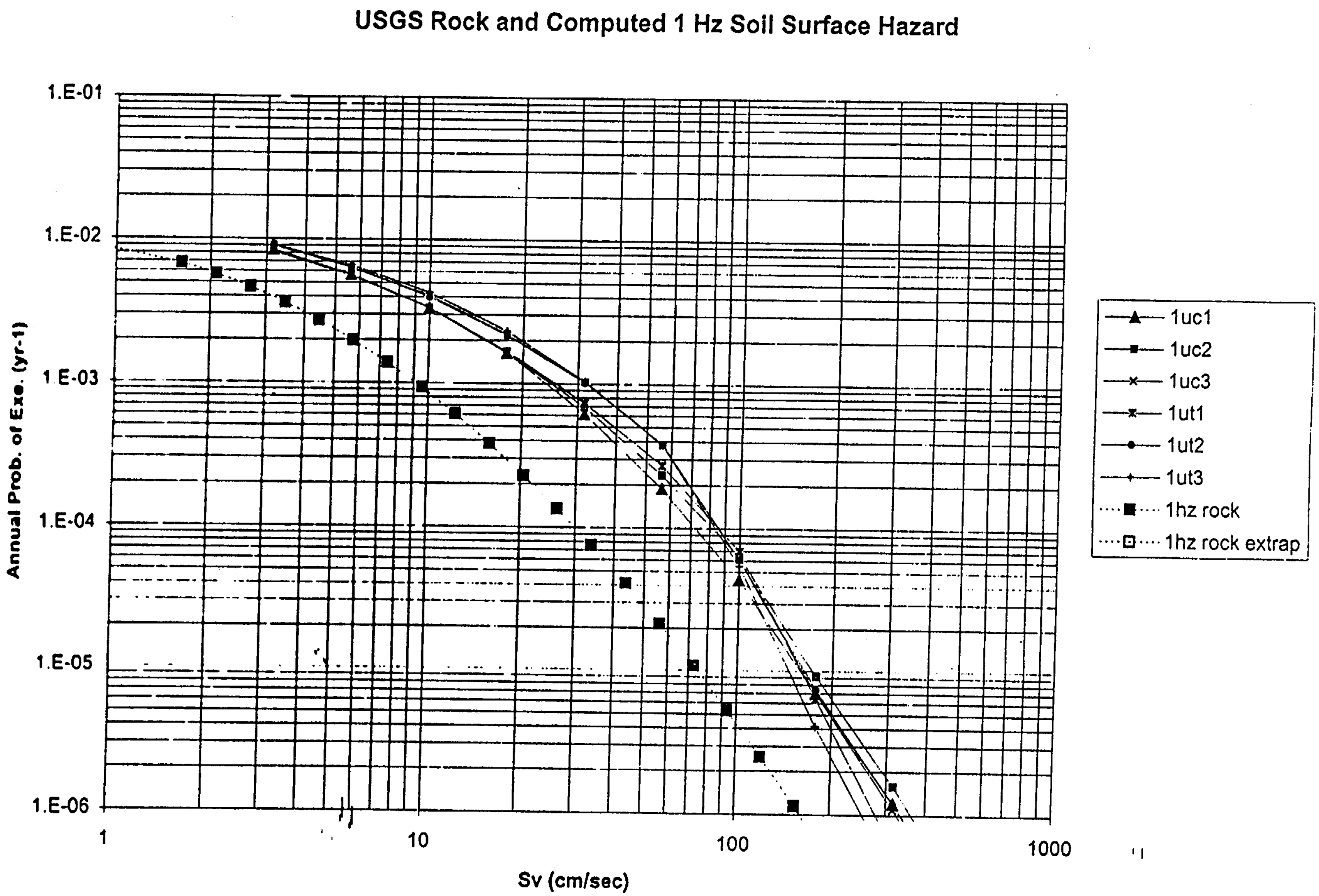

Figure 7a – Computed USGS 1-Hz soil surface hazard for six SRS site/bedrock conditions (solid lines). The letters "c" or "t" in the legend correspond to crystalline or Triassic bedrock respectively and the end numbers "1", "2", or "3" correspond to the soil column thickness category. USGS bedrock hazard shown by dotted line.

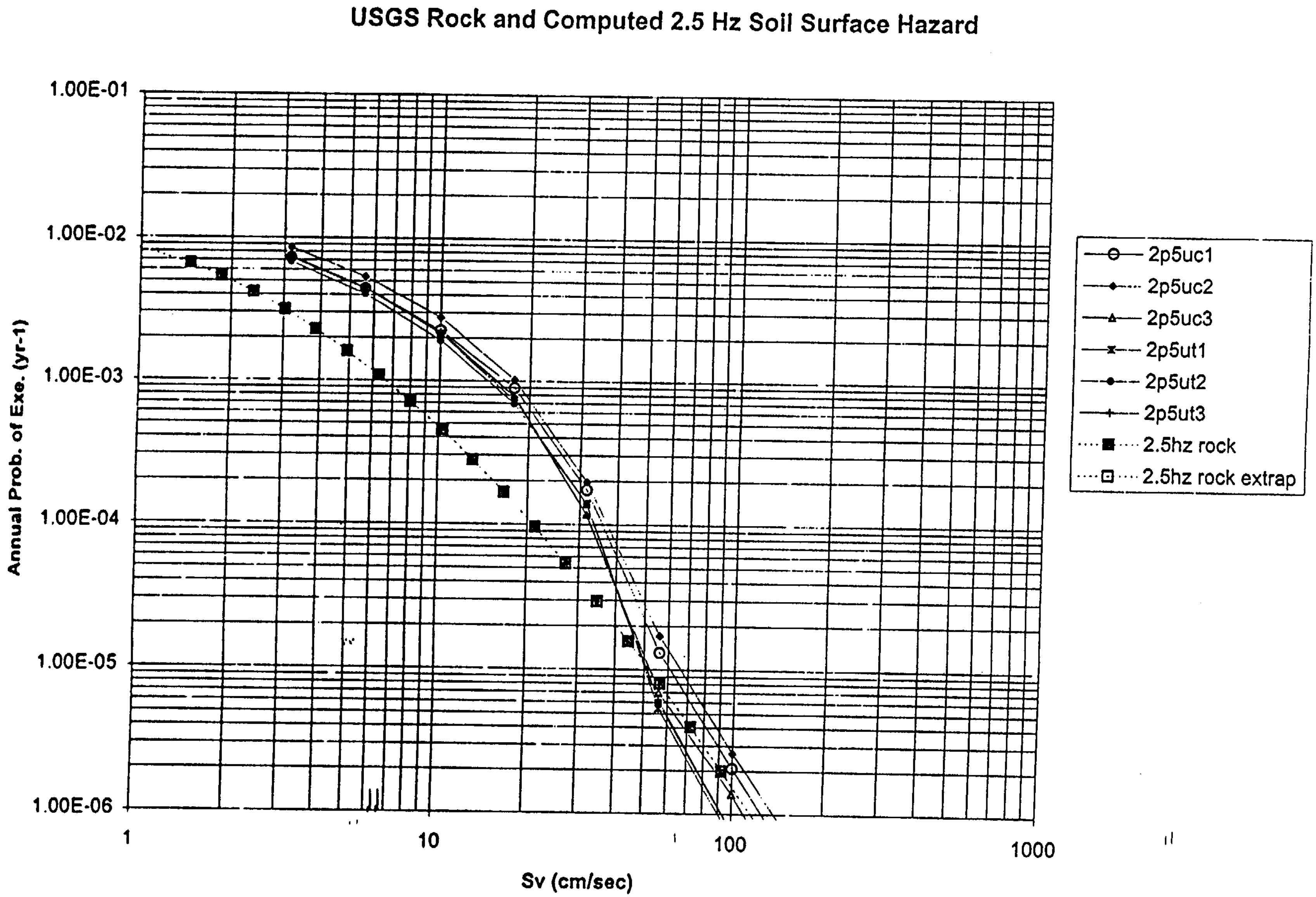

Figure 7b – Computed USGS 2.5-Hz soil surface hazard for six SRS site/bedrock conditions (solid lines). The letters "c" or "t" in the legend correspond to crystalline or Triassic bedrock respectively and the end numbers "1", "2", or "3" correspond to the soil column thickness category. USGS bedrock hazard shown by dotted line.

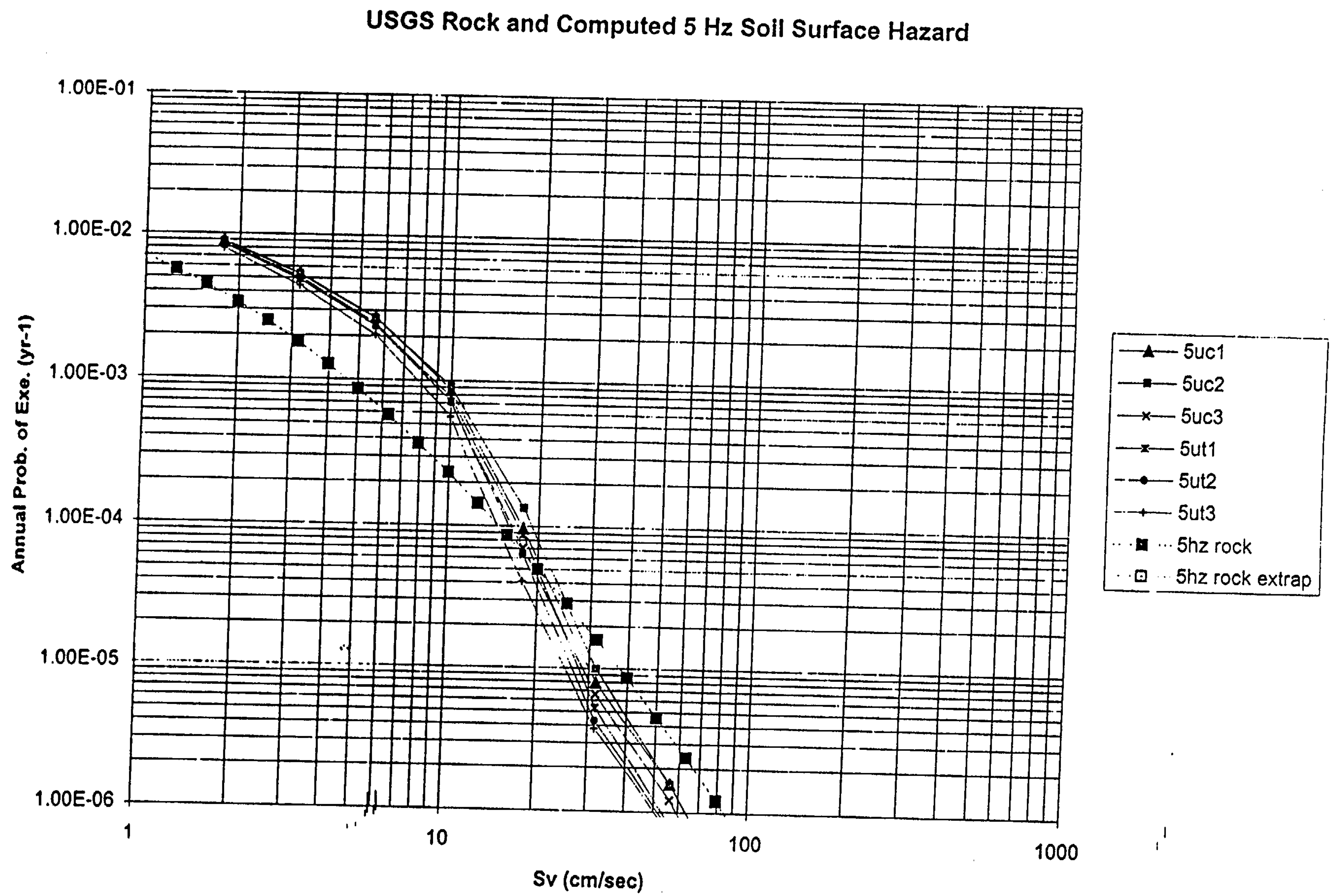

Figure 7c – Computed USGS 5-Hz soil surface hazard for six SRS site/bedrock conditions (solid lines). The letters "c" or "t" in the legend correspond to crystalline or Triassic bedrock respectively and the end numbers "1", "2", or "3" correspond to the soil column thickness category. USGS bedrock hazard shown by dotted line.

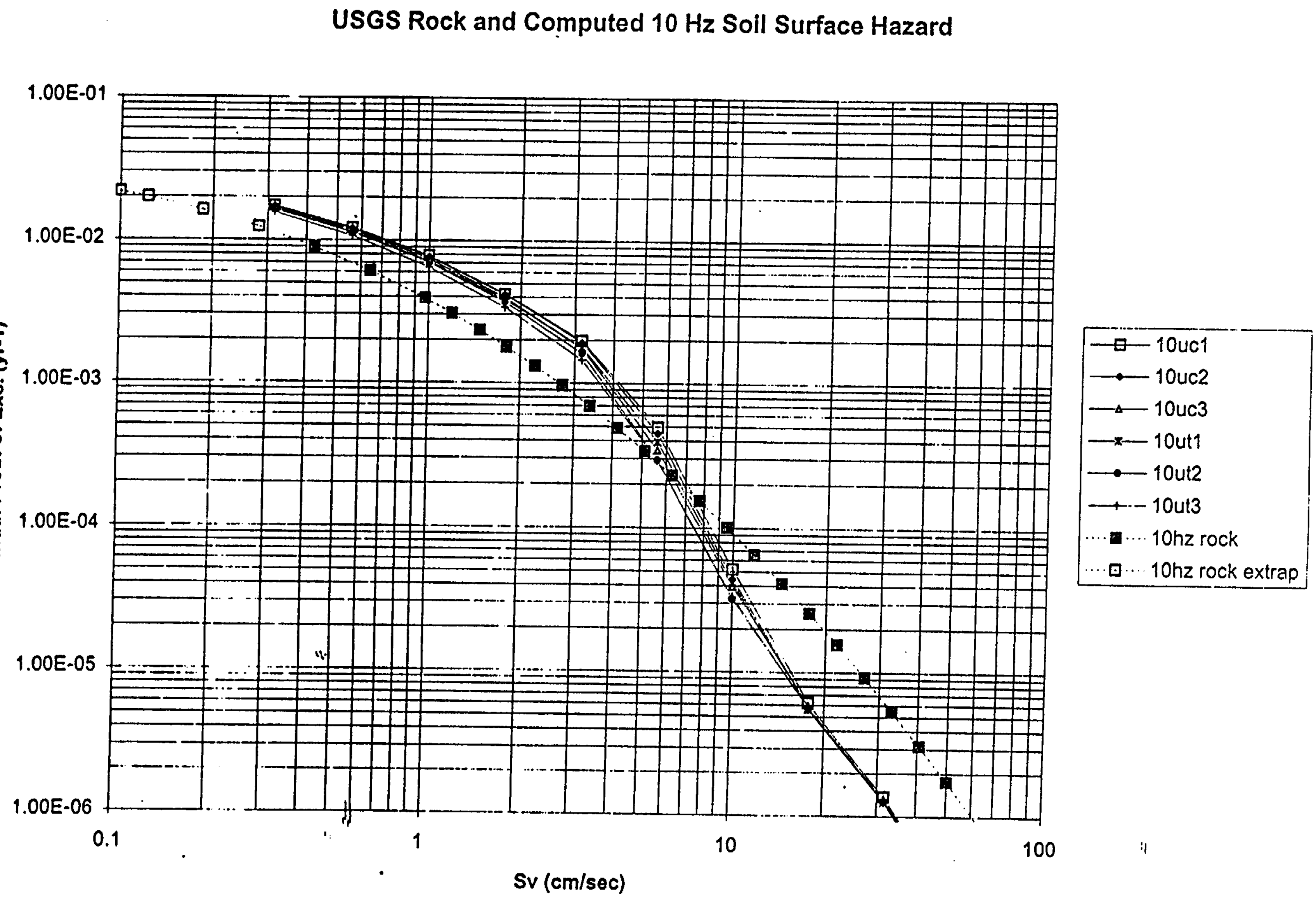

Figure 7d – Computed USGS.10-Hz soil surface hazard for six SRS site/bedrock conditions (solid lines). The letters "c" or "t" in the legend correspond to crystalline or Triassic bedrock respectively and the end numbers "1", "2", or "3" correspond to the soil column thickness category. USGS bedrock hazard shown by dotted line.

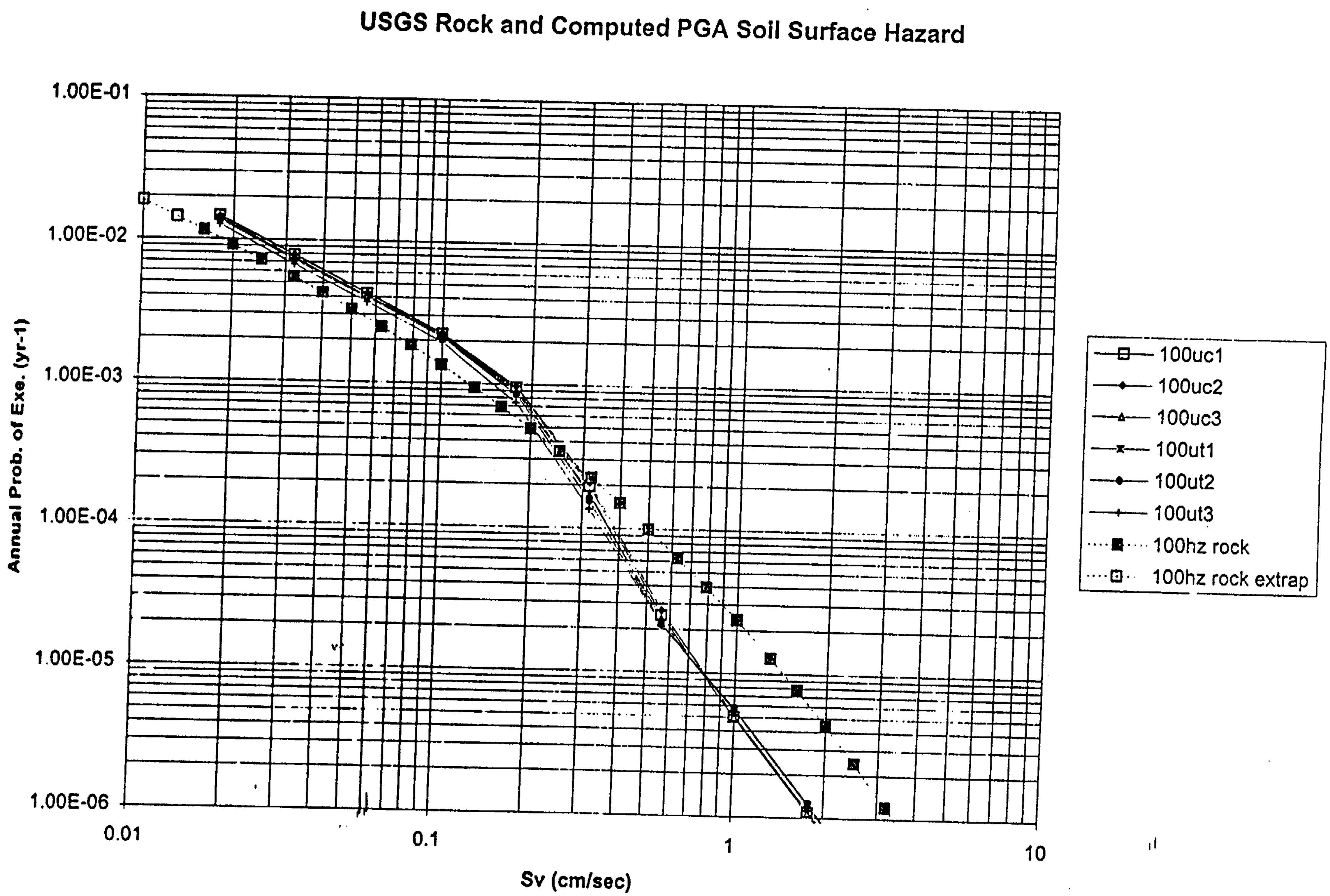

Figure 7e – Computed USGS PGA soil surface hazard for six SRS site/bedrock conditions (solid lines). The letters "c" or "t" in the legend correspond to crystalline or Triassic bedrock respectively and the end numbers "1", "2", or "3" correspond to the soil column thickness category. USGS bedrock hazard shown by dotted line.

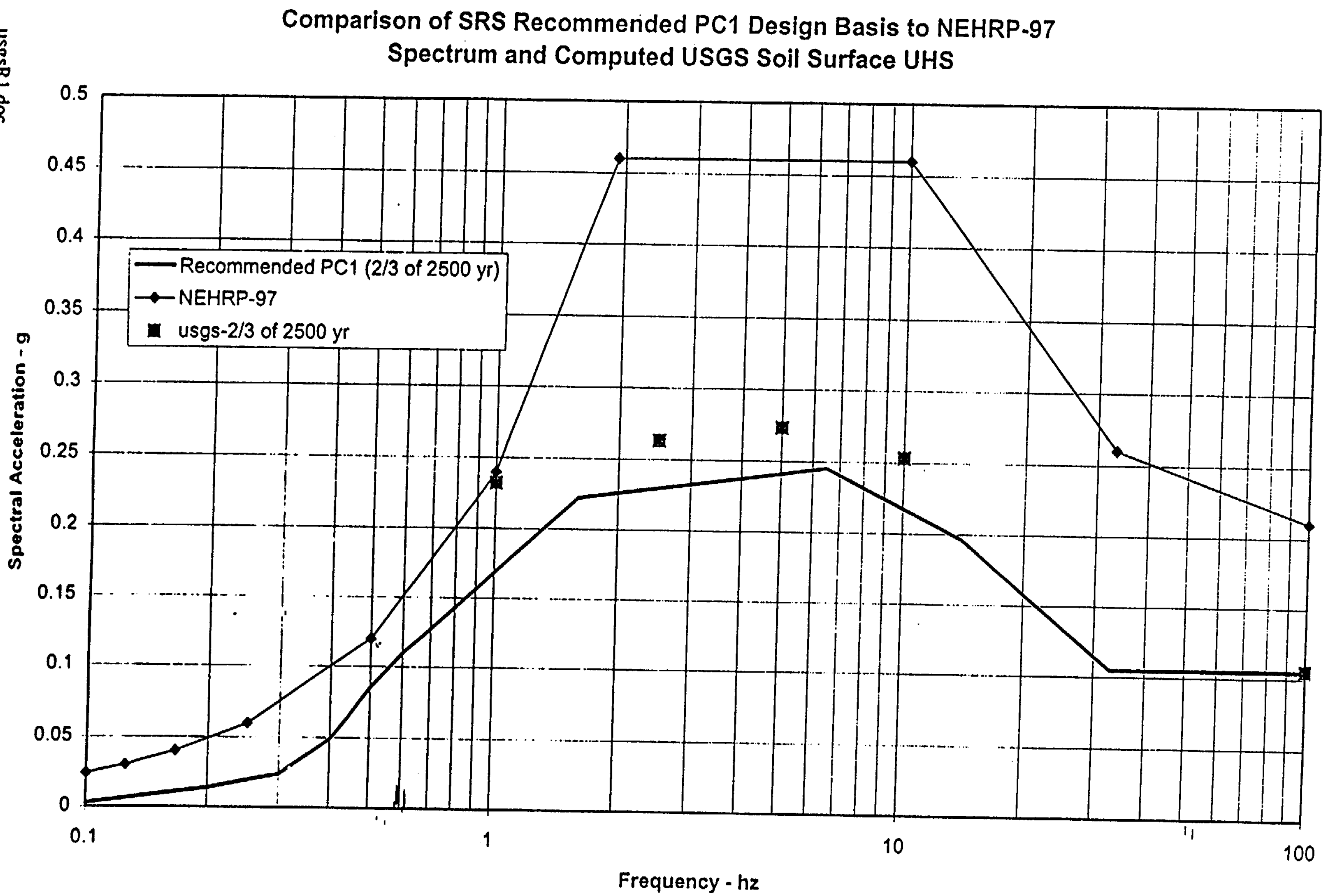

Figure 8 – Comparison of SRS PC1 spectrum to NEHRP-97 spectrum and USGS soil UHS for a criterion of 2/3 of the 2500-year return period.

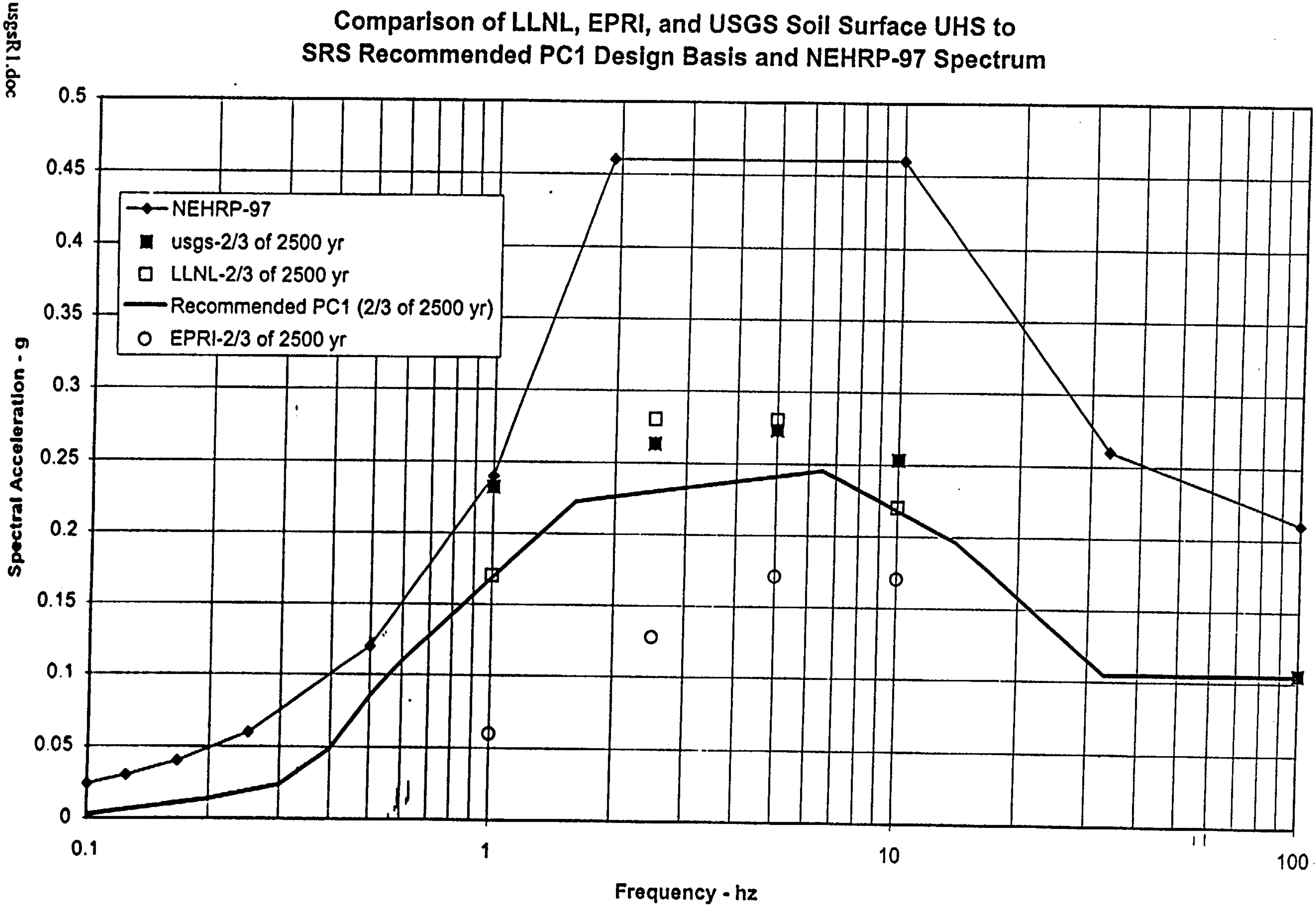

Figure 9a - Comparison of SRS site-specific soil UHS derived from USGS, LLNL and EPRI bedrock hazard evaluations and a criterion of 2/3 of the 2500 year return period. Also shown are the SRS PC1 and NEHRP-97 spectra.

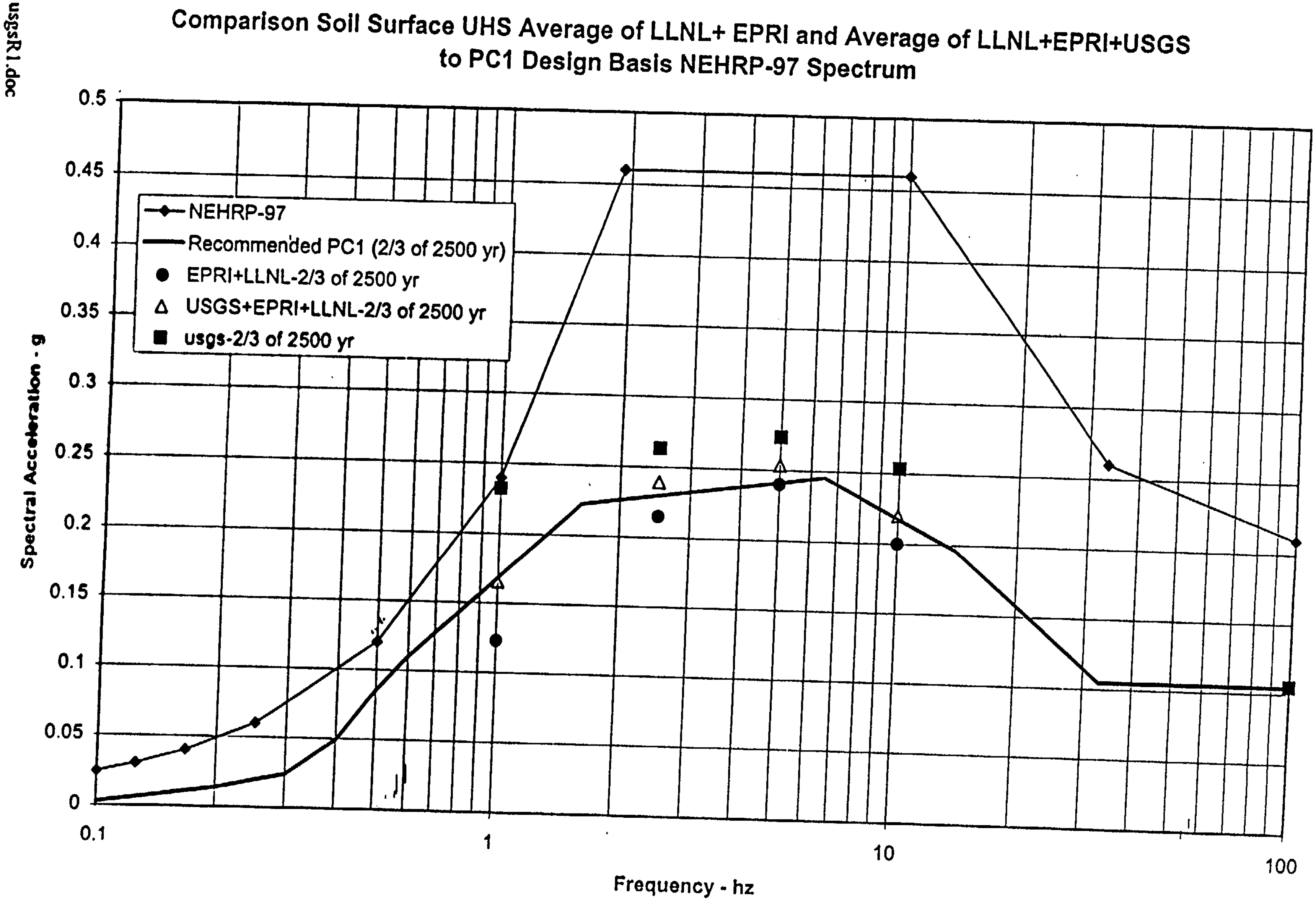

Figure 9b - Comparison of the average LLNL and EPRI soil hazard to the average LLNL, EPRI, and USGS soil hazard using a criterion of 2/3 of the 2500 year return period. Also shown are the SRS PC1, NEHRP-97 spectra and USGS soil UHS.

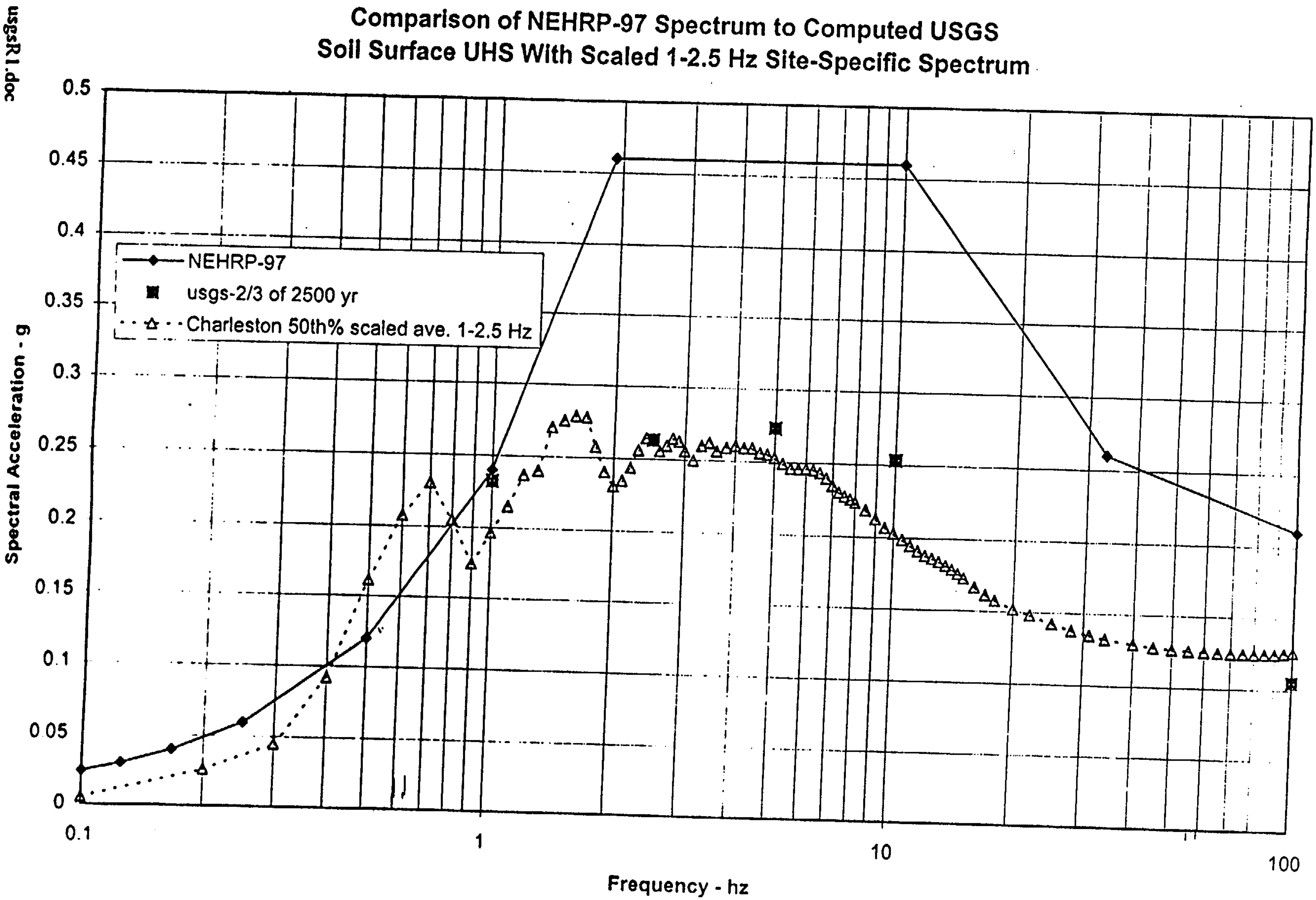

Figure 10 – Comparison of NEHRP-97 spectrum to USGS soil UHS with 1-2.5 Hz scaled Charleston 50th percentile spectrum for a criterion of 2/3 of the 2500-year return period.

Calculation Cover Sheet

Project **Mixed Oxide Fuel Fabrication Facility (MFFF)**	Calculation No. **K-CLC-F-00049**	Project Number **99-D-43 Task No. WTA-023**
Title **Applicability of SRS Site-wide Spectra to the MFFF Site**	Functional Classification **SS** Discipline **Geotechnical**	Sheet 1 of 26

☐ Preliminary ☒ Confirmed

Computer Program No.	Version / Release No.
☐ NA	NA

Purpose and Objective

The purpose of this calculation is to determine the applicability/suitability of SRS site-wide spectra to the MOX Fuel Fabrication Facility (MFFF) Site.

Summary of Conclusion

See Results and Conclusion Section on sheet 5.

Revision

Rev. No.	Revision Description
0	Original

Sign Off

Rev. No.	Originator (Print) Sign / Date	Verification / Checking Method	Verifier / Checker (Print) Sign / Date	Manager (Print) Sign / Date
0	Richard C. Lee Richard C. Lee 8/15/01	Document Review	Michael D. McHood Michael D. McHood 8/15/01	M. R. Lewis M. R. Lewis 8/16/01

Classification

Unclassified

UNCLASSIFIED
DOES NOT CONTAIN
UNCLASSIFIED CONTROLLED
NUCLEAR INFORMATION
ADC & Reviewing Official: C. B. Reeves RO
(Name and Title)
Date 8/15/01

TABLE OF CONTENTS

Purpose

The purpose of this calculation is to determine the applicability/suitability of SRS site-wide spectra to the MOX Fuel Fabrication Facility (MFFF). In March of 1997, the Site Geotechnical Services Department (SGS) issued SRS site-wide spectra (Lee et al., 1997) in a "committed" calculation. In order for the spectra to be used as "confirmed", SGS must review the stratigraphic conditions at the facility or site being considered for seismic evaluation.

Calculation Approach

There are four general areas (i.e., stratigraphic conditions) to examine to validate the suitability of the site-wide response spectra (SWRS) for a new facility: (1) the stratigraphy of soils to validate that there are no topographic or subsurface features that could significantly alter ground motion over the modeled cases; (2) validate that the soil column thickness and bedrock type matches one of the ranges used in developing the SWRS; (3) validate that the velocity profiles measured at the site are within the variances used in developing the SWRS; and (4) validate that the geologic formations at the site are reasonably close to the basecase formations used for the SWRS so that there is a consistent relationship between the dynamic properties applied in the SWRS and the new site.

Input Data and Evaluation

Site Topography and Soil Stratigraphy

The MFFF site CPT locations, boring locations and cross-sections are shown in Figure 1. The stratigraphy shown in Figures 2 through 10 were reviewed to verify that there are no topographic or subsurface features that could significantly alter ground motion over the modeled cases contained in the SWRS. The interpretations indicate that the formations underlying the MFFF site are relatively flat-lying. Thus, surface topography and soil stratigraphy are consistent with the approximation of a simple horizontal layered model and exhibit no features that could suggest the possible occurrence of anomalous seismic amplitudes at the MFFF site.

Soil Column Thickness and Bedrock Type

The soil column thickness is well constrained in F- and H-areas (Aadland et al., 1995; Agbabian, 1994). The MFFF site is within about a kilometer of several boreholes used to define the depth to bedrock. Based on the available data, the MFFF soil column fits within the classification of SRS soils in depth range-3 (800 to 1000 feet). Although basement shear-wave velocity directly under the site has not been measured, crystalline bedrock wave-speeds are anticipated based on the available bedrock measurements northwest of the Pen Branch Fault (Lee et al., 1997). Thus, due to the proximity of the MFFF site to the well-characterized F- and H-Areas, there is a very high confidence that the site is included in the range of models used to develop the SWRS.

Measured Soil Profile Wave-speeds

Down-hole SCPTU seismic surveys were performed as part of the geotechnical investigation for the MFFF site (DCS, 2000; 2001). Fifteen DCS SCPT shear-wave interpretations were reviewed for comparison to the site-wide velocity profiles used to develop site-wide spectra and for applicability of the site-wide spectra to the MFFF site. The fifteen DCS SCPT shear-wave interpretations are shown in Figure 11. One of the shear-wave interpretations (CPT-35) was revised, rejecting shallow and deep interpretations of the shear-wave speed that were based on complex arrivals or low signal-to-noise data. There are no deep shear-wave velocity profiles in the vicinity of the MFFF site.

Figure 11 also compares the MFFF shear-wave velocity interpretations to the statistical median and standard deviation derived from the randomized shear-wave soil models used to develop the SWRS. Figure 11 shows that there is a generally excellent overall agreement between the measured MFFF shear-wave speeds and the statistical median except for the upper 20 feet of the profile. In this upper 20 feet, the MFFF profiles appear to be somewhat faster on average than the median site-wide profile by approximately 200 ft/sec. This small increase in shear-wave speed over the upper 20 ft layer is considered insignificant. These profiles are within the range of velocity profile variability contained in the SWRS and are judged not to bias the mean MFFF profile as compared to the mean site-wide velocity profile. The measured MFFF velocity profiles are thus judged to be consistent with the SWRS.

Site Specific Shear Modulus and Damping

Figures 12 through 15 illustrate a comparison of the shear modulus and damping curves measured for the MFFF (DCS, 2001) to SRS recommended curves (WSRC, 1996). Laboratory resonant column and cyclic triaxial measurements were made from soil samples collected at the MFFF site. The testing was conducted to evaluate the applicability of the WSRC-recommended strain dependent modulus and damping curves (DCS, 2001). The modulus results (Figures 12 and 14) show good agreement with the SRS recommended curves, while MFFF-specific damping curves (Figures 13 and 15) suggest significantly greater damping than the SRS recommended curves. Stokoe et al. (1995) has reviewed the SRS dynamic property database and concluded that resonant column damping results are unreliable (WSRC, 1996). DCS (2001) also does not recommend the MFFF-specific resonant column damping results. Thus, the site wide dynamic properties used to develop the SRS design spectrum are appropriate for the MFFF site.

Geologic Formations

Figures 2 through 10 show engineering and geologic layering for the MFFF site. The stratigraphy and geologic formations are discussed in Lee et al. (1997) as well as Appendix A of this calculation. The fill layer in the illustrations will be removed before construction of the MFFF. Any fill that is not removed at the MFFF site will require a separate engineering analysis and a reassessment of the applicability of the SWRS. The thickness of the Altamaha Formation (TR1 layer) is about 5 feet. The thickness of the Tobacco Road Formation (layers TR1A and

TR2A) is about 30 feet. The Dry Branch Formation (layers TR2B, TR3/4, and DB1/3) is about 60 feet thick and the Santee/Tinker Formation is about 40 feet thick (see Appendix A, Figure A1).

The SWRS basecase formation thickness was 12 feet for the Altamaha, 72 feet for the Tobacco Road and 128 feet for the Dry Branch and Santee Formations. In the development of the SWRS, dynamic properties were applied on the basis of soil formation as prescribed in the work conducted for the SRS by the Univ. of Texas (Stokoe et al., 1995) and peer reviews (WSRC, 1996). Variability of modulus and damping were increased in the development of the SWRS because the occurrence, depth and/or thickness of specific formations and soil types were expected to vary across the site. Thus, the formation thickness of the MFFF Tobacco Road and Dry Branch is consistent with the site wide spectra model (Lee et al., 1997). Consequently the MFFF soils formation, while somewhat different from the site-wide basecase, is consistent with the range of soil properties used in the development of the SWRS.

Assumptions

For the SRS site-wide spectra to be applicable for design of the MFFF, the fill overlying the MFFF site must be removed prior to construction of the facility.

Results and Conclusions

General stratigraphic conditions have been examined to validate the suitability of the site-wide response spectra for the MFFF site. There are no topographic or subsurface features that could significantly alter ground motion over the modeled cases with the exception of a surficial fill layer. It is expected that this fill layer will be removed before construction of the MFFF. The soil column thicknesses and bedrock type match ranges used in developing the SWRS. The velocity profiles measured at the MFFF site are within the variances used in developing the SWRS. The formations at the MFFF site, while somewhat different from the assumed formation model used for the SWRS, would not lead to any significant bias in a predicted ground motion model for the MFFF. The variability used in developing the SWRS encompasses the dynamic properties expected at the MFFF.

It should be noted that the SWRS is intended for simple response analysis. It is not appropriate for soil-structure interaction analysis. In addition the SWRS represent a surface response and is not representative of an embedded response.

References

Aadland, R. K., Gellici, J. A., and Thayer, P. A., (1995). *Hydrogeologic Framework of West-Central South Carolina*, S. C. Department of Natural Resources, Water Resources Division, Report 5.

Agbabian Associates Engineers and Consultants (1994). *Suspension P- and SH-Wave Velocity Measurements at the Savannah River Site Boreholes MMP-2A-SB, MMP-3-SB, and MMP-4-SB*, Report 9507-6542, November 29, 1994.

Duke, Cogema, Stone and Webster (DCS) (2000). MOX Fuel Project Transmittal from James Meisenheimer to Lawrence A. Salomone, October 31, 2000.

Duke, Cogema, Stone and Webster (DCS) (2001). *MOX Fuel Fabrication Facility Site Geotechnical Report*, Report DCS01-WRS-DS-NTE-G-00005-C, DOE Contract DE-AC02-99CH10888, August 2001.

Lee, R.C., M.E. Maryak and M.D. McHood (1997). *SRS Seismic Response Analysis and Design Basis Guidelines*, WSRC-TR-97-0085, Revision 0, March 1997.

Stokoe, Kenneth. H., II, Hwang, Seon-Keun, Darendeli, Mehment, and N. K. James Lee (1995). *Correlation Study of Nonlinear Dynamic Soil Properties: Savannah River Site, Aiken, South Carolina*, Rev. 0, File No. SRS-FR-CDP-95, University of Texas at Austin, Department of Civil Engineering, September 13, 1995.

Toro, G.R. (1997). *Probabilistic Models of Shear-wave Velocity Profiles at the Savannah River Site, Aiken, South Carolina*, April 4, 1997 (also Appendix A in Lee et al., 1997).

WSRC (1996). *Investigations of Nonlinear Dynamic Soil Properties at the Savannah River Site*, WSRC-TR-96-0062, Rev. 0, March 22, 1996.

FIGURES

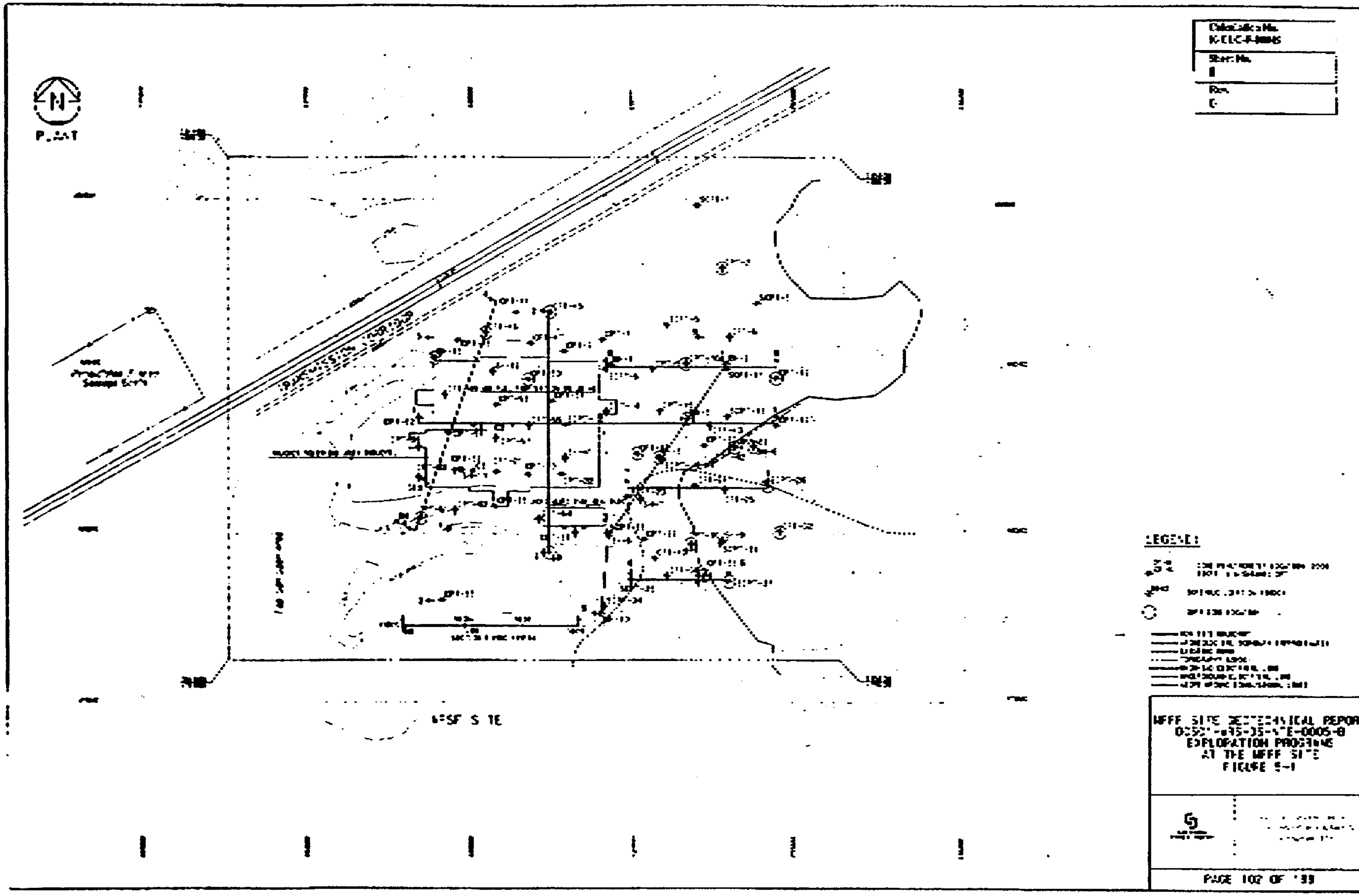

Figure 3 - MFFF Site Area with SCPTU Locations and Cross-Sections

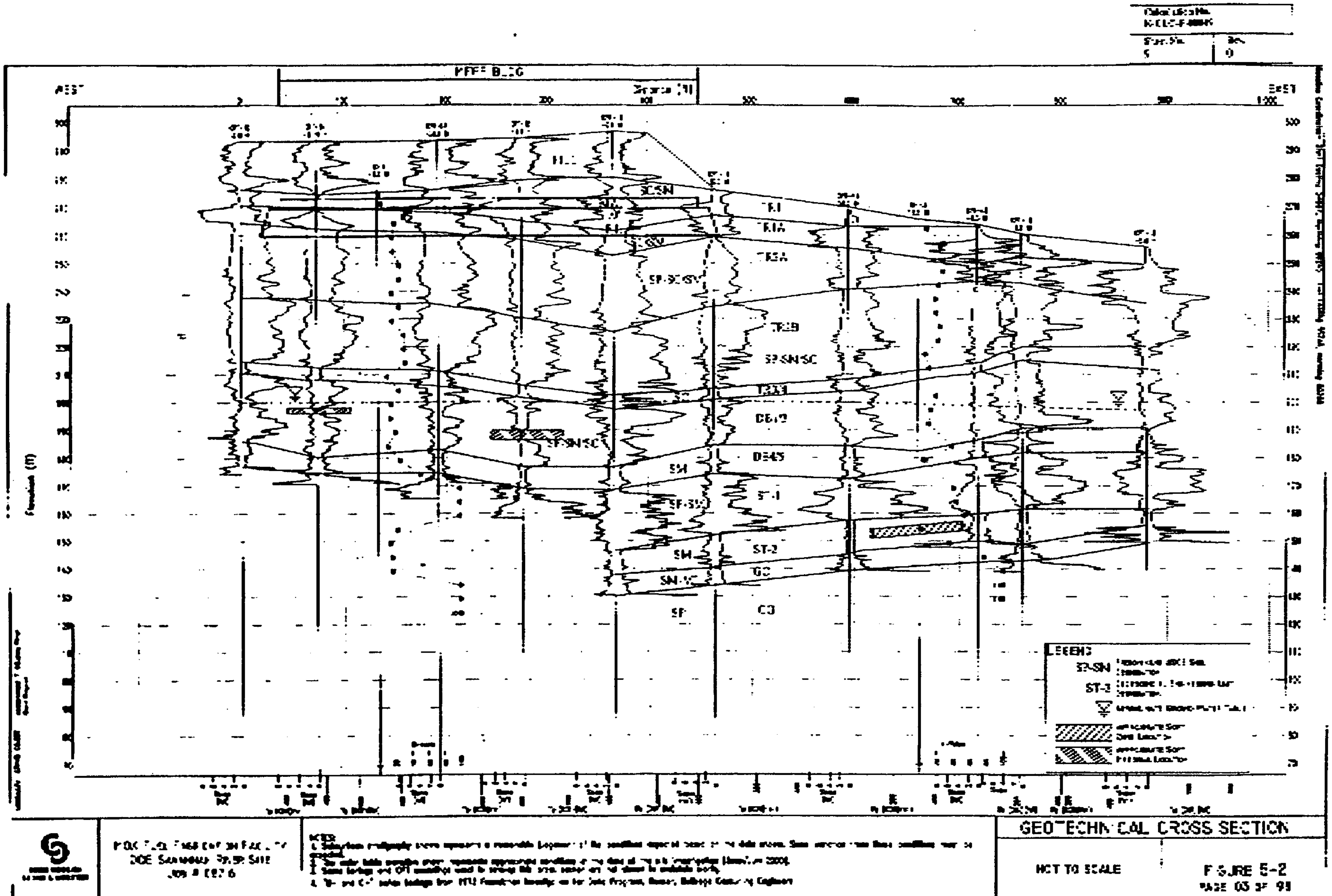

Figure 2 - SCPTU Log and Stratigraphic Formation Identification for MFFF Section 1

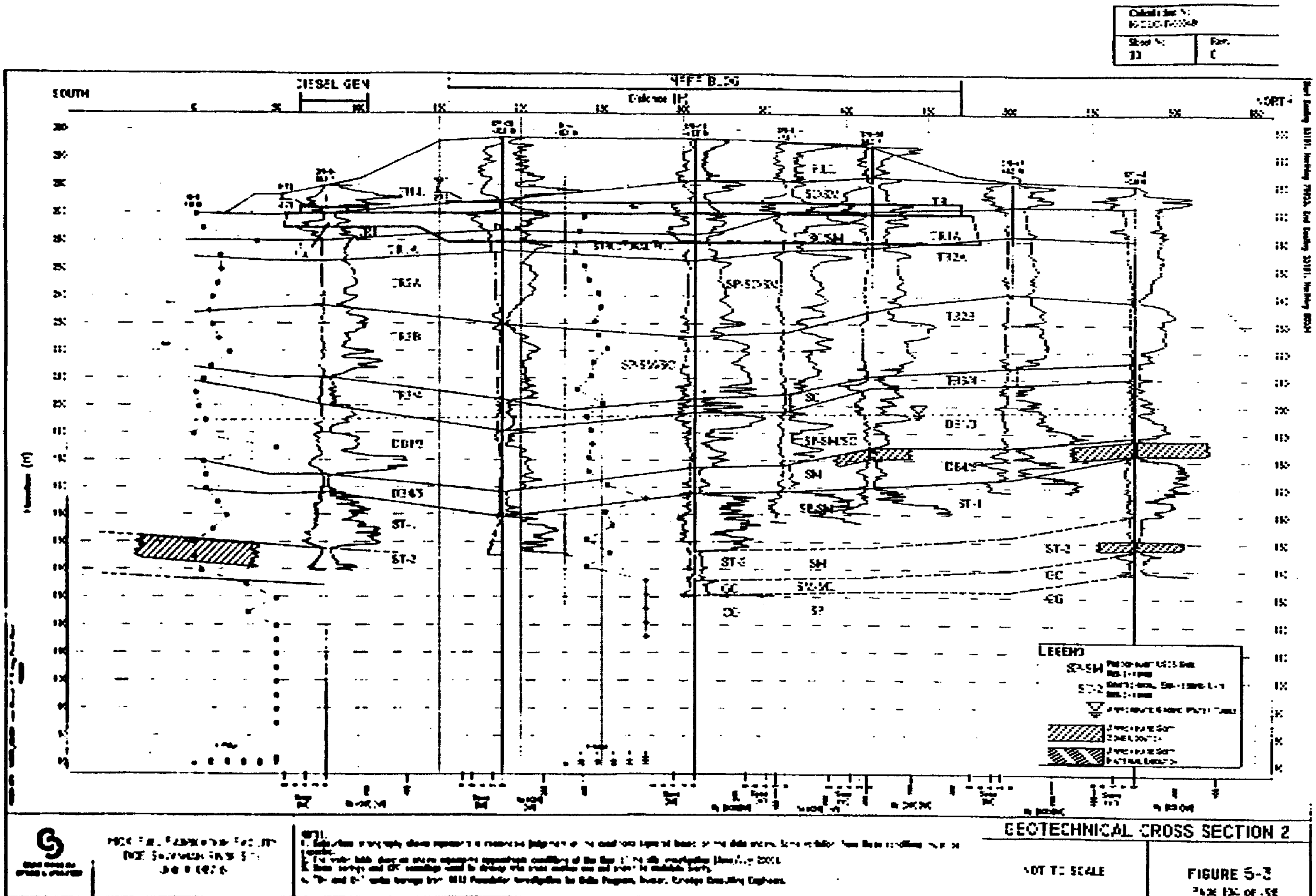

Figure 3 - SCPTU Log and Stratigraphic Formation Identification for MFFF Section 2

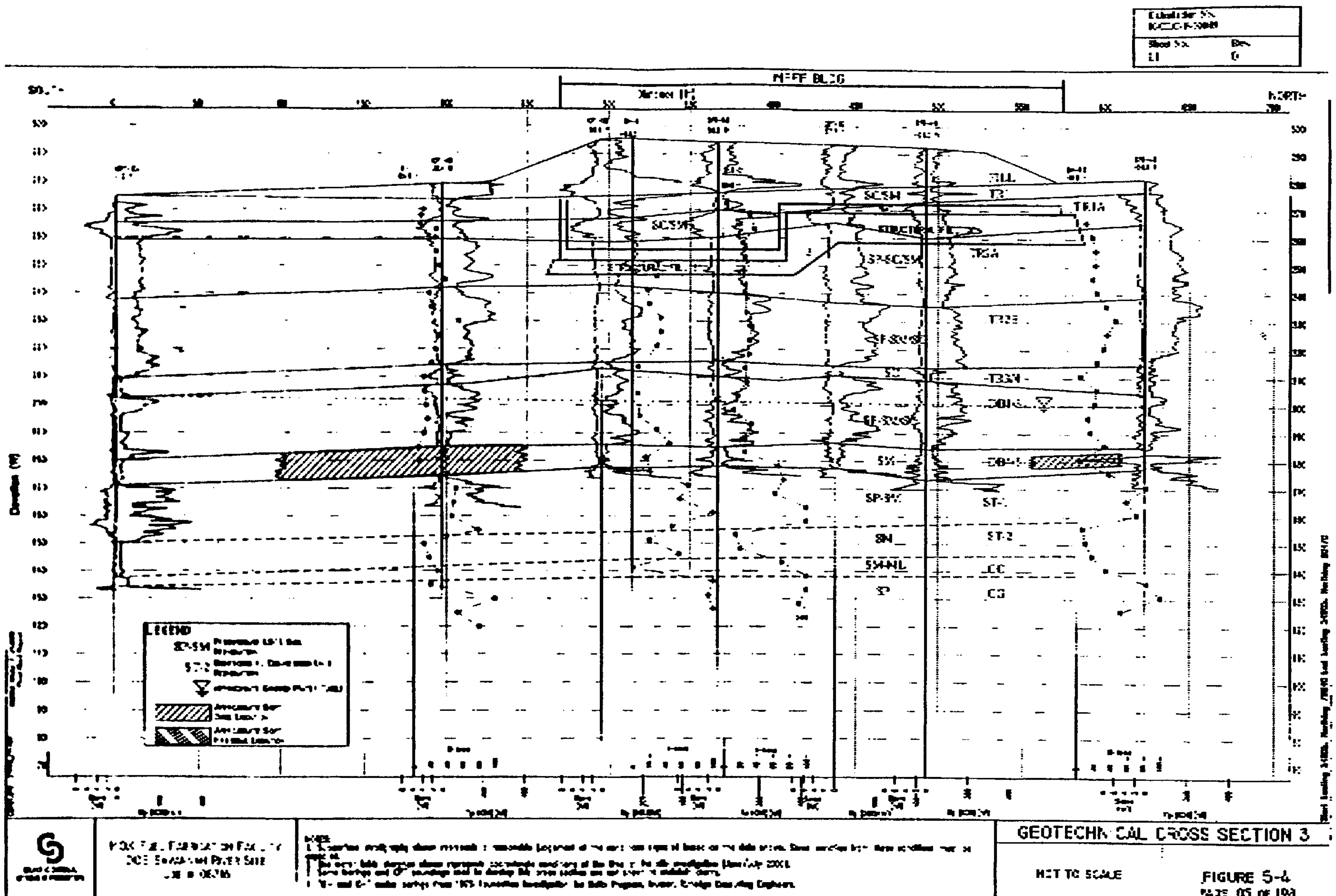

Figure 4 - SCPTU Log and Stratigraphic Formation Identification for MFFF Section 3
(Figure 5-4 from DCS, 2001)

Calculation No. K-CLC-F-00049	
Sheet No. 12	Rev. 0

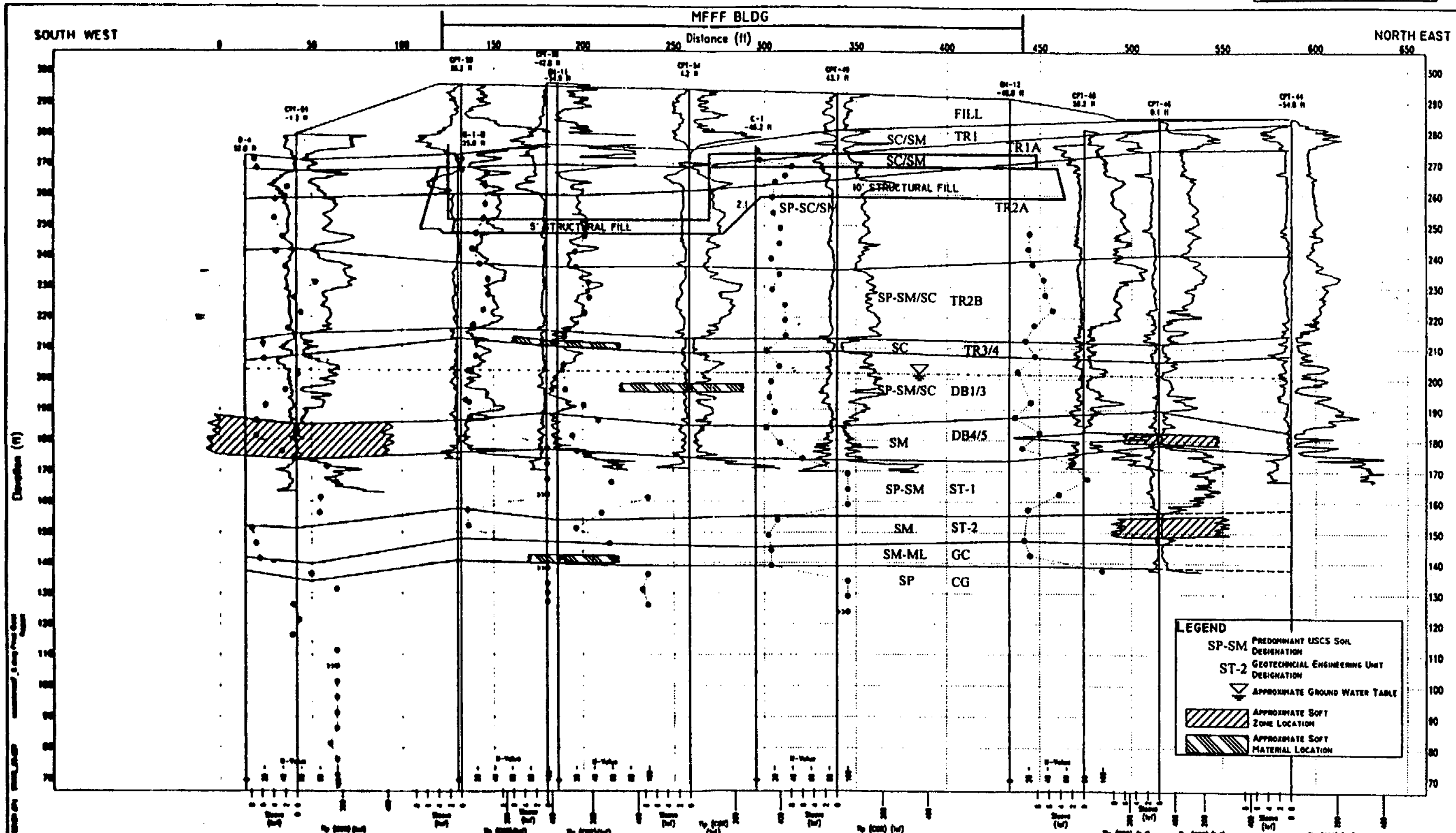

MOX FUEL FABRICATION FACILITY
DOE SAVANNAH RIVER SITE
JOB # 08716

NOTES:
1. Subsurface stratigraphy shown represents a reasonable judgement of the conditions expected based on the data shown. Some variation from these conditions must be expected.
2. The water table elevation shown represents approximate conditions at the time of the site investigation (June/July 2000).
3. Some borings and CPT soundings used to develop this cross section are not shown to maintain clarity.
4. "B- and C-" series borings from 1973 Foundation Investigation for Duke Program, Mueser, Rutledge Consulting Engineers.

GEOTECHNICAL CROSS SECTION 4

NOT TO SCALE

FIGURE 5-5

PAGE 106 OF 198

Figure 5 - SCPTU Log and Stratigraphic Formation Identification for MFFF Section 4
(Figure 5-5 from DCS, 2001)

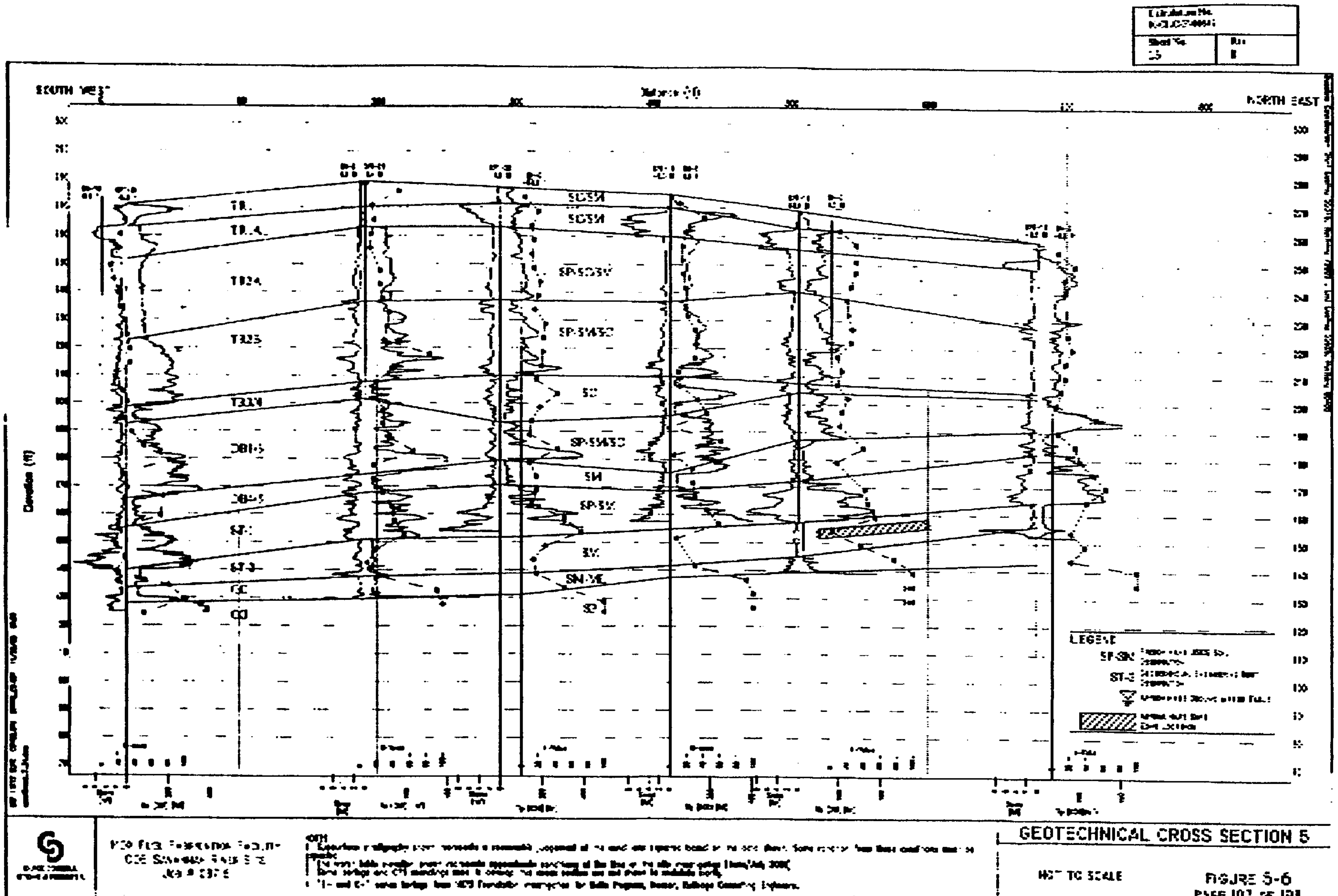

Figure 6 - SCPTU Log and Stratigraphic Formation Identification for MFFF Section 5
(Figure 5-6 from DCS, 2001)

Sheet No. 34	Rev. 0

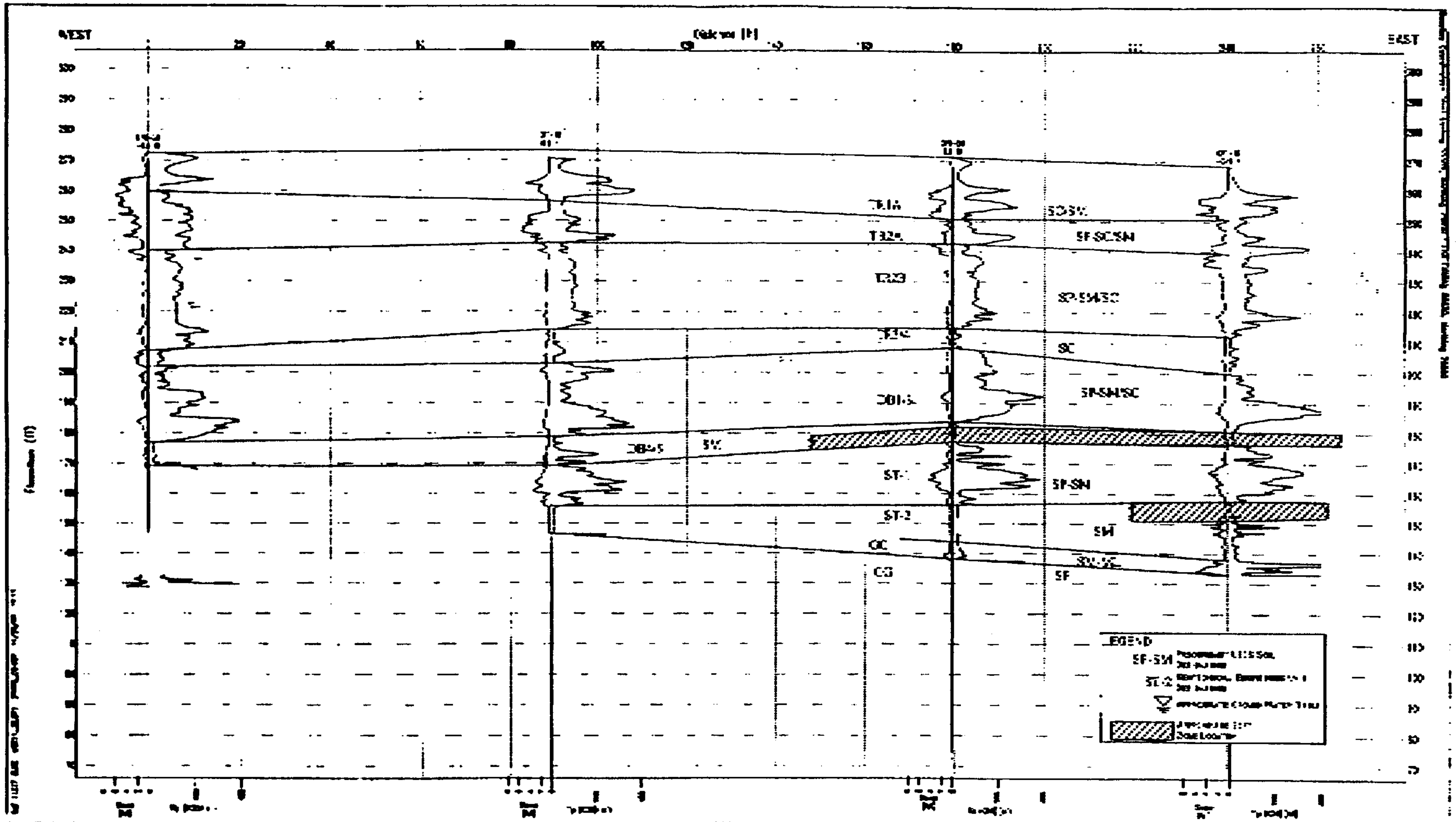

MOX FUEL FABRICATION FACILITY DCS Savannah River Site	NOTES:	GEOTECHNICAL CROSS SECTION 6	
		NOT TO SCALE	FIGURE 5-7 PAGE 106 OF 193

Figure 7 - SCPTU Log and Stratigraphic Formation Identification for MFFF Section 6 (Figure 5-7 from DCS 2001)

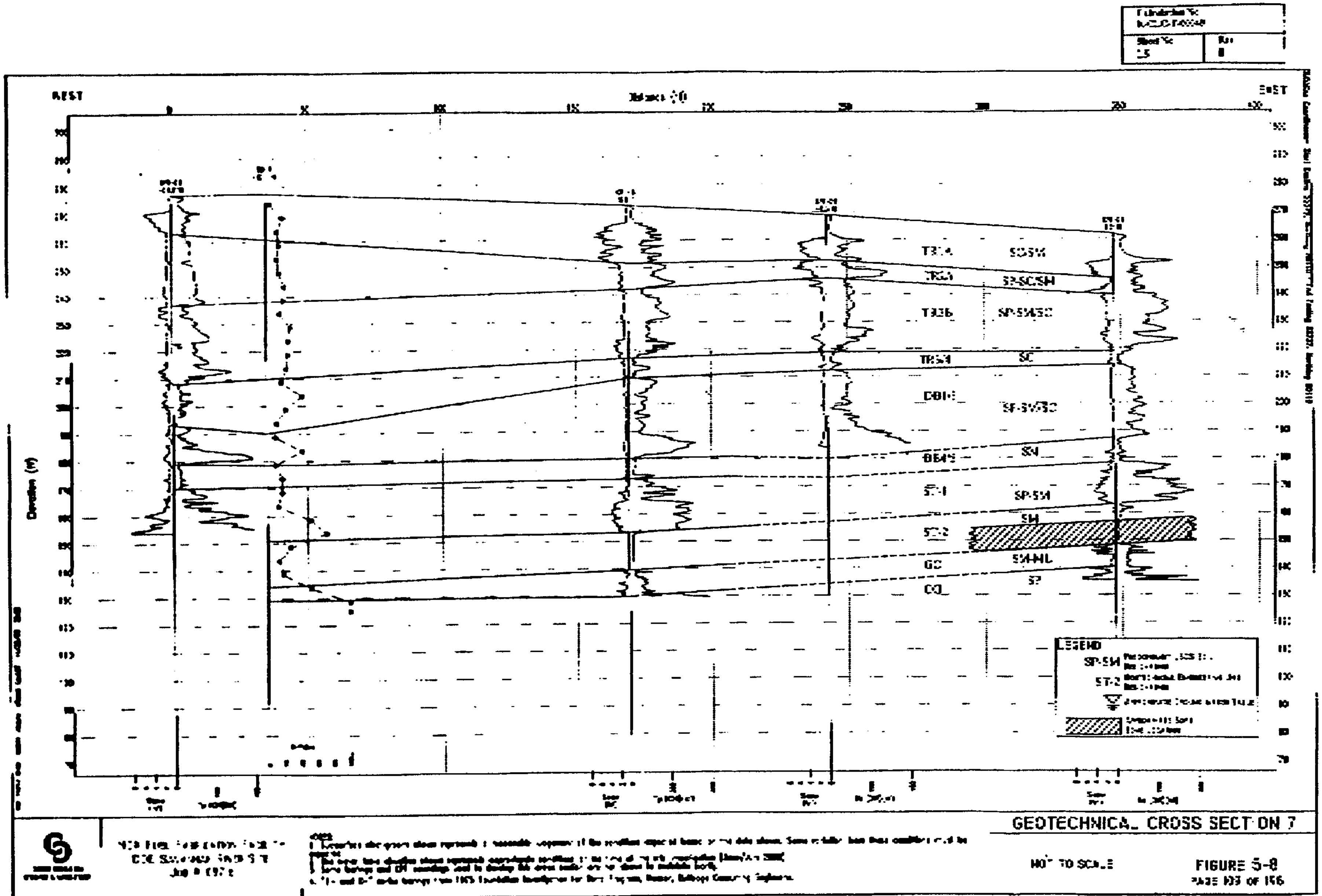

Figure 8 - SCPTU Log and Stratigraphic Formation Identification for MFFF Section 7
(Figure 5-8 from DCS 2001)

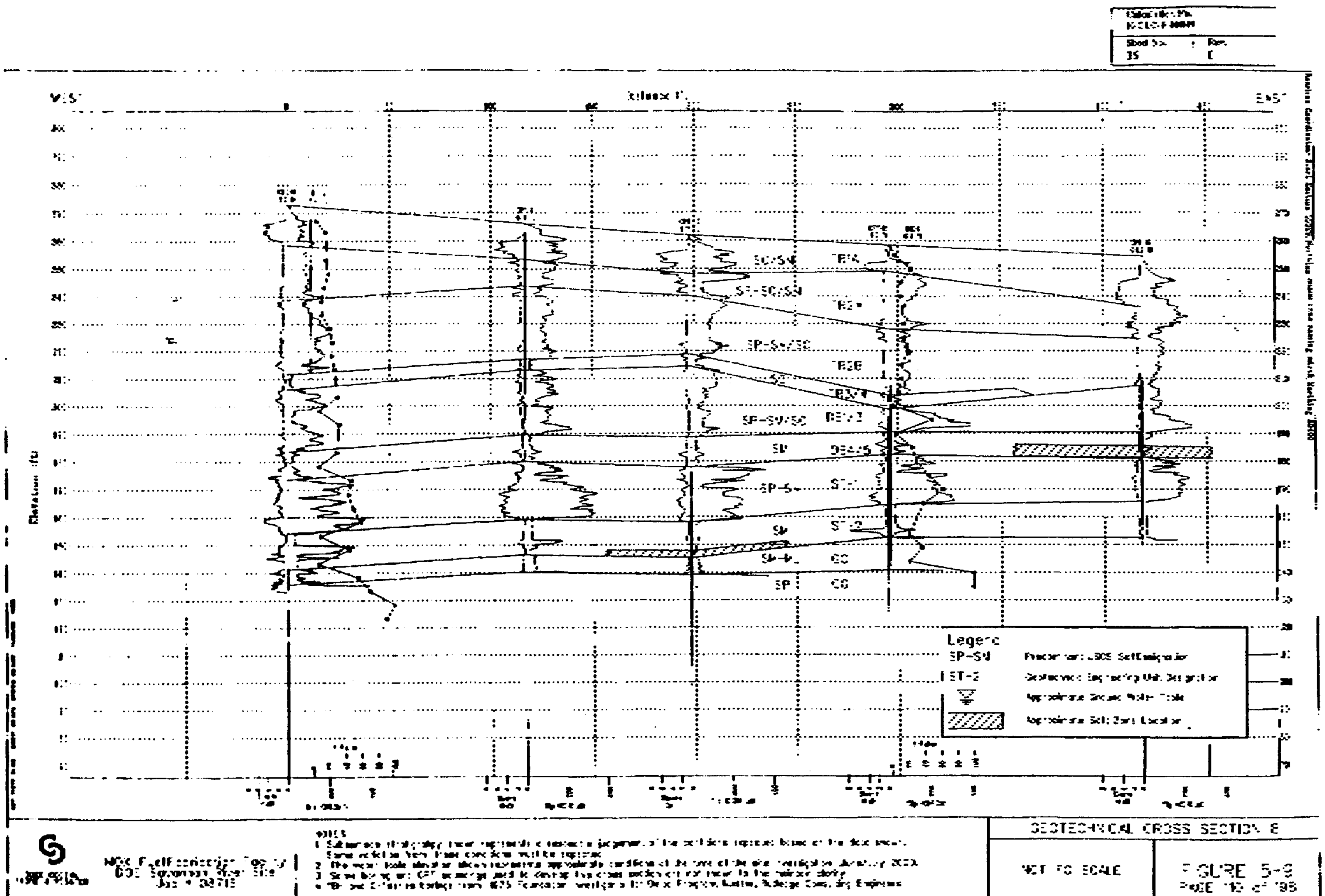

Figure 9 - SCPTU Log and Stratigraphic Formation Identification for MFFF Section B
(Figure 5-8 from DCS, 2001)

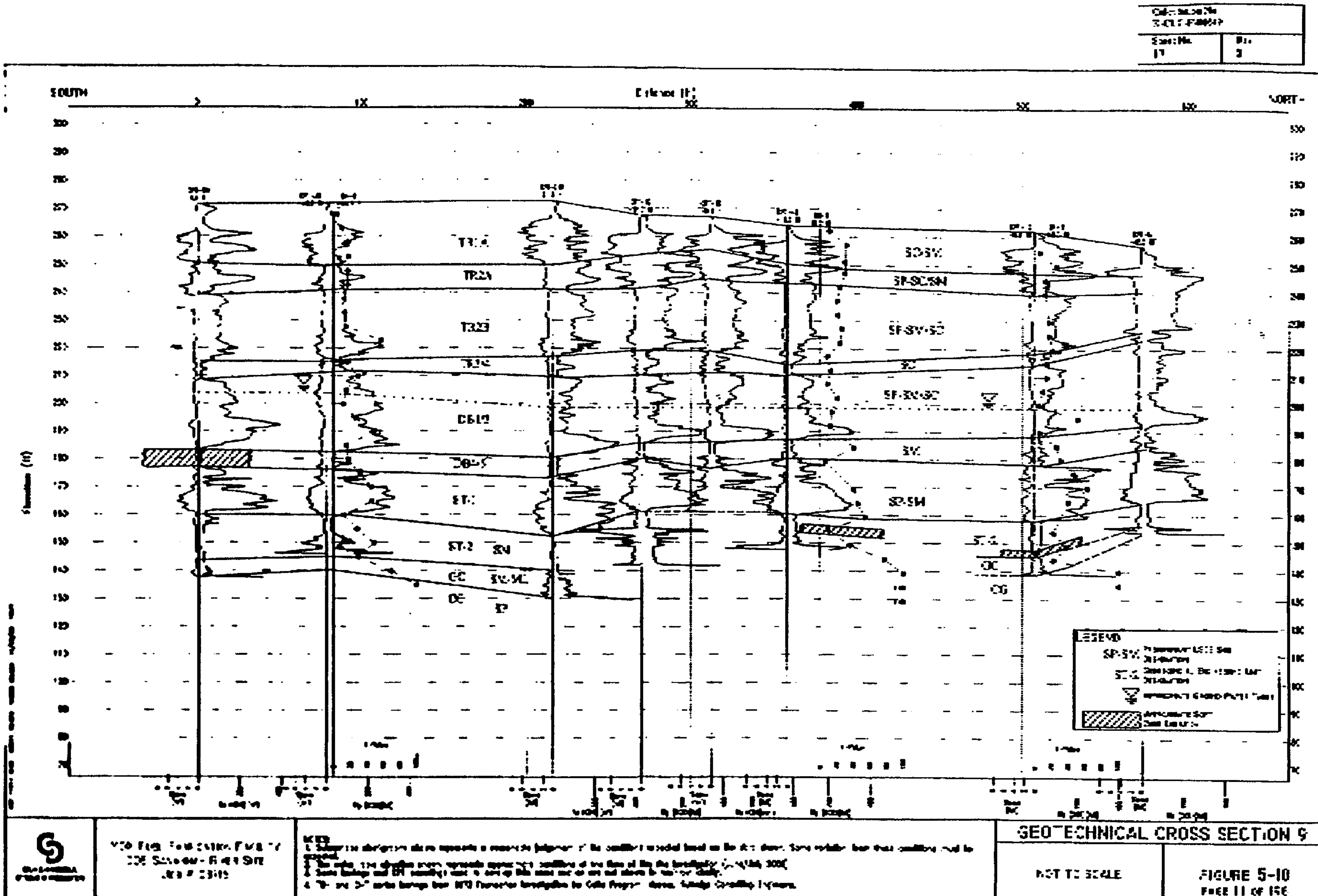

Figure 8 - SCPTU Log and Stratigraphic Formation Identification for MFFF Section 9
(Figure 5-10 from DCS, 2002)

Calculation No. K-CLC-F-00049	
Sheet No. 18	Rev. 0

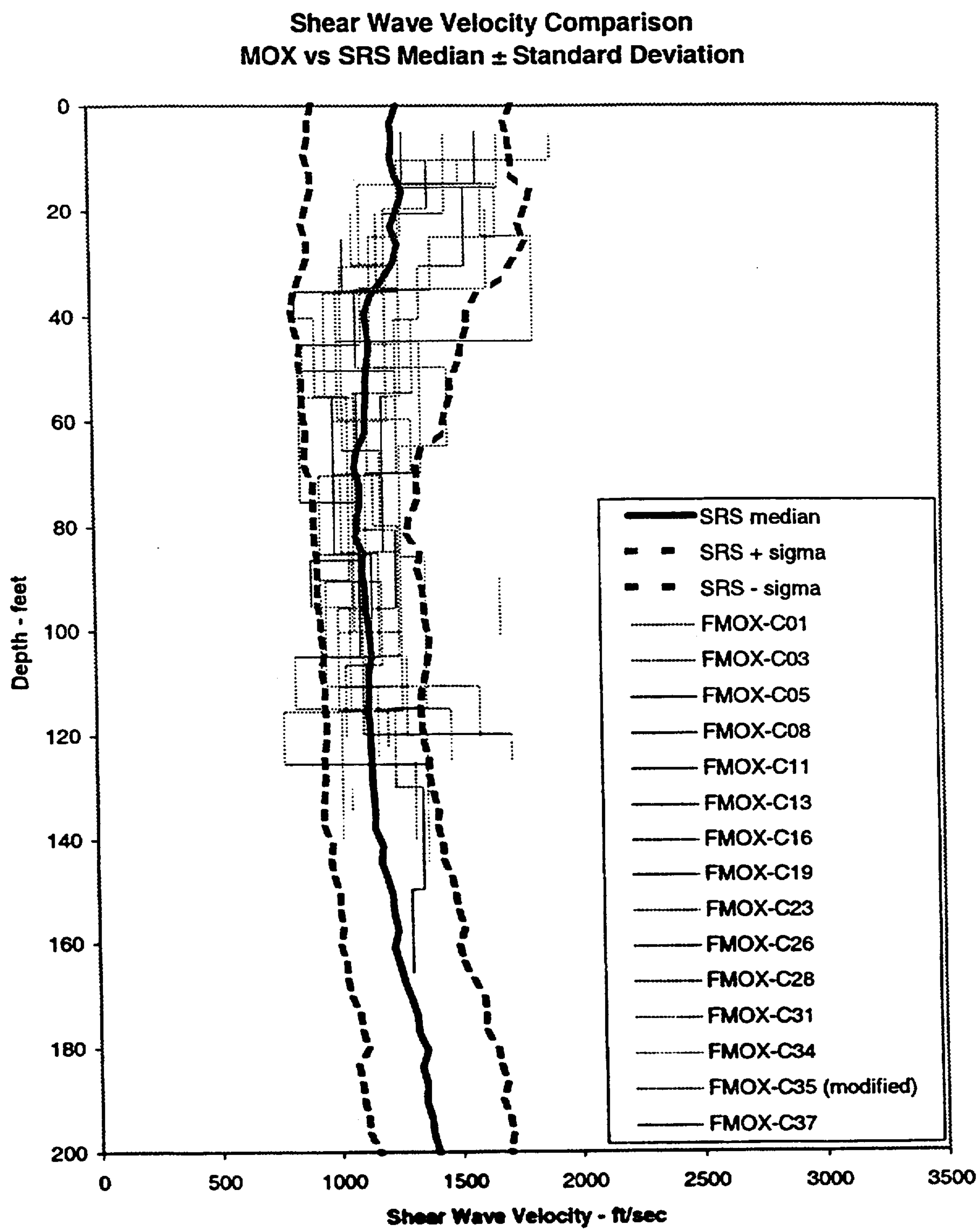

Figure 11 - Comparison of MFFF Measured SCPT Shear-Wave Profiles with Statistical Median and ± σ Derived from Velocity Profiles Used in Developing SRS Response Spectra (data from DCS, 2000 and Toro, 1997)

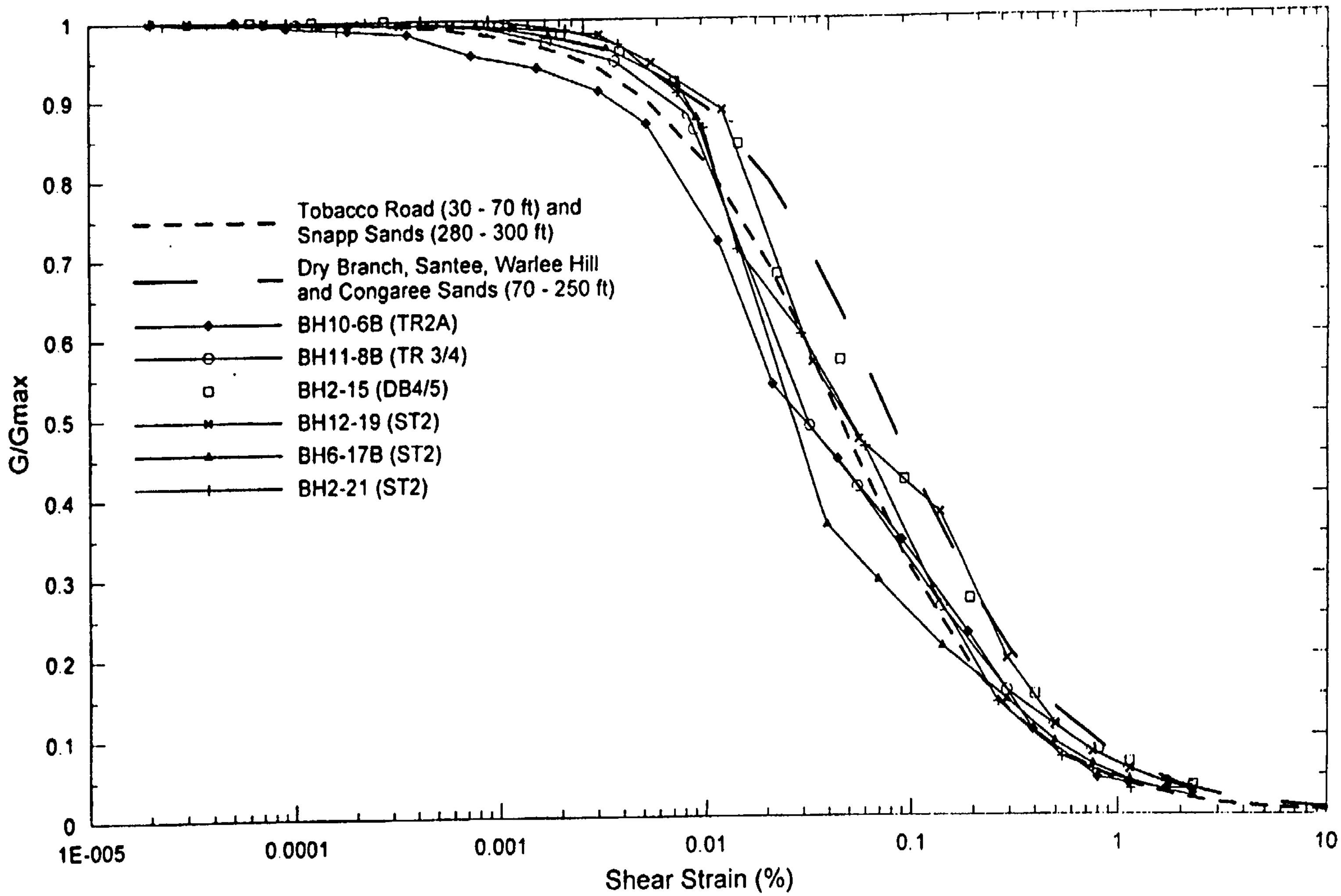

Figure 12 - Comparison of MFFF Site-Specific and SRS-Recommended Shear Modulus Reduction Curves for Sands
(Figure 6-6 from DCS, 2001)

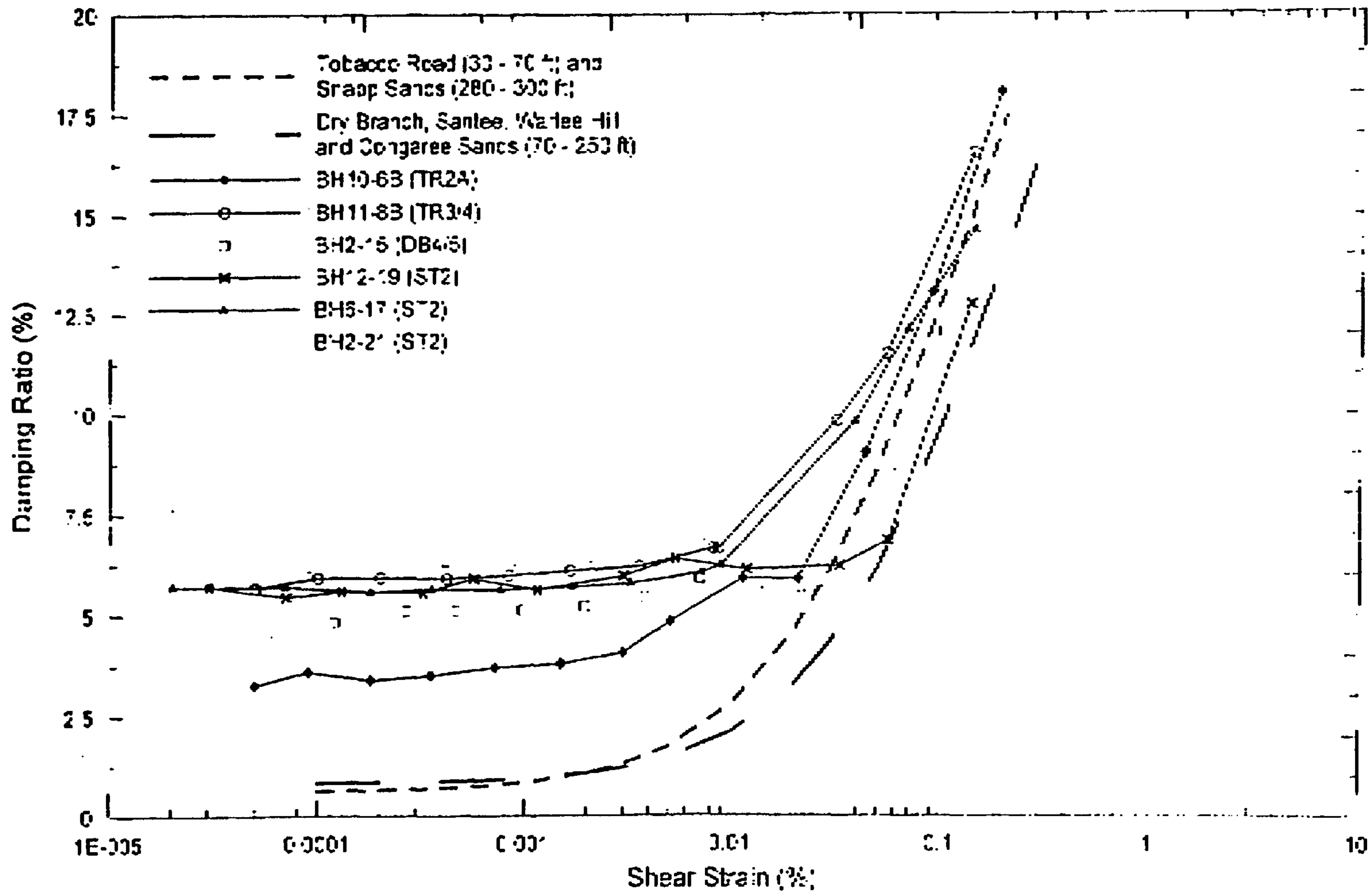

Figure 13 - Comparison of MFFF Site-Specific and SRS-Recommended Damping Ratio Curves for Sands
(Figure 6.7 from DCS, 2001)

Calculation No. K-CLC-F-00049	
Sheet No. 20	Rev. 0

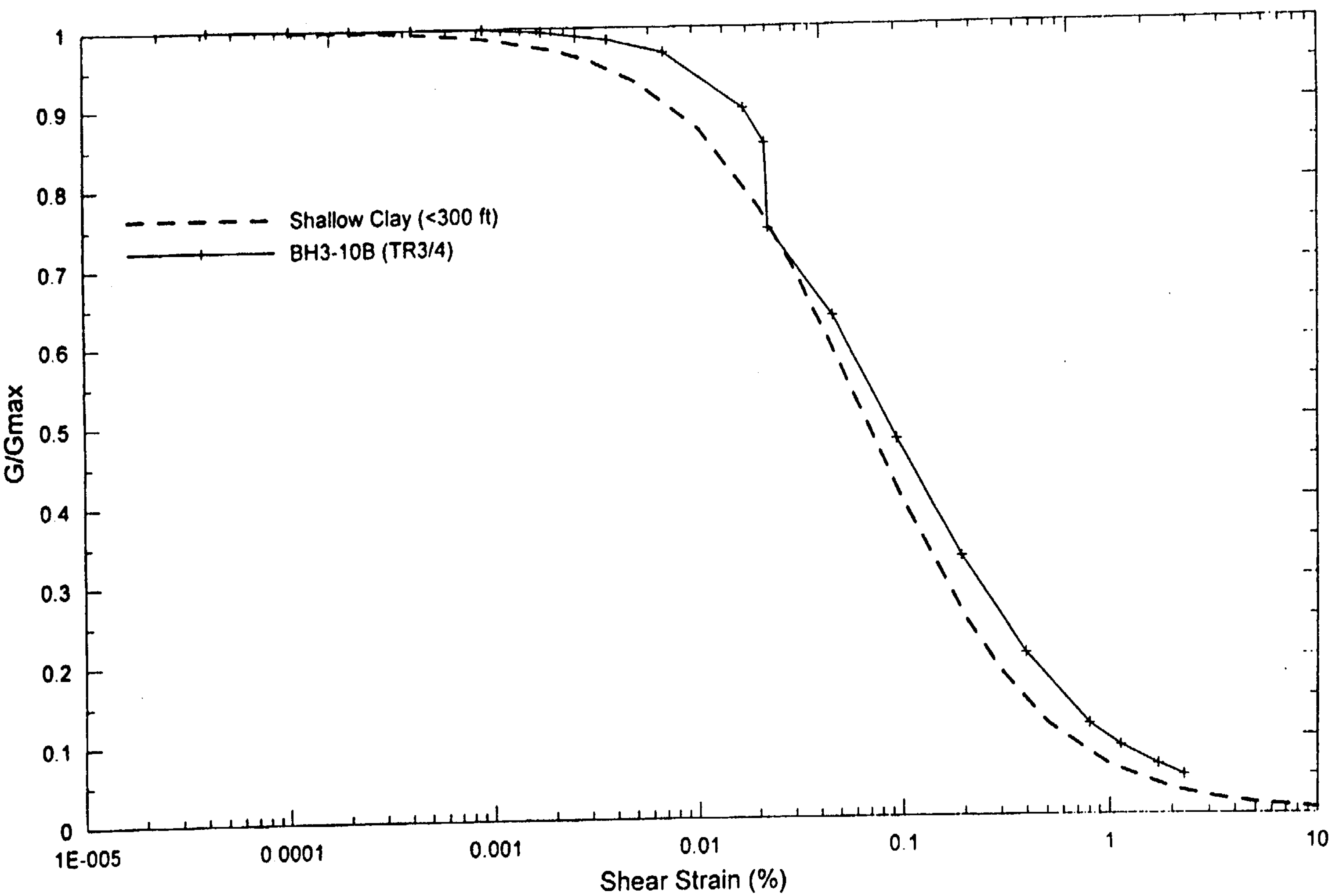

Figure 14 - Comparison of MFFF Site-Specific and SRS-Recommended Shear Modulus Reduction Curves for Clays
(Figure 6-8 from DCS, 2001)

Calculation No. K-CLC-F-00049	
Sheet No. 21	Rev. 0

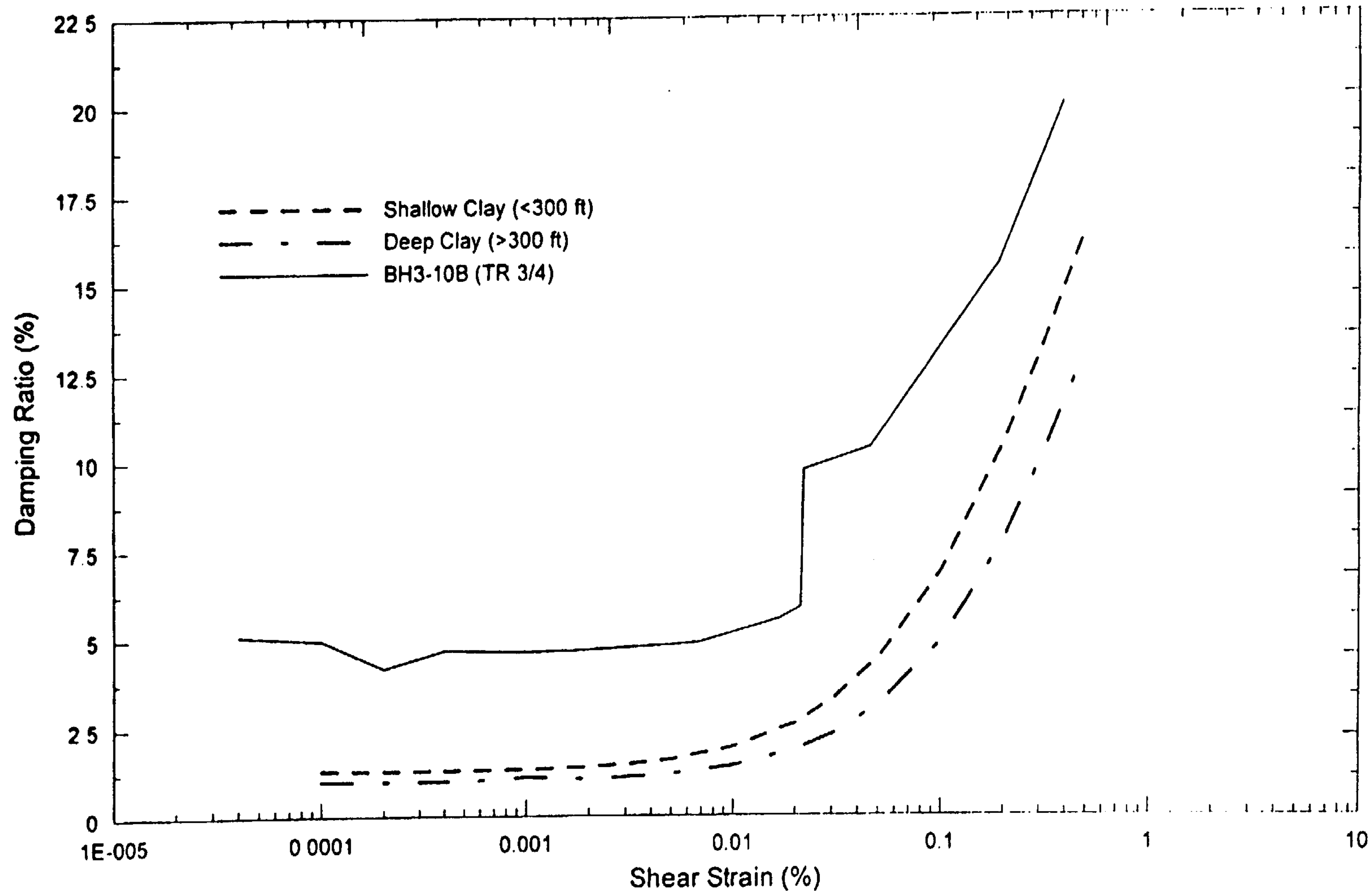

Figure 15 - Comparison of MFFF Site-Specific and SRS-Recommended Damping Ratio Curves for Clays (Figure 6-9 from DCS, 2001)

Calculation No. K-CLC-F-00049	
Sheet No. 22	Rev. 0

Appendix A – Engineering Stratigraphy

Information obtained from the field exploration has been used to establish the engineering stratigraphy for the subsurface (surface to about 180 feet in depth) for F-Area and at the MOX Fuel Fabrication Facility (MFFF) (WSRC, 2001). The subsurface engineering stratigraphy was determined from CPTU measurements including tip resistance, sleeve resistance, friction ratio, and pore pressure signatures, as well as correlation with adjacent soil borings. The layering system is based on observed changes in the CPTU measurements that correlate between CPTU soundings and nearby borings. The layer nomenclature was developed for mapping subsurface units across various parts of the SRS. It is only used to differentiate units based on similar engineering characteristics that can be mapped in the investigation area. A generalized cross section for the MFFF site is shown on Figure A1. Figure A1 illustrates thickness of engineering layers and geologic formations, and how engineering layers at the MFFF site correlate with geologic formations.

The layer nomenclature follows an alphanumeric system with layer numbers increasing from top to bottom. Subdivided layers are identified with a letter designation (e.g., TR1A). Some layer boundaries correspond to geologic formations. Layer TR1 is most probably the Altamaha formation. In fact, some upper portion of Layer 1A may also be Altamaha. However, due to the similar material properties and an irregular erosional surface that separates these units, defining the contact between the Altamaha and Tobacco Road formation is difficult. In some parts of the F-Area, the TR1 and TR2 layers have been subdivided to recognize sublayers with distinct soil properties (TR1A, TR2A, and TR2B). As described in the F-Area Geotechnical Characterization Report (WSRC, 1996), the TR3/4 layer was first correlated to the lower portion of the Tobacco Road formation but based on more recent geologic investigations in the area has been reassigned to the upper portion of the Dry Branch formation. Layers DB1 through DB3 were combined into a DB1/3 layer because of similar properties. Likewise, layers DB4 and DB5 were combined into a DB4/5 layer. The DB1/3 layer corresponds to the Dry Branch formation while the DB4/5 layer corresponds to the upper Santee/Tinker formation. The Santee/Tinker formation is the most variable layer in the shallow subsurface. It has been further subdivided into the ST1 and ST2 layers where practical. The green clay, an informal stratigraphic interval at the SRS, is considered the base unit for the shallow engineering stratigraphy and is labeled as GC. This geologic unit is locally continuous and provides a reliable marker bed. The Green Clay overlays the Congaree Formation which is predominantly dense silty sands.

The following sections describe the physical attributes used to delineate each layer, as well as, depositional environment and lithologic variability.

TR1 Layer

The TR1 layer is most probably the Altamaha formation consisting of red, purple and brown poorly sorted sands ranging from fine to gravel size with the dominant soil classification being clayey to silty sands (SC to SM). The depositional environment of these sediments is characterized as high energy fluvial such as river and stream channels. The base of the Altamaha is distinguished by an irregular erosional surface and can reach thicknesses of up to 70 feet at the

SRS. The TR1 layer is characterized by moderate CPTU tip resistances and relatively high friction ratios.

TR1A and TR2A Layers

The TR1A and TR2A layers have been used to differentiate the Tobacco Road formation. Sediments of the Tobacco Road formation were deposited in low energy shallow marine transitional environments such as tidal flats. Much of the sediments are laminated or otherwise bioturbated (mixed by burrowing organisms after deposition) red, purple and brown poorly sorted sands and clayey sands.

The TR1A, and TR2A layers are predominantly clayey sands and sands (SC/SM to SP-SC/SM) as determined by laboratory classification tests. The TR2A layer is distinguished from the overlying TR1A layer by increased tip resistance and notably lower sleeve friction values resulting in a lower friction ratio.

TR2B, TR3/4, and DB1/3 Layers

The Dry Branch Formation consists of sands and clays deposited in a transitional sequence between near shore and bay or lagoon environments. The upper contact of the TR2B layer is defined by an increase in tip resistances. The TR3/4 layer is defined by a marked decrease in CPTU tip resistance and an increase in both the friction ratio and pore pressure measurements. As determined by laboratory classification tests, the TR2B layer consists of sands with minor amounts of clay and silts (SP-SC/SM) and the TR3/4 layer is predominantly clays and sandy clays (SC).

The DB1/3 layers correspond to the Irwinton Sands. On the CPTU logs, the DB1/3 layer is a zone of variable, but generally high, CPTU tip resistances and low friction ratios. In general, pore pressures are low or slightly above hydrostatic. The dominant unified soil classification for the DB1/3 is SP-SM with minor layers of CL material occurring as laminations.

DB4/5, ST1 and ST2 layers

The Santee/Tinker Formations represent the most complex geologic unit in the shallow subsurface of F-Area. It is depositionally complex and highly variable in both its lithology and material properties. Soils in the Santee/Tinker range from sands to silty sands (SP-SM). The contact between the Santee/Tinker Formation and the overlying Dry Branch Formation is generally seen on the CPTU logs as a sharp decrease in the pore pressure measurement. This layer is characterized by thin, alternating layers of low and high CPTU tip resistances and friction ratios. Characteristically, CPTU soundings in this layer show a pronounced sawtooth trace with large variations over relatively small vertical intervals. This highly variable pattern suggests interfingering of alternating lenses of clayey and silty sands with more resistant, silica-cemented sediments and less resistant, calcareous sediments, and appears to be a result of rapid lateral and vertical changes in the nature of the materials originally deposited in this interval. The unit consists of complex sequences of limestones, carbonate muds, carbonate sands, and muddy sands.

The soils of the DB4/5 interval are much more plastic than the overlying Irwinton Sand (DB1/DB3) and the underlying ST1 layer. Soils of the DB4/5 typically classify as SM to CL materials. The DB4/5 layer has moderate to low tip resistances and moderate friction ratios. The DB4/5 layer has been subject to extensive characterization within the APSF area because of observed soft zones (tip resistances less than 15 tsf and N-values of 5 or less). The ST1 layer is characterized by higher tip resistances than the overlying DB4/5 layer underlying ST2 layer. Not all soundings penetrate this layer. Soils of the ST2 layer are generally characterized by lower tip resistances and sleeve resistances than the overlying ST1 layer. Soils of the ST1 and ST2 layers generally classify and SM to SP-SM materials.

GC Layer
The "green clay" (GC) is an informal stratigraphic name at SRS for stiff, green to gray clays, silts, and clayey sands that are commonly found at the base of the Santee/Tinker Formation. In general, these soils classify as SM to ML with varying amounts of clay. This layer is locally continuous at F-Area and has been used to define the lower boundary of the shallow stratigraphy. Layer elevations and thicknesses have been determined from those borings and soundings that penetrate this layer. Most borings and CPTU soundings do not reach or penetrate the GC layer. The top of the layer ranges from around El. 126 feet MSL in the south and northwestern portions of the area to a high of around 140 feet MSL in the east-central part of the area. This is consistent with the correlating Gordon Confining Unit as mapped by Aadland (1995) which corresponds to the "green clay" unit.

References

Aadland, R. K., Gellici, J. A., and Thayer, P. A., 1995. *Hydrogeologic Framework of West-Central South Carolina*, S. C. Department of Natural Resources, Water Resources Division, Report 5.

WSRC 1996. *F-Area Geotechnical Characterization Report*, WSRC-TR-96-0069, Rev. 0, September 1996.

WSRC, 2001. *Determination of Stratagraphic Tops for F and H Area Tobacco Road, Dry Branch and Santee Formations*, K-CLC-G-00069, Rev. 1, January 2001.

Calculation No. K-CLC-F-00049
Sheet No. 26
Rev. 0

GEOLOGIC FORMATION	ENGINEERING LAYER	Bottom Elevation (feet MSL)
		276.0 (±11.9) Ground Surface
ALTAMAHA FORMATION	TR1	271.0 (±5.0)
TOBACCO ROAD FORMATION	TR1A	258.7 (±3.9)
	TR2A	239.7 (±4.5)
DRY BRANCH FORMATION	TR2B	214.0 (±5.9)
	TR3/4	206.6 (±6.5)
	DB1/3	182.8 (±6.0)
SANTEE/TINKER FORMATION	DB4/5	173.5 (±6.1)
	ST1	156.4 (±6.7)
	ST2	140.4 (±3.3)
WARLEY HILL FORMATION	GC	

Numbers shown are averages, numbers in parentheses are standard deviations.

Figure A1 - Generalized Cross Section for the MFFF Site

Development of MFFF-Specific Vertical-to-Horizontal Seismic Spectral Ratios

By

R. C. Lee

UNCLASSIFIED
DOES NOT CONTAIN
UNCLASSIFIED CONTROLLED
NUCLEAR INFORMATION
~~ADC &~~ Reviewing Official: C. G. Reeves/RO
(Name and Title)
Date: 8/13/01

Westinghouse Savannah River Co.
Savannah River Site
Aiken, SC 29808

Site Geotechnical Services
Geotechnical Engineering Section

Approved by: M. R. Lewis

M. R. Lewis, Manager, Geotechnical Engineering Section

L. A. Salomone

L. A. Salomone, Site Chief Geotechnical Engineer

R. R. Beckmeyer, Manager, Site Geotechnical Services Dept.

DISCLAIMER

Executive Summary

Significant advances have been made during the past ten years in understanding the amplitude of vertical seismic response spectra relative to horizontal response spectra (V/H). Recent observations of vertical and horizontal spectra at strong motion recording sites in the western United States (WUS) demonstrate the importance of considering the vertical to horizontal seismic spectral ratio (V/H) in the design of new facilities. Soil sites that were in close proximity to an earthquake or subject to a large magnitude earthquake exhibited high V/H seismic spectral ratios. These studies have shown that there is significant variation of V/H with response spectral frequency. Earthquake magnitude, earthquake source mechanism, distance to the earthquake source, regional crustal rock properties and site geology all contribute to this variation. Because of this improved understanding of the importance of considering the vertical component of an earthquake, Duke-Cogema Stone and Webster (DCS) asked Westinghouse Savannah River Company (WSRC) to perform a study of the relative magnitude of the vertical component of earthquake motion for the MOX Fuel Fabrication Facility (MFFF).

The purpose and scope of the study was to establish the vertical-to-horizontal seismic spectral ratio specific to the MFFF site for an appropriate range of selected response frequencies. To accomplish this purpose, WSRC used WUS empirical V/H relationships that are earthquake magnitude and distance dependent. These empirical relationships were then corrected for MFFF site conditions using site properties consistent with the development of SRS-specific design spectra (WSRC, 1997). The computational model used for the site correction was developed for the Electric Power Research Institute (EPRI) in 1993. The site correction model has been validated using strong motion recordings at sites in the WUS (EPRI, 1993). To account for the specific magnitude and distance dependence affecting the SRS hazard, the United States Geological Survey (USGS) (Frankel, 1999) bedrock hazard disaggregation with an annual probability of 10^{-4} was used to properly weight the corrected V/H.

Several important assumptions regarding wave propagation through the soil and the linear (low-strain) response of the soil are made in the implementation of the V/H modeling. The linear assumptions as well as assumptions about the level of the water table can strongly influence the model-derived V/H.

The results of the study show that;

- V/H varies with frequency
- MFFF site (deep soil eastern U.S. site) V/H shows a stronger dependency on earthquake magnitude and distance than does the WUS empirical V/H primarily because of the effects of a deep water table enhancing the vertical component motions
- Application of the SRS hazard disaggregation to the earthquake magnitude and distance dependent V/H is an objective way to provide a smooth site-specific V/H that adequately accounts for SRS earthquake hazards
- For frequencies greater than about 3 hz, the MFFF site-specific V/H is greater than the standard (ASCE 4-86) used by SRS

Based upon the empirical data used, the corrections to that data, and the earthquake magnitudes and distances that control the evaluation, the MFFF V/H are considered best estimate values. However, consistency with V/H observations is the key measure of the acceptability of the technical results presented herein. Because of limited observed values of V/H in the eastern U.S., the uncertainty of the results presented in Figure 8 is unknown. Thus, use of the results requires caution until additional sensitivity studies can be completed and the uncertainties quantified.

Introduction

This report documents a site-specific assessment of the ratio of vertical and horizontal component response spectra for the MFFF. This study is based on observations of vertical and horizontal spectra at strong motion recording sites in the western U.S. (WUS), with corrections for eastern U.S. (EUS) conditions, SRS-specific bedrock and soil properties and MFFF site conditions. In addition, the SRS probabilistic hazard disaggregation is included in the evaluation, so that appropriate earthquake magnitudes and distances are incorporated into the vertical component spectrum. This study was originated to address and validate the preliminary vertical component design basis.

This study was performed using the SRS-specific dynamic and material property database documented in WSRC (1997) and probabilistic hazards assessments reported in WSRC (1998) and WSRC (1999a). Transfer functions to correct the existing WUS empirical database for EUS site conditions were provided under contract by Pacific Engineering and Analysis.

Although SRS guidelines exist for V/H (WSRC, 1997), there have been no site-specific assessments made for V/H. Current SRS guidelines for V/H design are that the vertical response spectrum should be taken as 2/3 of the horizontal, based on ASCE 4-86 recommendations (also consistent with Newmark and Hall, 1978). New requirements in ASCE 4-98 are being reviewed along with site-specific studies that will likely alter the current SRS guidelines for assigning a V/H ratio to the SRS PC-3 site free-field spectra. A guideline incorporating oscillator frequency dependence is Regulatory Guide 1.60 (USNRC, 1977) where V/H is 1.0 for higher oscillator frequencies ($f > 3.5$ Hz) and V/H is 2/3 for lower oscillator frequencies ($f < 0.25$ Hz).

Scope of Work

The scope of work was to establish an MFFF-specific V/H by applying MFFF-specific and EUS crust corrections to empirical WUS data for V/H. The USGS hazard disaggregation was used to define the composition of the hazard by earthquake magnitude and distance. The complete scope of work for this task as it appears in the Work Task Agreement (WTA) with DCS is contained in Attachment 1.

The tasks performed by WSRC and subcontractor to produce this report were conducted in accordance with the WSRC QA Program and requirements specified in WTA-023, Revision 1.

Empirical Estimates of V/H

Recent investigations of measured WUS vertical and horizontal spectra have indicated that V/H has strong dependencies on oscillator frequency, earthquake magnitude and distance, and site response (Bozorgnia et al., 1999, Abrahamson and Silva, 1997, and Campbell, 1997). The ratio between the vertical and horizontal response spectrum can be evaluated in two ways: (1) evaluate the vertical to horizontal response spectral ratio and statistically summarize all observations; or (2) statistically summarize the vertical and horizontal components separately and ratio the result (the method employed by Abrahamson and Silva, 1997). Bozorgnia et al. (1999) found that computation of V/H using the latter approach (2) provides an unbiased estimator although the alternate scheme of regressing on observed spectral values of (V/H) instead of V and H separately gave consistent results.

As an example of empirical V/H exhibiting oscillator frequency and earthquake distance dependence, Figure 1 illustrates V/H for moment magnitude (Mw) 6.5 WUS earthquakes for soil sites at distances of 10, 20, 40 and 100 km (Abrahamson and Silva, 1997). The regressions are well constrained for Mw 6.5 at the range of distances shown. Figure 1 shows that for frequencies less than 3 Hz, V/H is relatively low (< 0.5), and increases for increasing oscillator frequency and decreasing earthquake distance. At higher frequencies, V/H increases to about 1.7 (in the 10-20 Hz frequency range) for a Mw 6.5 at 10 km. Similarly, Figure 2 illustrates empirical V/H for earthquake magnitudes (Mw) 5.0, 5.5, 6.0, 6.5, 7.0 and 7.5 at a distance of 20 km. V/H in these cases show that that at lower frequencies, V/H is relatively low (about 0.5), and increases for increasing oscillator frequency and increasing earthquake magnitude. Bozorgnia et al. (1999) have shown that rock site V/H shows less magnitude and distance dependence than soil sites, suggesting non-linear behavior in the soils as a likely mechanism for the dependencies. Figures 1 and 2 also show that a design basis using a constant V/H over a wide range of frequencies is not supported by empirical data.

Silva (1997) has made a number of important observations about V/H and has been successful at modeling V/H for the 1989 Loma Prieta, 1994 Northridge and 1992 Landers earthquakes. Noting the character of WUS rock and soil time histories, he observes that: (1) for rock sites at near epicentral distances, vertically-polarized shear-waves (SV) dominate the vertical component and are phased about the same time as horizontally-polarized shear-waves (SH) on the horizontal components; (2) for soil sites at near-epicentral distances, the vertical component is dominated by compressional (P) waves arriving earlier than the dominant horizontal shear (S) waves and having more high frequency; and (3) for distant rock and soil sites, the vertical component is dominated by compression waves. Because generally lower amplitude P- and SV-waves dominate the vertical motions, induced dynamic strains are lower as compared to the dynamic strains induced by generally higher amplitude SH-waves that dominate the horizontal motions. The higher strains induced by SH-waves may induce non-linear behavior which would reduce horizontal amplitudes. This is especially important in the range of distances where angles of incidence become steep enough that SV-waves transition to SH-waves (Silva, 1997). The consequence is that with increasing earthquake magnitude or with decreasing distance from the earthquake source non-linear effects, especially for soil sites, may cause significantly large V/H values, particularly at higher response spectra frequencies. This effect is apparent in the empirical V/H results shown in Figures 1 and 2.

The WUS earthquake spectra also exhibit consistent trends (Silva, 1997): (1) vertical component spectra for both rock and soil sites exhibit a high frequency shift relative to the horizontal components, which can be explained by differences in vertical and horizontal site attenuation; (2) the horizontal component shows more low-strain damping than the vertical component; and (3) with increasing shear strain (closer and/or larger earthquakes), horizontal component spectra shapes also exhibit a shift to longer periods which can be explained by the nonlinear response of the soil.

In addition to the V/H trends based on the WUS data, there are well-documented differences in the spectral content of EUS earthquake recordings (EPRI, 1993). Although there are limited data in the EUS, available data show that eastern rock recordings of both the vertical and horizontal components are richer in high frequency energy. This observation is attributed to differences in crustal attenuation and damping. Thus, an MFFF-specific V/H design that is based on empirical WUS data, including earthquake magnitude and distance dependency, must be corrected for SRS crust and soil conditions to appropriately account for differences between the EUS and WUS spectral content.

In summary, strong motion data are extremely limited in the EUS, and any modeling done must account for the observations discussed above and site-specific data. For the MFFF, the model is based on SRS-specific conditions, such as crust and soil velocity, crustal attenuation (Q), site damping, and strain-dependent soil properties. Modeling techniques, successfully used to model observations of V/H in the west, are used to predict V/H for the MFFF. These modeling techniques, described in EPRI (1993), are the most credible techniques available.

Development of V/H Transfer Functions for the MFFF

The computational model used to estimate V/H for this study is that described in EPRI 1993. The model has been validated against measured observations using strong ground motion recordings at sites in the WUS, and has been recommended for modeling V/H at central and eastern U.S. (CEUS) sites (EPRI, 1993). For purposes of applying the model to compute the MFFF site-specific V/H, a WUS-to-EUS V/H transfer function is derived in this study. A number of modeling assumptions have been made based on the validations: (1) vertical motions are modeled as a combination of pure SV-waves and SV-P converted waves arriving at the base of the soil/alluvial materials at inclined angles of incidence computed using ray tracing methods; (2) horizontal component spectra are computed assuming pure SH-waves arriving at vertical incidence; (3) linear elastic analysis is assumed for computing the vertical motions; (4) low strain behavior (i.e. no wave induced dynamic strain degradation) compressional and shear wave site velocity profiles are used in computing vertical spectra; (5) damping for computing vertical spectra is the low strain level damping used to compute horizontal spectra; (6) for computing horizontal motions, wave induced dynamic strain degradation of the shear wave velocity and increased damping of the profile is permitted (in an equivalent linear analysis). The consequence is that model-derived V/H values particularly for the MFFF site, may be conservatively high over some range of spectral frequencies and at high loading levels. If these conservative assumptions affect the model-derived V/H values for the MFFF site more than the model-derived generic V/H values for the WUS, the derived MFFF site-specific V/H values would be conservative by an unknown amount over some frequency range. Parametric assessments on input parameters used in the V/H computations (recommended below) will assist in understanding these uncertainties and possible conservatisms.

To correct the WUS empirical V/H for each earthquake magnitude and distance relevant to the MFFF, a frequency-dependent transfer function is computed for: (1) generic WUS soil sites, approximating the conditions at the soil recording sites ($V/H_{wus}(f)$); and (2) generic SRS site conditions ($V/H_{MFFF}(f)$) (note that SRS-specific velocity profiles and dynamic properties and the MFFF-specific water table depth were used in the computations). These transfer functions are applied to the empirical $V/H_{emp}(f)$ (Figure 1) as follows:

$$V/H_{corr}(f) = \underbrace{[V/H_{MFFF}(f) \,/\, V/H_{wus}(f)]}_{\text{V/H Transfer Function}} * V/H_{emp}(f) \qquad (1)$$

V/H Transfer Function

Figure 3 illustrates the resulting model V/H for WUS Mw 6.5 earthquakes for soil sites using WUS velocity profiles (derived for Geomatrix C and D site conditions; Silva, 1997) and crustal conditions. Table 1 summarizes the soil and crustal parameters used in the development of the model. Comparison of the soil model V/H (Figure 3) and empirical V/H (Figure 1) shows generally good agreement although the model V/H is broadened at higher frequencies and V/H is somewhat smaller for lower frequencies. There is, however, a very close comparison between the modeled and empirical results that validates the modeling approach.

Figure 4 illustrates the results of applying the model V/H for SRS soil and crust conditions and MFFF water table elevation (V/H_{MFFF}) for Mw 6.5 earthquakes. Table 2 summarizes the SRS soil and crustal parameters used for the model. Note that very high V/H are possible at higher frequencies and for close earthquake distances owing to the high horizontal component soil loads and consequent reduction in horizontal amplitude levels as compared to the increasing vertical component motions modeled linearly. An additional condition at the MFFF is the effect of a deep (60-70 ft below grade) water table on the vertical component motions. At the water table elevation a significant impedance contrast exists for vertically propagating P-waves. This P-wave velocity contrast induces a P-wave resonance between the surface layers and the water table elevation, also significantly increasing V/H. A water table depth of 70 ft below finished grade was taken based on cross sections 1 through 4 given in DCS (2001). Note that the effect of the water table depth is included in the analysis as a contrast in Poisson's ratio in the soil column, resulting in a significant contrast in the P-wave velocities above and below the water table. Also note that the water table effect is implicit in the WUS model.

To illustrate the steps used to incorporate Equation (1) for the MFFF, a Mw 6.0 earthquake at 40 km is considered. Figure 5a shows the empirical WUS soil V/H for a Mw 6.0 at 40 km. Figure 5b shows the computed WUS model V/H for a Mw 6 at 40 km. The WUS model results were computed using the WUS soil models and modeling parameters shown in Table 1. Figure 5c shows the MFFF model V/H for a Mw 6 at 40 km. The MFFF model uses the SRS crust and soil models used previously with modeling parameters shown in Table 2 together with a Poisson's ratio that reflects the depth of the water table. Figure 5d illustrates the ratio of the MFFF-to-WUS V/H ratios. The result of Equation 1 is illustrated in Figure 5e where the transfer function (Figure 5d) is applied to the empirical V/H (Figure 5a).

To illustrate the magnitude and distance dependence in the MFFF specific V/H, Figure 6 illustrates the results of applying Equation (1). Figure 6a shows the MFFF V/H for a Mw 5.0 at distances of 10, 20, 40 and 100 km. The effects of nonlinearity on the horizontal component are most obvious at frequencies greater than 5 Hz. The effects of increasing magnitude are illustrated for magnitudes 5.5, 6.0, 6.5, 7.0 and 7.5 in Figures 6b, c , d, e respectively for the same earthquake distances of 10, 20, 30, 40 and 100 km. Note that the V/H ratio increases dramatically for larger earthquakes closer to the site. Magnitude dependency in the MFFF V/H is illustrated in Figures 7a and b for distances of 20 and 100 km respectively. For earthquakes at 20 km distance, soil nonlinear behavior significantly reduces the horizontal component, increasing V/H for frequencies above 1 Hz whereas at greater distances the effect of nonlinearity on the horizontal component is reduced.

MFFF-Specific V/H

For development of MFFF-specific V/H, a selection must be made for the appropriate magnitude and distance dependent V/H transfer functions corresponding to the dominant or controlling earthquake magnitudes and distances affecting the SRS and MFFF. Thus, it is appropriate to incorporate the probabilistic seismic hazard assessment (PSHA) magnitude and distance disaggregations for the SRS. The average of the EPRI and Lawrence Livermore National Laboratory (LLNL) PSHAs, modified for SRS-specific soils, are currently used for SRS design basis (those PSHAs and their disaggregations are described in WSRC (1997) and WSRC (1998)). However, the most recently available PSHA having up-to-date source models is that conducted by Frankel (1999) and reported in WSRC (1999a). For this evaluation we have selected the Frankel (1999) bedrock hazard disagregations with an annual probability of 10^{-4}. Although the soil surface disaggregation would be preferred, the rock outcrop disaggregation is not expected to differ significantly. Note that for the MFFF mean seismic design basis, the 10^{-4}/yr disaggregation would be conservative for V/H design as the controlling earthquakes are somewhat larger in magnitude and closer in distance as compared to a design basis having greater exceedence probability. Table 3 shows the hazard disaggregation for the SRS (Frankel, 1999) for the available frequencies of 1, 2, 3.33, 5, 10 and 100 Hz for an annual probability of exceedence of 10^{-4}. To illustrate the sensitivity of computed V/H to the annual probability of exceedence of the disaggregation, a 5 x 10^{-4}/yr USGS hazard disaggregation is also developed for comparison. The hazard disaggregation for the SRS (Frankel, 1999) for an annual probability of exceedence of 5 x 10^{-4} is tabulated in Table 4.

Nonlinearity of the soil column complicates the adoption of a vertical component design recommendation. Ideally, the bedrock control motions used to develop the horizontal component design basis motions would be the same level as the motions used for the V/H analysis. For this analysis, the assumption is made that the hazard disaggregation captures the appropriate level of soil nonlinearity for the design basis.

Our approach to develop a site-specific V/H, for each oscillator frequency, is to form the products:

$$V/H_{weight} = \Sigma_{ij} P_{ij} * V/H_{corr\ ij} \qquad (2)$$

Where i is the index over all distances in the disaggregation and j is the index over all magnitudes in the disaggregation. P_{ij} is the fraction of the earthquakes in the ith distance bin and jth magnitude bin contributing to the hazard ($\Sigma_{ij} P_{ij} = 1.0$). $V/H_{corr\ ij}$ is the corrected MFFF V/H for the ith distance and jth magnitude (Equation 1). For each magnitude and distance, interpolation was used from the values shown in Figure 6. Interpolation was also used between disaggregation oscillator frequencies.

The resulting MFFF V/H (V/H_{weight}) using Equation 2 is illustrated in Figure 8. For frequencies greater than about 3 Hz, the ASCE 4-86 recommendations of V/H = 2/3 are unconservative as compared to V/H_{weight}. For frequencies greater than about 8 Hz, the MFFF V/H is in excess of 1.0.

To demonstrate the sensitivity of the analysis to the location of the water table an evaluation for the MFFF site was performed with the groundwater table at the ground surface. The results are also shown in Figure 8. The results show the same trend as the MFFF-specific V/H except the magnitude is less. The deeper water table creates a contrast in P-wave velocity that enhances the vertical component motions as a result of a P-wave resonance. The effect of the water table at depth is oscillator frequency dependent and generally increases V/H over a wide frequency range, in this case significantly for frequencies greater than about 3 Hz.

To demonstrate the sensitivity of the analysis to hazard disaggregation probability of exceedence, the MFFF-specific V/H was evaluated using the Frankel (1999) hazard disaggregation at a probability of exceedence of 5×10^{-4}/yr. For increasing probabilities of exceedence the hazard disaggregation exhibits greater contributions from earthquakes of somewhat lower magnitude and greater distance. Consequently, the MFFF site V/H would in general be lower for greater exceedence rates. Figure 9 illustrates the effect of the 5×10^{-4}/yr exceedence rate, indicating an approximate 30% reduction in V/H at higher frequencies. At low frequencies, V/H is unchanged as the distant Charleston earthquake dominates the hazard contribution for both 5×10^{-4}/yr and 10^{-4}/yr exceedences.

Summary

Based on EUS ground motion models, corrections have been applied to a well-constrained empirical WUS V/H, which is based on the most recently available strong motion data. Corrections for SRS and MFFF soil, bedrock and crust conditions indicate very high V/H for sites that are in close proximity to an earthquake or subject to a large magnitude earthquake. Such events would load the soil, reducing the horizontal component spectra, thus increasing V/H. Using the USGS developed bedrock hazard disaggregation for the SRS (Frankel, 1999), a weighted-average of V/H is computed resulting in an appropriate composition of V/H that reflects the dominant earthquake magnitudes and distances affecting the SRS. As shown in

Figure 8 the MFFF weighted V/H is frequency dependent, reaches a peak of nearly 1.4 at frequencies greater than about 3 Hz and is higher than the ASCE 4-86 recommendations.

It should be noted that there is significant uncertainty in the correction to the empirical WUS V/H relationship. There is uncertainty in the model for WUS V/H, and even greater uncertainty in the EUS V/H model. However, the necessity to model V/H in the EUS is a result of the shortage of strong motion data (in the EUS), particularly on deep soil sites. The uncertainties in the dynamic properties of the soil, the properties of the crustal model and the depths and model of eastern seismic sources all contribute to this uncertainty. Additional uncertainty is introduced by assuming the same modeling approach in the EUS as is used to model WUS vertical component motions. The importance of these uncertainties and the sensitivity of the V/H corrections to the input parameters are best evaluated in a parametric study that is beyond the scope of this task.

While there is significant uncertainty in the results, there is no apparent bias in the models used. There is a possibility of a conservative bias in the transfer functions at higher loading levels because the entire soil column is allowed to degrade, reducing the horizontal component, possibly excessively, while the vertical component response is treated linearly. However, the earthquake magnitude and distance composition defined by the USGS hazard disaggregation gives low weight to those events that would heavily load the soil. Thus, based upon the empirical data used, the corrections to that data, and the earthquake magnitudes and distances that control the evaluation, the MFFF V/H are considered best estimate values.

If the MFFF-specific V/H (Figure 8) is to be used to develop a vertical design spectrum, then the MFFF-specific V/H should only be applied to a site-specific mean horizontal spectrum derived at the appropriate exceedence level (WSRC, 1997). The spectrum resulting from this operation would then be enveloped for appropriate engineering analysis.

A parametric study should be completed to evaluate the importance of parameters used in the evaluation of V/H. Parameters that could be evaluated for V/H sensitivity are: (1) EUS and WUS source models including stress drop and single/double corner models; (2) EUS and WUS crustal models and depth ranges of earthquakes; (3) EUS and WUS crustal attenuation and site damping models; (4) range of Poisson models (including various water table depths) for the MFFF site; (5) alternate strain-dependent soil properties for the WUS and MFFF site; and (6) alternate models for predicting the response of the vertical component including strain dependent modulus and damping.

The greatest uncertainty in this analysis is the use of analytical models to estimate corrections for EUS deep soil site conditions. This analysis reinforces the importance of continuing the strong motion monitoring at the SRS at multiple levels in the soil column.

Acknowledgements

Walt Silva (Pacific Engineering and Analysis) computed the V/H corrections to the empirical relationships and provided valuable insight on their development. Jeff Kimball, Carl Stepp, Carl Costantino, Tom Houston, Mike Lewis, Larry Salomone and Mike McHood all contributed to improvements in the text.

References

Abrahamson, N.A., and W. J. Silva, 1997. Empirical Response Spectral Attenuation Relations for Shallow Crustal Earthquakes. Seis. Res. Lett., Vol. 68, No. 1, 94-127.

ASCE 4-86. American Society of Civil Engineers Seismic Analysis of Safety Related Nuclear Structures, Standard and Commentary.

ASCE 4-98. American Society of Civil Engineers Seismic Analysis of Safety Related Nuclear Structures, Standard and Commentary.

Bozorgnia, Y., K.W. Campbell, and M Niazi, 1999. Vertical Ground Motion: Characteristics, Relationship with Horizontal Component, and Building-Code Implications. Proceedings of SMIP99 Seminar on Utilization of Strong Motion Data, San Francisco, Sept 15, 1999.

Campbell, K.W., 1997. Empirical Near-Source Attenuation Relationships for Horizontal and Vertical Components of Peak Ground Acceleration, Peak Ground Velocity, and Pseudo-Absolute Acceleration Response Spectra, Seis. Res. Lett., Vol. 68, No. 1, 154-179.

DCS, 2001. MOX Fuel Fabrication Facility Site Geotechnical Report, DCS01-WRS-DS-NTE-G-0005-B.

Electric Power Research Institute (1993). "Guidelines for determining design basis ground motions." Palo Alto, Calif: Electric Power Research institute, vol. 1-5, EPRI TR-102293.

Frankel, A., 1999. Letter report of calculation results to R.C. Lee, March 9, 1999.

McConaghy Jr., John M., e-mail to M.R. Lewis on May 2, 2001.

Newmark, N.M., and W.J. Hall, 1978. Development of criteria for seismic review of selected nuclear power plants. NUREG/CR-0098, Nuclear Regulatory Commission.

Silva, W.J., 1997. Characteristics of Vertical Strong Ground Motions for Applications to Engineering Design, in Proceedings of the FHWA/NCEER Workshop on the National Representation of Seismic Ground Motion for New and Existing Highway Facilities, edited by I.M. Friedland, M.S. Power and R.L. Mayes, September 22, 1997.

U.S. Nuclear Regulatory Commission, 1977. Regulatory Guide 1.60 Design Response Spectra for Seismic Design of Nuclear Power Plants, Washington, D.C.

WSRC, 1997. SRS Seismic Response Analysis and Design Basis Guidelines, by R.C. Lee, M.E. Maryak and M.D. McHood, WSRC-TR-97-0085, Rev. 0.

WSRC, 1998. Soil Surface Seismic Hazard and Design Basis Guidelines for Performance Category 1 & 2 SRS Facilities, WSRC-TR-98-00263.

WSRC, 1999a. Computation of USGS Soil UHS and Comparison to NEHRP and PC1 Seismic Response Spectra for the SRS. Westinghouse Savannah River Company, WSRC-TR-99-00271, Rev. 0, 9/30/99.

WSRC, 1999b. Engineering Standard No. 01060, September, 1999, Rev. 4

Table 1
PARAMETERS FOR WUS SOIL OUTCROP SIMULATIONS

M	5.0, 5.5, 6.0, 6.5, 7.0, 7.5		
D(km)	1, 5, 10, 15, 20, 40, 100		
30 simulations for each **M**, *R* pair			
Randomly vary source depth, Δσ, kappa, Q_o, profile			
<u>Depth</u>, $\sigma_{lnH} = 0.6$, $\overline{H}$ (M > 5) = 8 km; Source, California Seismicity			
M	Lower Bound (km)	$\overline{H}$ (km)	Upper Bound (km)
5.0, 5.5	2	6	25
6.0, 6.5	4	8	20
7.0, 7.5	5	8	15
<u>Δσ</u>, $\sigma_{ln\Delta\sigma} = 0.5$, Based on California earthquake inversions (Silva et al., 1997)			
M	Δσ (bars)	AVG. Δσ (bars) = 65	
5.5	65	Based on inversions of the A&S 97 relation (BNL, 1997)	
6.5	65		
7.5	65		
<u>*Q(s)*</u>, $\overline{Q_o} = 275$, *Southern California inversions;* $\sigma_{lnQ_o} = 0.4$, (Silva et al., 1997) $\eta = 0.60$, *Southern California inversions;* $\sigma_\eta = 0$, (Silva et al., 1997) Varying Q_o only sufficient, ± 1 σ covers range of Southern California inversions from 1 to 20 Hz			
<u>Kappa</u>, $\overline{\kappa} = 0.04$ sec, $\sigma_{ln\kappa} = 0.3$ (EPRI, 1997):total kappa			
<u>Profile</u>, GEOMATRIX C + D over generic California crust (Silva et al., 1997) randomize depth 100 to 1,000 ft.			
Geometrical attenuation $R^{-(a + bM)}$, $R^{-(a + bM)/2}$, R > 60 km, a = 1.0296, b = -0.0422 Based on inversions of the Abrahamson and Silva (1997) relation			

Table 2
PARAMETERS FOR CEUS ROCK OUTCROP SIMULATIONS

M	5.0, 5.5, 6.0, 6.5, 7.0, 7.5
D(km)	1, 5, 10, 15, 20, 40, 100

30 simulations for each **M**, *R* pair

Randomly vary source depth, $\Delta\sigma$, kappa, Q_o, η, profile

Depth, $\sigma_{lnH} = 0.6$, $\overline{H}$ (M > 5) = 10 km; Intraplate Seismicity (EPRI, 1993)

M	Lower Bound (km)	$\overline{H}$ (km)	Upper Bound (km)
5.0, 5.5	3	8	30
6.0, 6.5	4	10	30
7.0, 7.5	5	12	30

$\Delta\sigma$, $\sigma_{ln\Delta\sigma} = 0.7$ (EPRI, 1993)

M	$\Delta\sigma$ (bars)	
5.5	120	AVG. $\Delta\sigma$ (bars) = 122; Assumes M 5.5 = 160 bars (Atkinson, 1993) with magnitude scaling taken from WUS (Table 1)
6.5	120	
7.5	120	

Q(s), $\overline{Q_o} = 351$, *Saguenay inversions;* $\sigma_{lnQ_o} = 0.4$, (Silva et al., 1997)
$\eta = 0.84$, *Saguenay inversions;* *sigmaSUB*$\eta = 0$, (Silva et al., 1997)
Varying Q_o only sufficient, ± 1 σ covers range of CEUS inversions from 1 to 20 Hz

Kappa, $\overline{\kappa} = 0.02$ sec (Fletcher, 1995) $\sigma_{ln\,\kappa} = 0.3$, (EPRI, 1993): total kappa

Profile, SRS, randomize 800 to 1,000 ft

Geometrical attenuation $R^{-(a+bM)}$, a = 1.0296, b = -0.0422
$R^{-(a+bM)/2}$, R > 80 km

Based on inversions of the Abrahamson and Silva (1997) relation

Table 3

USGS Bedrock hazard disaggregation (in percent) for the SRS at an annual probability of exceedence of $1x10^{-4}$ (WSRC, 1999) for oscillator frequencies of 1, 2, 3.3, 5, 10, and 100 Hz.

Freq (Hz)	**R** (km)	**Bin Magnitude** (Mw)					
		4.75	5.25	5.75	6.25	6.75	7.5
1.00							
	7.5	0.04	0.40	1.15	1.37	1.28	0.00
	20	0.01	0.12	0.63	1.19	1.67	0.00
	37.5	0.00	0.08	0.63	1.82	3.99	0.00
	75	0.00	0.02	0.31	1.61	0.00	20.07
	150	0.00	0.00	0.13	1.20	0.00	53.83
	250	0.00	0.00	0.01	0.11	0.00	6.46
	550	0.00	0.00	0.00	0.04	0.00	1.81
2.00							
	7.5	0.46	1.61	2.41	1.97	1.47	0.00
	20	0.07	0.53	1.41	1.84	2.06	0.00
	37.5	0.02	0.28	1.29	2.72	4.94	0.00
	75	0.00	0.05	0.48	1.92	0.00	21.81
	150	0.00	0.01	0.16	1.12	0.00	46.77
	250	0.00	0.00	0.00	0.06	0.00	4.09
	550	0.00	0.00	0.00	0.01	0.00	0.43
3.33							
	7.5	2.05	3.31	3.25	2.22	1.51	0.00
	20	0.41	1.28	2.15	2.27	2.19	0.00
	37.5	0.13	0.70	1.97	3.33	5.29	0.00
	75	0.01	0.12	0.66	2.14	0.00	21.32
	150	0.00	0.02	0.20	1.13	0.00	39.43
	250	0.00	0.00	0.00	0.04	0.00	2.69
	550	0.00	0.00	0.00	0.00	0.00	0.16
5.00							
	7.5	4.57	4.84	3.84	2.34	1.53	0.00
	20	1.13	2.10	2.74	2.47	2.24	0.00
	37.5	0.43	1.24	2.55	3.64	5.35	0.00
	75	0.04	0.21	0.81	2.17	0.00	20.42
	150	0.00	0.03	0.21	1.03	0.00	32.37
	250	0.00	0.00	0.00	0.03	0.00	1.63
	550	0.00	0.00	0.00	0.00	0.00	0.05

Table 3 (cont.)

USGS Bedrock hazard disaggregation (in percent) for the SRS at an annual probability of exceedence of $1x10^{-4}$ (WSRC, 1999) for oscillator frequencies of 1, 2, 3.3, 5, 10, and 100 Hz.

Freq (Hz)	**R** (km)	**Bin Magnitude** (Mw)					
		4.75	5.25	5.75	6.25	6.75	7.5
10.00							
	7.5	8.82	6.86	4.57	2.54	1.57	0.00
	20	2.55	3.48	3.62	2.88	2.38	0.00
	37.5	0.83	1.95	3.37	4.25	5.70	0.00
	75	0.05	0.23	0.82	2.13	0.00	18.56
	150	0.00	0.02	0.17	0.76	0.00	21.33
	250	0.00	0.00	0.00	0.01	0.00	0.56
	550	0.00	0.00	0.00	0.00	0.00	0.01
100.00							
	7.5	13.44	8.20	4.93	2.61	1.58	0.00
	20	4.09	4.40	4.06	3.00	2.38	0.00
	37.5	1.12	2.20	3.51	4.20	5.39	0.00
	75	0.04	0.17	0.63	1.65	0.00	15.52
	150	0.00	0.01	0.09	0.43	0.00	15.90
	250	0.00	0.00	0.00	0.00	0.00	0.43
	550	0.00	0.00	0.00	0.00	0.00	0.01

Table 4

USGS Bedrock hazard disaggregation (in percent) for the SRS at an annual probability of exceedence of $5x10^{-4}$ (WSRC, 1999) for oscillator frequencies of 1, 2, 3.3, 5, 10, and 100 Hz.

Freq (Hz)	**R** (km)	**Bin Magnitude** (Mw)					
		4.75	5.25	5.75	6.25	6.75	7.5
1.00							
	7.5	0.14	0.49	0.69	0.49	0.32	0.00
	20	0.04	0.26	0.62	0.64	0.54	0.00
	37.5	0.02	0.26	0.99	1.51	1.83	0.00
	75	0.00	0.13	0.95	2.49	0.00	15.21
	150	0.00	0.05	0.74	3.13	0.00	53.31
	250	0.00	0.00	0.07	0.51	0.00	9.10
	550	0.00	0.00	0.03	0.30	0.00	5.13
2.00							
	7.5	0.79	1.28	1.05	0.58	0.33	0.00
	20	0.25	0.80	1.09	0.83	0.60	0.00
	37.5	0.13	0.77	1.75	2.07	2.11	0.00
	75	0.02	0.31	1.42	3.01	0.00	16.80
	150	0.01	0.12	0.91	3.16	0.00	50.77
	250	0.00	0.00	0.05	0.33	0.00	6.88
	550	0.00	0.00	0.01	0.10	0.00	1.69
3.33							
	7.5	2.14	1.94	1.21	0.60	0.34	0.00
	20	0.92	1.48	1.41	0.93	0.61	0.00
	37.5	0.56	1.55	2.39	2.37	2.20	0.00
	75	0.11	0.62	1.85	3.34	0.00	16.72
	150	0.02	0.22	1.11	3.20	0.00	45.86
	250	0.00	0.00	0.04	0.25	0.00	5.22
	550	0.00	0.00	0.00	0.05	0.00	0.73
5.00							
	7.5	3.58	2.36	1.30	0.61	0.34	0.00
	20	1.93	2.05	1.62	0.97	0.62	0.00
	37.5	1.42	2.36	2.87	2.52	2.23	0.00
	75	0.33	1.00	2.21	3.46	0.00	16.51
	150	0.05	0.29	1.15	3.00	0.00	40.91
	250	0.00	0.00	0.03	0.17	0.00	3.78
	550	0.00	0.00	0.00	0.02	0.00	0.30

Table 4 (cont.)

USGS Bedrock hazard disaggregation (in percent) for the SRS at an annual probability of exceedence of $5x10^{-4}$ (WSRC, 1999) for oscillator frequencies of 1, 2, 3.3, 5, 10, and 100 Hz.

Freq (Hz)	**R** (km)	**Bin Magnitude** (Mw)					
		4.75	5.25	5.75	6.25	6.75	7.5
10.00							
	7.5	5.25	2.82	1.39	0.63	0.34	0.00
	20	3.58	2.92	1.93	1.05	0.63	0.00
	37.5	2.67	3.59	3.70	2.90	2.36	0.00
	75	0.47	1.27	2.58	3.78	0.00	16.56
	150	0.07	0.32	1.10	2.61	0.00	33.33
	250	0.00	0.00	0.01	0.07	0.00	2.00
	550	0.00	0.00	0.00	0.00	0.00	0.06
100.00							
	7.5	6.26	3.03	1.43	0.63	0.34	0.00
	20	4.87	3.38	2.07	1.08	0.64	0.00
	37.5	3.52	4.10	3.96	2.98	2.36	0.00
	75	0.45	1.17	2.38	3.46	0.00	15.87
	150	0.04	0.21	0.77	2.00	0.00	30.89
	250	0.00	0.00	0.01	0.05	0.00	1.94
	550	0.00	0.00	0.00	0.00	0,00	0.11

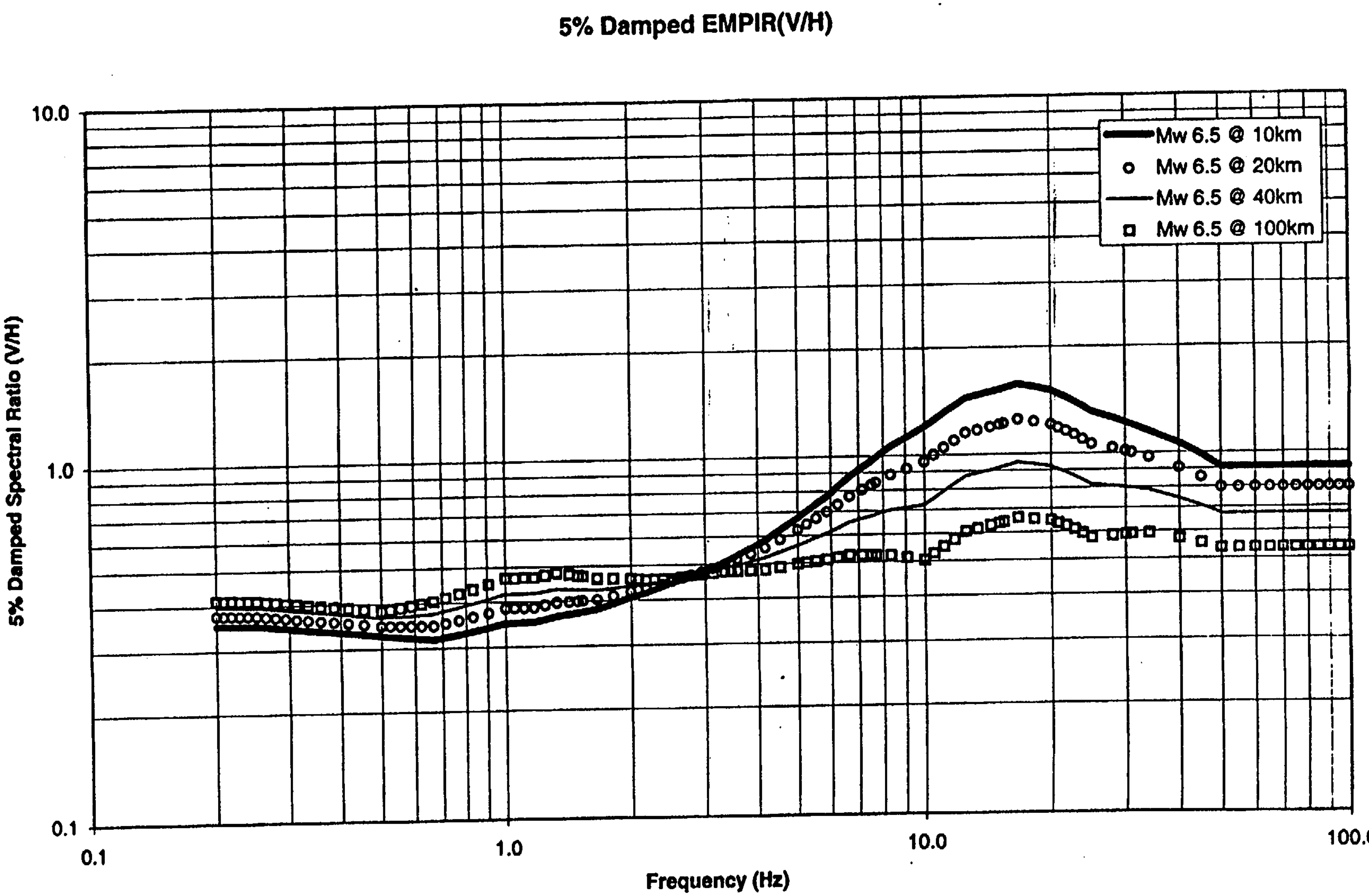

Figure 1. WUS empirical V/H based on motions recorded on soil sites 10, 20, 40 and 100 km distant from an Mw 6.5 earthquake.

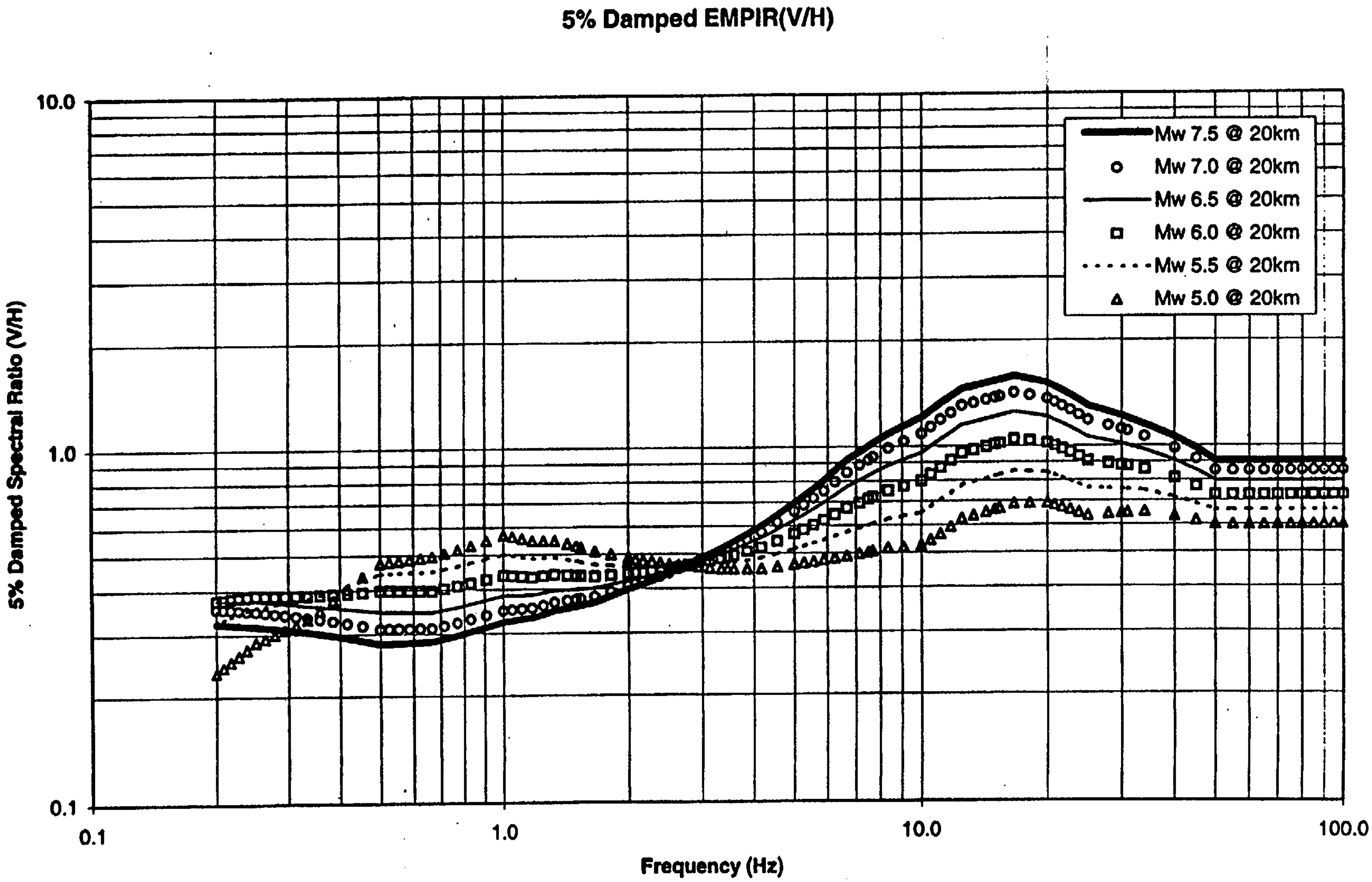

Figure 2. WUS empirical V/H based on motions recorded on soil sites 20 km distant from Mw 5.0, 5.5, 6.0, 6.5, 7.0 and 7.5 earthquakes.

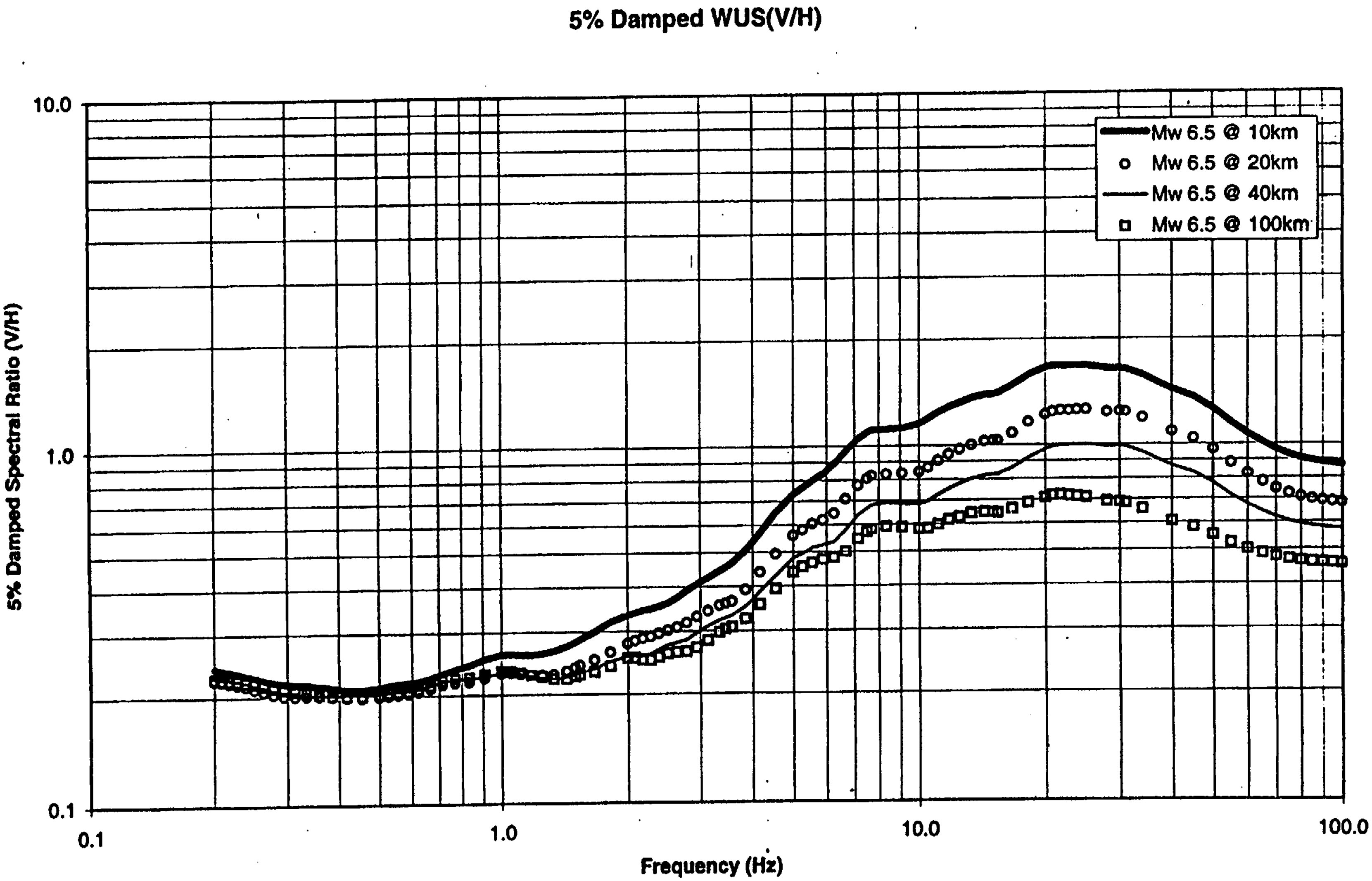

Figure 3. WUS model V/H for soil sites 10, 20, 40 and 100 km distant from an Mw 6.5 earthquake.

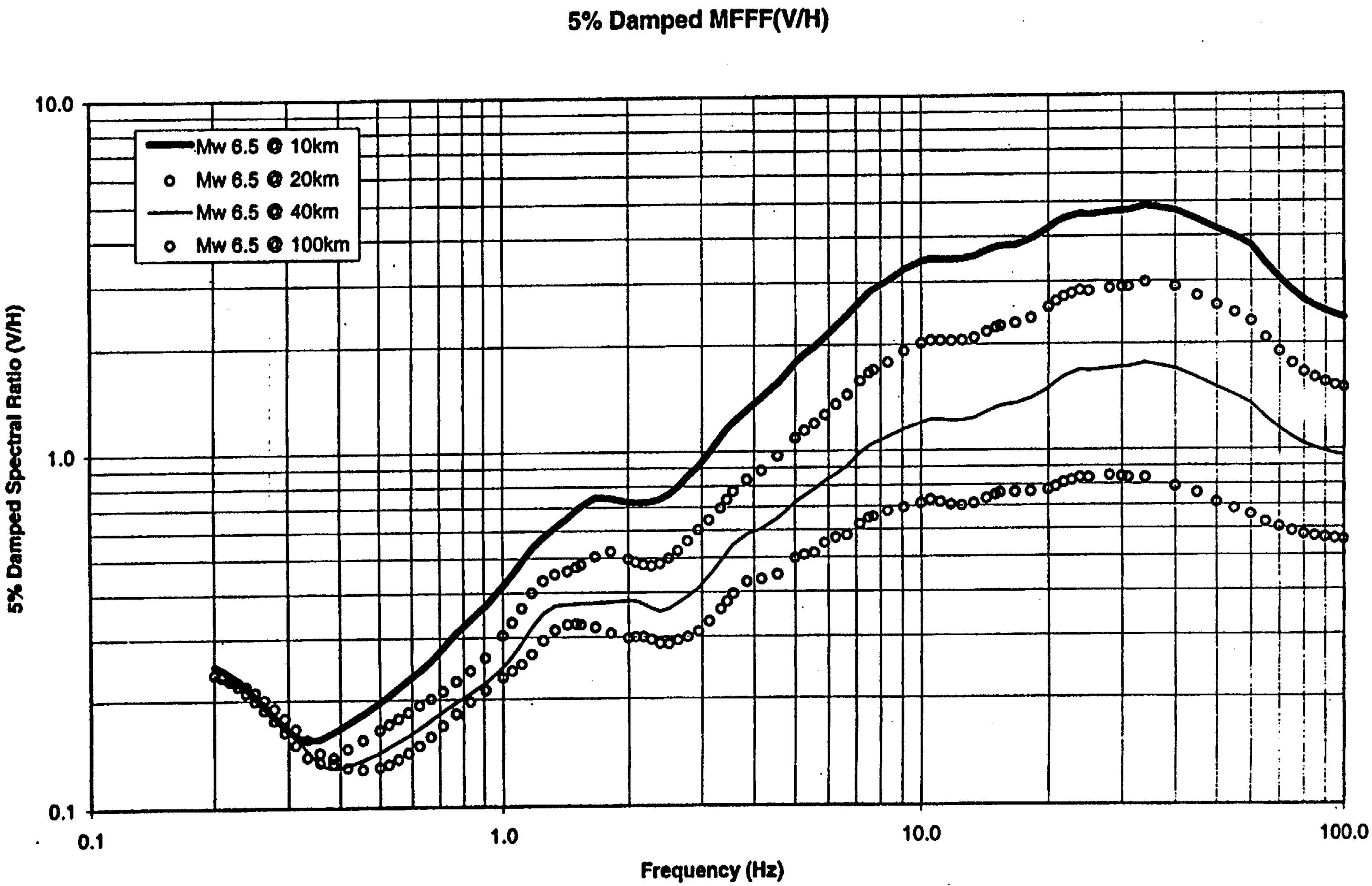

Figure 4. MFFF model V/H 10, 20, 40 and 100 km distant from an Mw 6.5 earthquake.

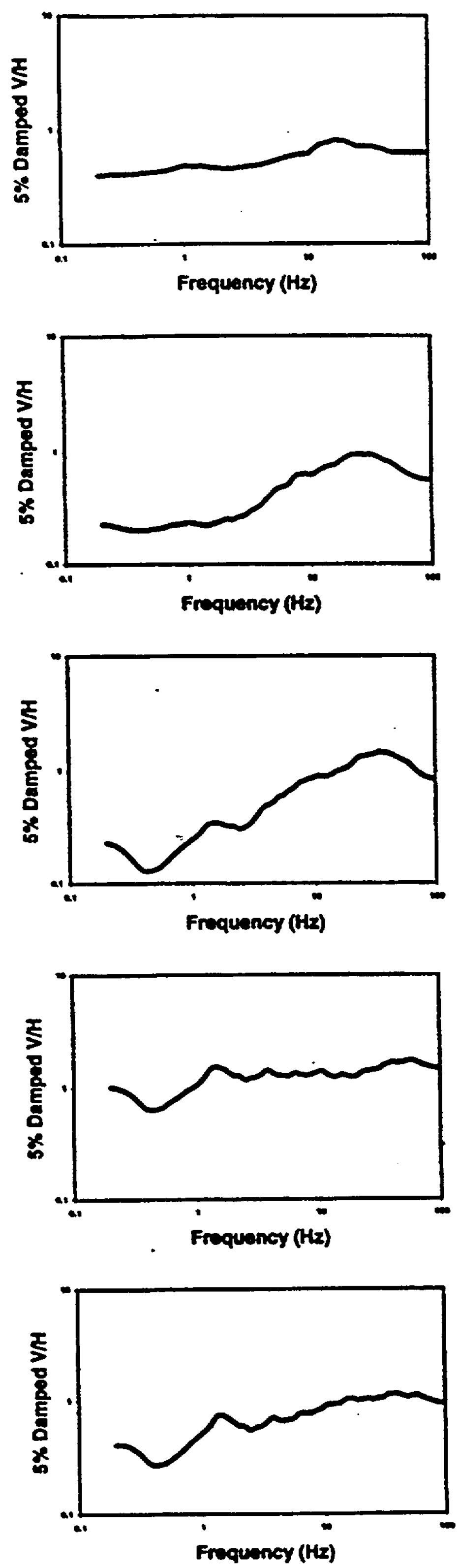

(a) WUS empirical V/H

(b) WUS model V/H

(c) MFFF model V/H

(d) Ratio of MFFF model V/H (V/H_{MFFF}) to WUS model V/H (V/H_{wus})
(c) / (b)

(e) Product of empirical WUS V/H (V/H_{emp}) and the ratio of MFFF model V/H (V/H_{MFFF}) to WUS model V/H (V/H_{wus})
(d) x (a)

Figure 5. Illustration of V/H operations using Equation 1 for a Mw 6.0 at 40 km distance

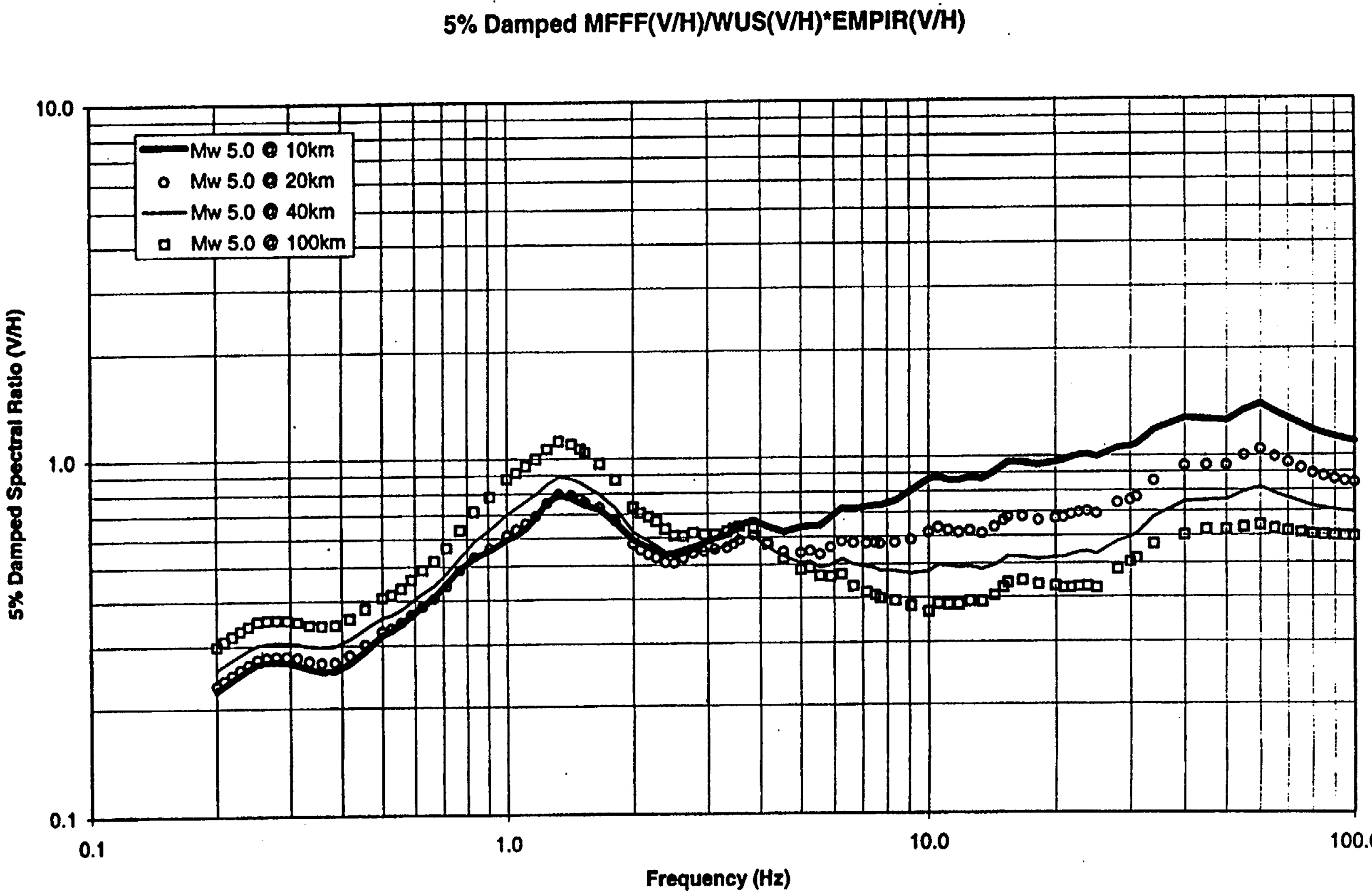

Figure 6a. MFFF corrected empirical V/H for Mw 5.0 at distances of 10, 20, 40 and 100 km.

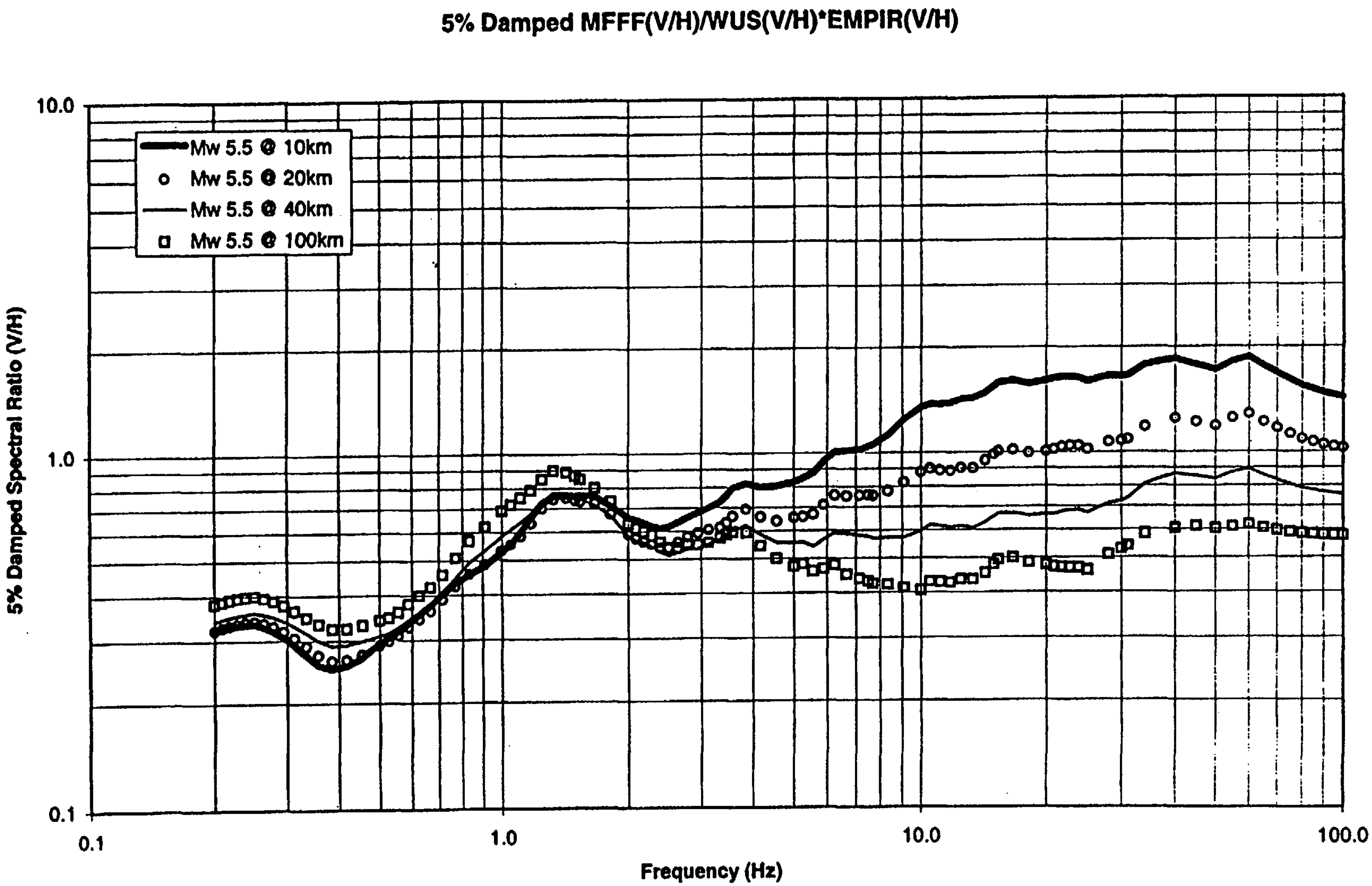

Figure 6b. MFFF corrected empirical V/H for Mw 5.5 at distances of 10, 20, 40 and 100 km.

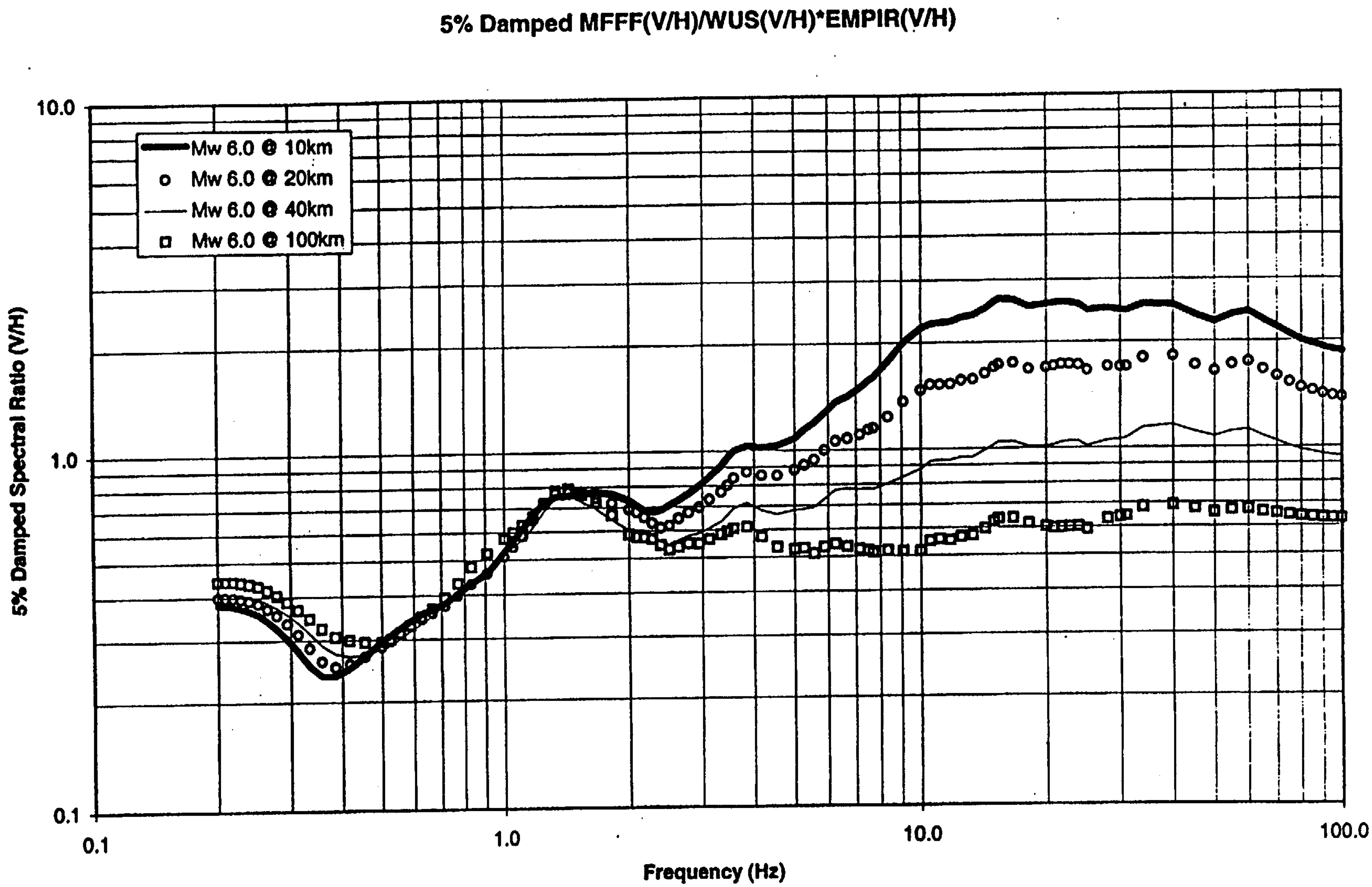

Figure 6c. MFFF corrected empirical V/H for Mw 6.0 at distances of 10, 20, 40 and 100 km.

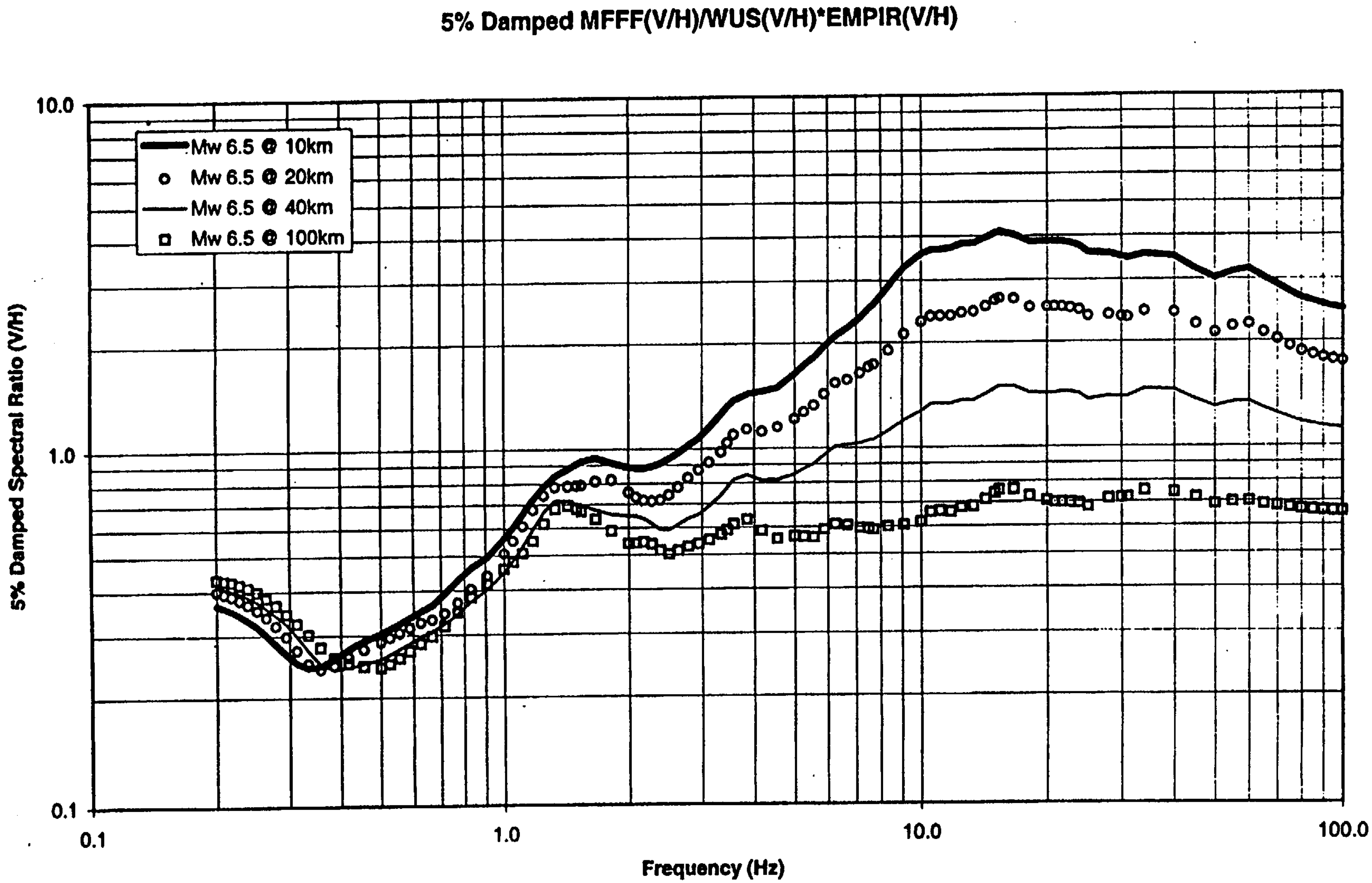

Figure 6d. MFFF corrected empirical V/H for Mw 6.5 at distances of 10, 20, 40 and 100 km.

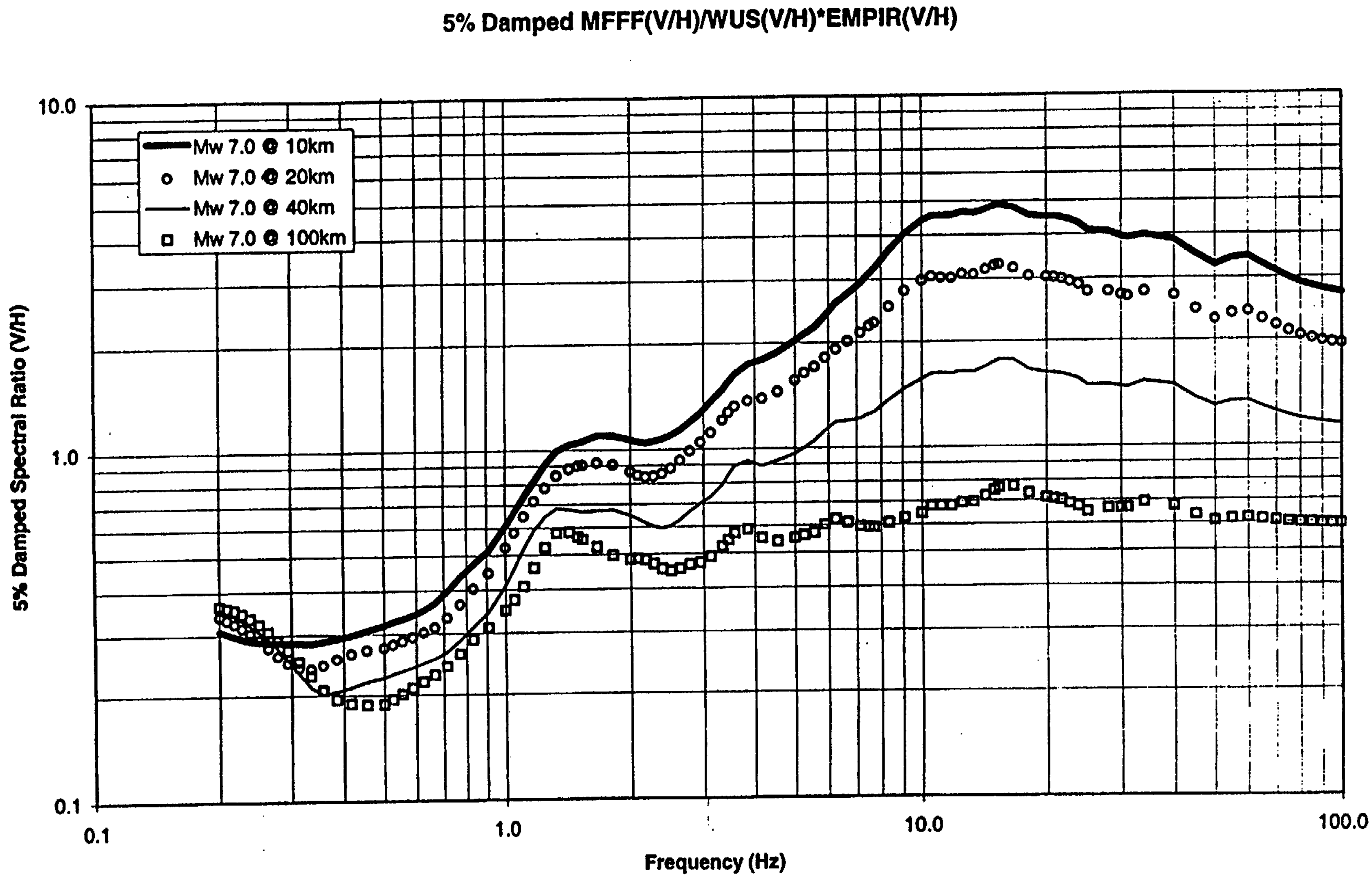

Figure 6e. MFFF corrected empirical V/H for Mw 7.0 at distances of 10, 20, 40 and 100 km.

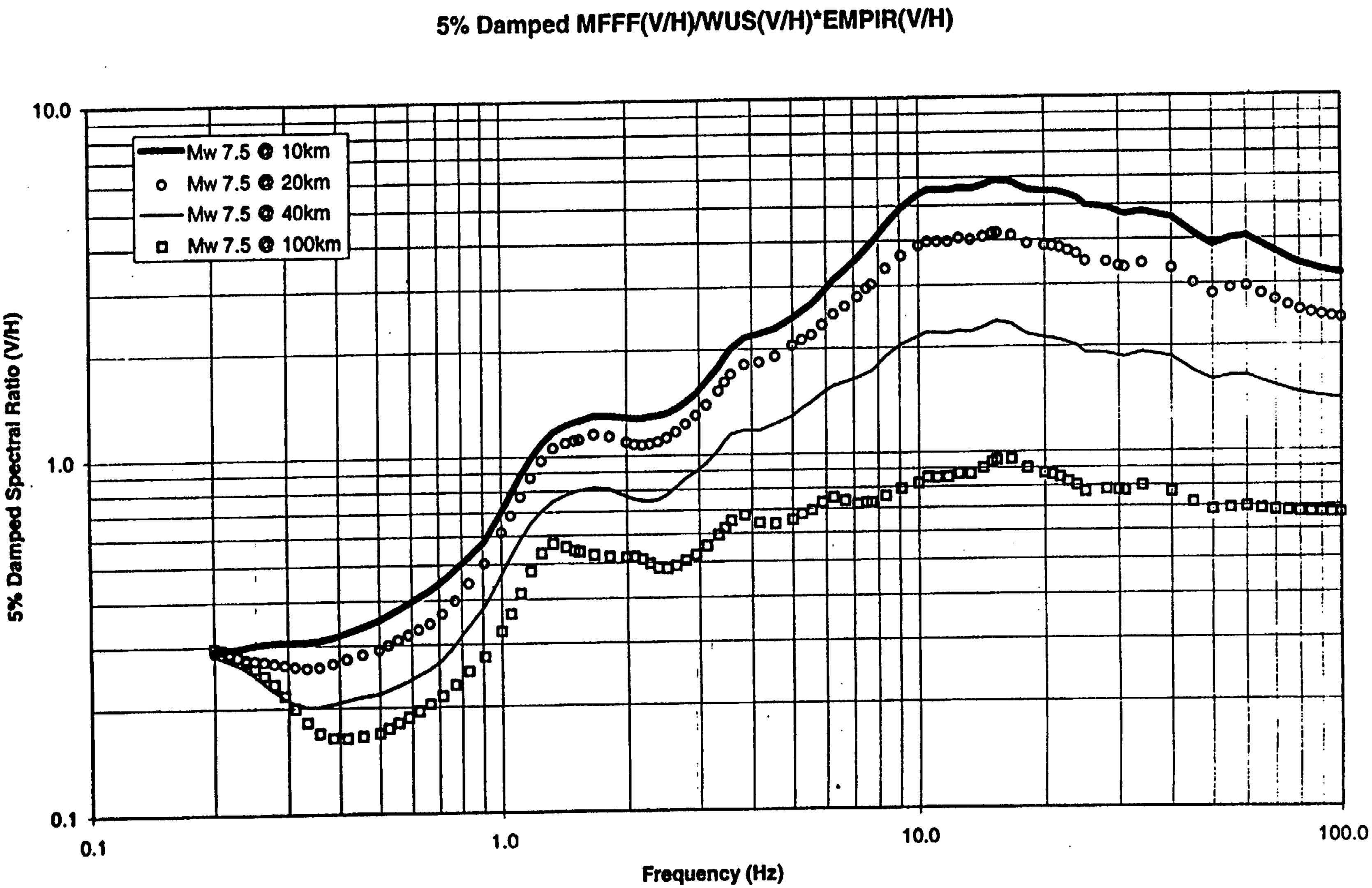

Figure 6f. MFFF corrected empirical V/H for Mw 7.5 at distances of 10, 20, 40 and 100 km.

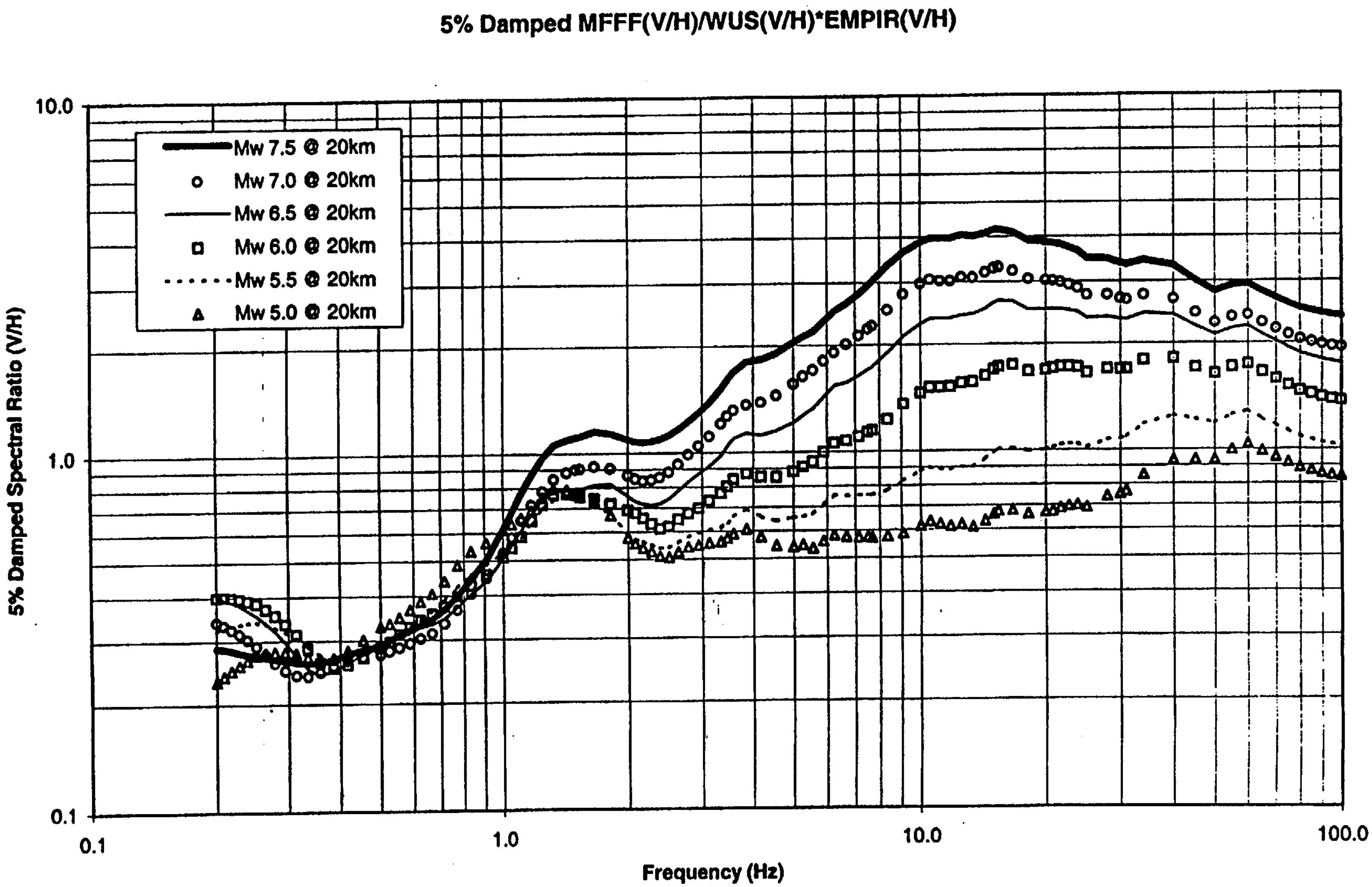

Figure 7a. Magnitude dependency in the MFFF-specific V/H. MFFF-specific V/H for Mw 5.0, 5.5, 6.0, 6.5, 7.0 and 7.5 at distance of 20 km.

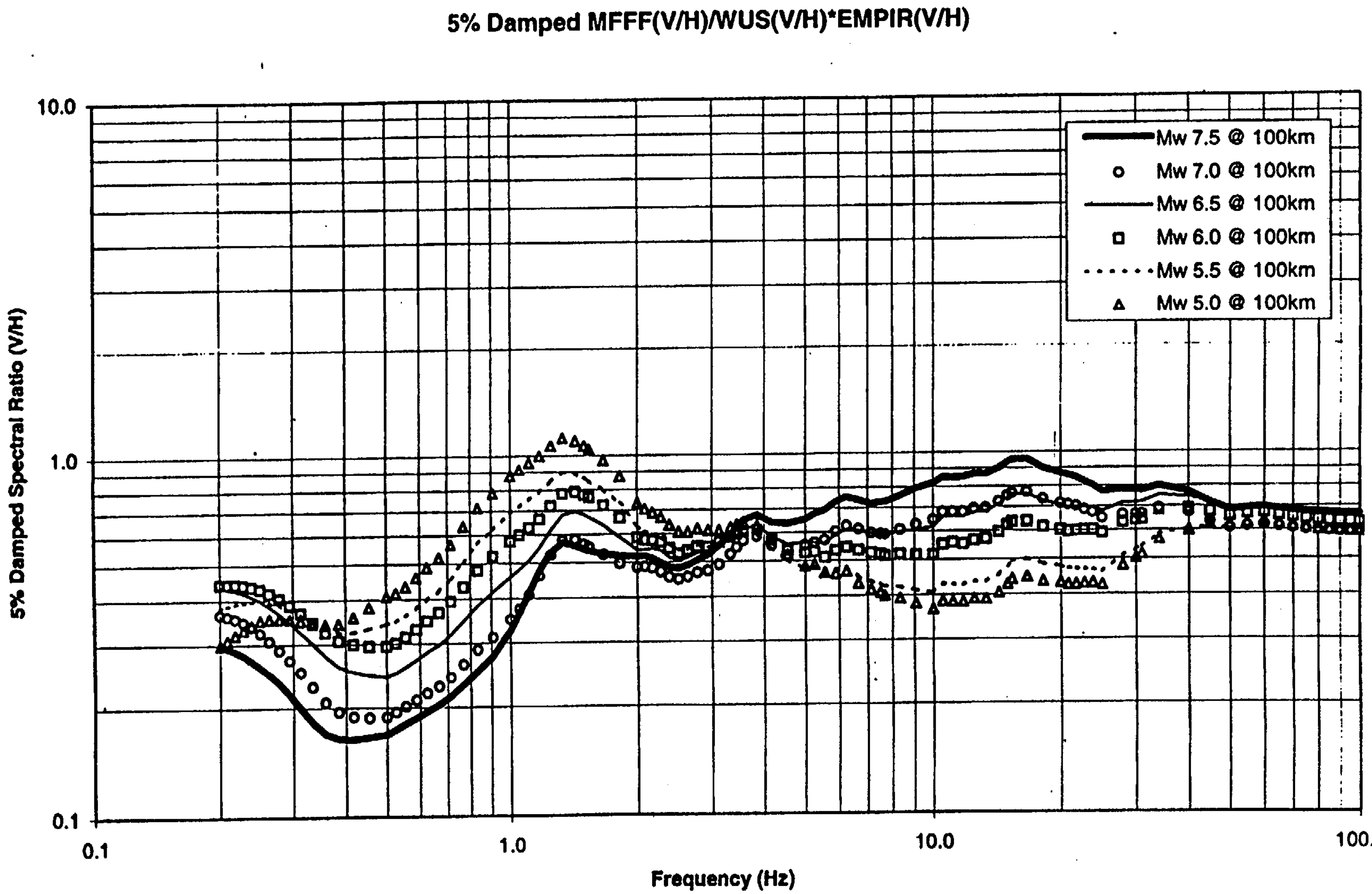

Figure 7b. Magnitude dependency in the MFFF-specific V/H. MFFF-specific V/H for Mw 5.0, 5.5, 6.0, 6.5, 7.0 and 7.5 at distance of 100 km.

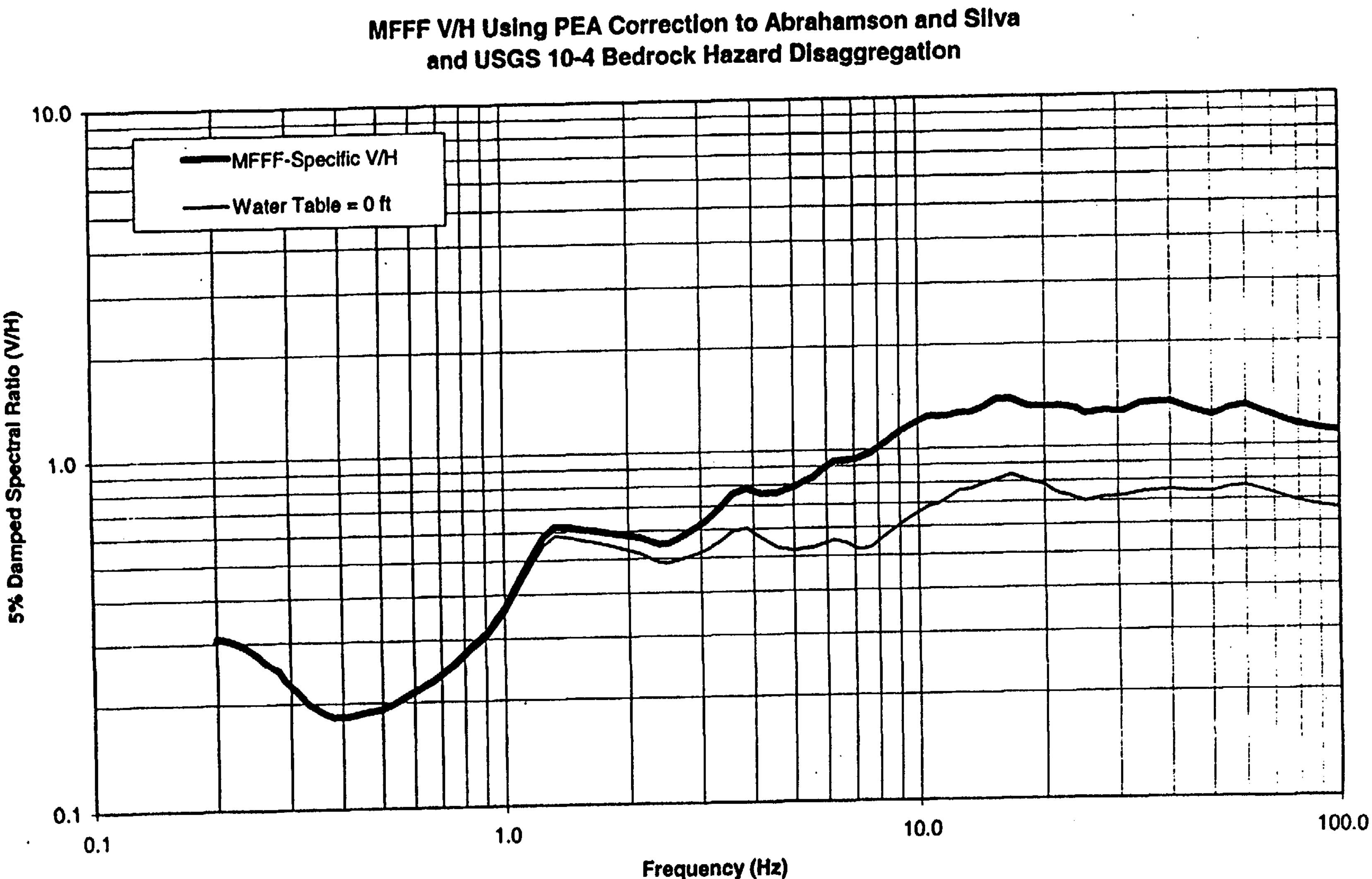

Figure 8. MFFF-specific V/H using USGS disaggregation to weight earthquake magnitudes and distances at the 1×10^{-4}/yr probability of exceedence. Also shown is the MFFF-specific V/H for water table at ground surface.

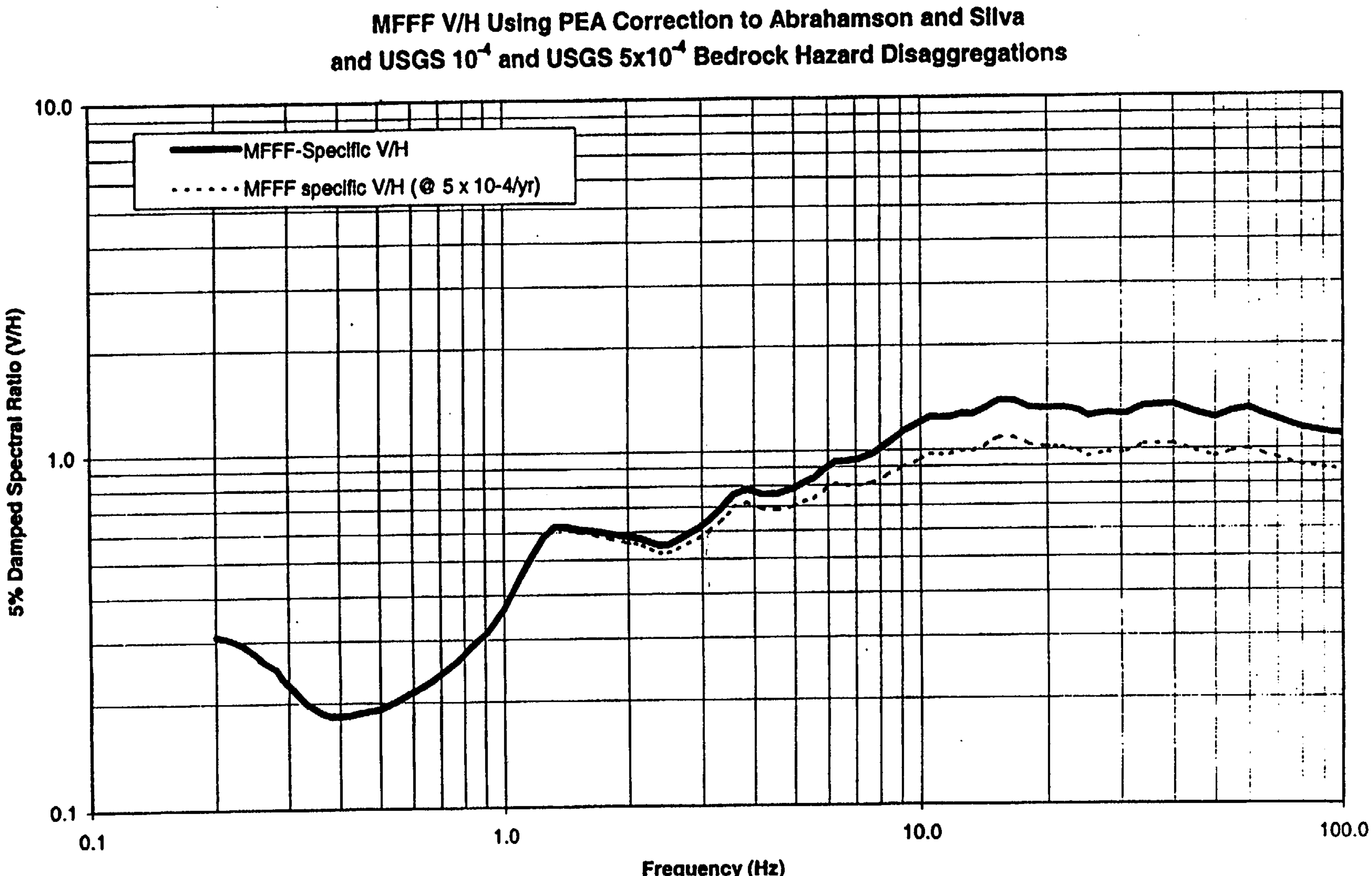

Figure 9. MFFF-specific V/H using USGS disaggregation to weight earthquake magnitudes and distances at the $1x10^{-4}$/yr probability level (V/H_{weight}). Also shown is the MFFF-specific V/H for USGS disaggregation at the $5x10^{-4}$/yr probability level.

Attachment 1

WTA 023 Rev. 1 Scope of Work

WSRC to perform a study of the relative magnitude of the vertical component of earthquake motion for the MFFF site. The study shall address peak ground acceleration level (PGA) of about 0.2g for consistency with the selected MFFF horizontal Design Earthquake spectrum. Evaluations shall be performed to develop results applicable to a deep soil site such as the MFFF. The information shall be conveyed to DCS in the form of a letter report that will be suitable for inclusion as a project record, and acceptable for use as a design input for facility design.

Methodology:

The relative vertical to horizontal evaluation is to be performed for representative frequencies between the PGA and approximately 5 hz. Suggested frequencies are at intervals of 5hz between 5hz and 30 hz, and the PGA. In any case, selected frequencies shall be appropriate to characterize the range and variability of the V/H ratio for all frequencies, but especially between 5 hz and the ZPA. Deaggregation matrix data from the USGS seismic hazard database (or equivalent) shall be used to derive a weighted V/H ratio using each magnitude-distance bin, applying the appropriate site-specific V/H ratio. An overall weighted V/H ratio will then be developed using the percentage contribution for each bin, yielding a composite V/H ratio based on the entire deaggregation matrix. This process would then be repeated at each frequency of interest. USGS deaggregation data for 5 and 10 Hz and PGA shall be used and interpolated for frequency dependency accordingly.

The work performed for this WTA shall be developed per the approved WSRC QA Program that complies with Criterion 1-6 and 15-18 of ASME/NQA-1-1989. At the completion of the documentation effort a final letter report will be prepared which satisfies the requirements of this WTA

OSR 31-688 (Rev 11-20-97)
Stores 26-8910.00

WESTINGHOUSE SAVANNAH RIVER COMPANY
INTEROFFICE MEMORANDUM

BNFL

Date: August 15, 2001 PEC-SGS-2001-00035

To: Richard Geddes, 703-45A/156

jl for

From: Russ Beckmeyer, 730-2B/130

Subject: Development of MFFF-Specific V/H Seismic Spectral Ratios (U)

Please find the subject report attached, WSRC-TR-2001-00342, Rev. 0. If you have any questions or need further assistance, please contact me at 2-6854 or Mike Lewis at 2-6847.

c: Jimmy Angelos, 703-45A/195
Mike Lewis, 730-2B/116
Larry Salomone, 730-B/304
Richard Lee, 730-2B/1078
William Martin, 703-45A/151
Mike McHood, 730-2B/1070
SGS Files, 730-2B/1102

Westinghouse
Savannah River Company
Aiken, SC 29808

PDP-MOX-2001-00032
RETENTION: Lifetime
RSM#10560

Mr. Sterling M. Franks, Acting Director
Office of Defense Nuclear Nonproliferation
National Nuclear Security Agency
Savannah River Operations Office
P. O. Box A
Aiken, SC 29802

Dear Mr. Franks:

MFFF SPECIFIC V/H SEISMIC SPECTRAL RATIOS

Ref: WTA-023, Rev. 1

In accord with the authorized tasking of the reference WTA, WSRC has completed development of site-specific V/H seismic spectral ratios. The enclosed report documents the results of the WSRC study. A draft of this study was reviewed by DCS and your staff and all comments dispositioned.

The report is now provided for your approval and issuance.

Sincerely,

James G. Angelos

J. G. Angelos, Director
Plutonium Disposition Program

RLG:jn

Enc.

Enclosure:

Development of MFFF Specific Vertical-to-Horizontal Seismic Spectral Ratios (WSRC-TR-2001-00342, Rev. 0, 8/12/01)

c: D. L. Bruner, 703-46A, w/enc.
A. M. Blackmon, 703-46A, w/enc.
W. P. Martin, 703-45A, w/o enc.
I. K. Sullivan, 703-45A, w/o enc.
R. R. Tansky, 703-45A, w/o enc.
R. L. Geddes, 703-45A, w/o enc.
R. R. Beckmeyer, 730-2B, w/o enc.
L. A. Salomone, 730-B, w/o enc.
M. R. Lewis, 730-2B, w/o enc.
R. C. Lee, 730-2B, w/o enc.
A. P. Poon, 703-45A, w/o enc.
PDP MOX Files #4700, 703-45A, w/enc.

National Nuclear Security Administration
Office of Defense Nuclear Nonproliferation
Savannah River Site
P.O. Box A
Aiken, South Carolina 29802
August 28, 2001

Mr. Jack P. Clemmens
Duke Cogema Stone & Webster
400 South Tryon Street, WC-32G
Charlotte, NC 28202

Dear Mr. Clemmens:

SUBJECT: Mixed Oxide Fuel Fabrication Facility (MFFF) Specific V/H Seismic Spectral Ratios

Please find enclosed the subject report that documents the results of the Westinghouse Savannah River Company study to establish an MFFF-specific V/H seismic spectral ratios. Duke Cogema Stone & Webster (DCS) requested this task under Work Task Agreement 023, *NPH Design Basis for MOX Facility Site*, revision 1. A draft of this report was reviewed by DCS staff and comments were incorporated. Additionally, this report has undergone a technical review by Office of Defense Nuclear Nonproliferation and Department of Energy-Savannah River Operation Office staff, and comments have been resolved and incorporated.

Please confirm that this report is responsive to WTA-023 revision 1.

This has been discussed with John McConaghy. Should you have any questions concerning this subject, please contact Allison Blackmon, of my staff, at 803-725-9910.

Sincerely,

Sterling Franks, Acting Manager
Office of Defense Nuclear Nonproliferation

ODNN:AAB:kas

WA-01-094

Enclosure:
~~Archeological Information~~ V/H Report

cc w/encl:
J. McConaghy, DCS

cc w/o encl:
J. Johnson, NN-60
B. Gutierrez, AMHSTS
R. Geddes, WSRC